

81-1-209  
M. J. ...

THE POMERON IN QCD

Alan R. White  
CERN - Geneva

A B S T R A C T

We develop a general formalism based on multiparticle dispersion theory and multi-Regge theory for describing the Pomeron in QCD. To avoid a phase-transition we use Higgs scalars in the fundamental representation only, and keep a transverse momentum cut-off except when we have asymptotic freedom. This allows the analytic continuation of a perturbative Reggeon diagram description of high-energy behaviour in the Higgs régime, of parameter space, to the confining régime of a pure gauge theory. By restoring the gauge symmetry first to  $SU(2)$  and extracting the infra-red singular part of the multiparticle Reggeon formalism we find a confining string-like result for both the Pomeron and the physical states, with the Pomeron carrying odd colour charge parity. All the features of super-critical Reggeon field theory are present and there is no rising cross-section.

When a higher gauge symmetry is restored, with the asymptotic freedom constraint on the number of fermions saturated, there is a critical phenomenon producing rising cross-sections, whose nature is associated with the complexity of closed strings (flux tubes) allowed by the symmetry. It seems that  $SU(3)$  produces the purely even signature "Critical Pomeron", with the odd colour charge parity of the vacuum (Pomeron) possibly implying Nambu-Goldstone chiral symmetry breaking.  $SU(4)$  and higher gauge groups are anticipated to produce, in addition, a non-falling odd-signature amplitude.

It seems, therefore, that the experimental Pomeron requires  $SU(3)$  gauge theory for its description and the continued rise of total cross-sections may anticipate the existence of many flavours of heavy quarks.

## 1. - INTRODUCTION

The purpose of this paper is to set up the machinery for what we hope will prove to be reliable calculations of the Pomeron in QCD. In doing so, we shall be led firstly to some rather striking conclusions on the dependence of the critical nature of the Pomeron on the number of fermions and the size of the gauge group in general Yang-Mills theories. Secondly, we shall derive a partial description of the physical states which is sufficient to demonstrate that there is confinement of colour, with the Pomeron (and, by implication, the vacuum) odd under colour charge conjugation, implying, we suspect, the spontaneous breaking of chiral symmetry when the Pomeron is sub-critical.

The vacuum quantum numbers of the Pomeron clearly suggest that it might be closely related to all the fundamental problems of quantization in non-Abelian gauge theories. For this and other related reasons it is often argued that it is fruitless to search for its correct description before solving such problems<sup>1)</sup>. Certainly the popularly anticipated picture of the Pomeron as associated with closed strings in a string theory of hadrons suggests that we should first have an adequate description of closed strings. Since this is thought by many<sup>2)</sup> to be the fundamental problem of the quantization of confining Yang-Mills theories, the fruitlessness of our purpose in this paper may be thought to be inevitable. Fortunately (and remarkably perhaps), we have found that by pursuing the construction of the Pomeron to the end, we have been led towards a resolution of the quantization problems. We also believe we may have uncovered the "tip of the iceberg" of a fascinating connection between the dynamics of the Pomeron and the dynamics of chiral symmetry breaking.

The reason for these (largely unexpected) bonuses is, perhaps, the following. During the barren years of quantum field theory (for strong interactions), the most sophisticated analyticity methods were developed to study the Pomeron<sup>3)</sup>. Using multidispersion theory and multi-Regge theory (generalized complex angular momentum theory), it became possible to construct very complicated multiparticle amplitudes almost completely from general principles in multi-Regge regions of phase-space, the construction being most complete for Pomeron amplitudes. At present, it is unclear whether field-theoretic methods will succeed, in principle or in practice, to define and calculate QCD away from the short-distance region. Clearly, if we can input enough of the defining structure of QCD into the S matrix methods we may succeed not only in defining (at least the high-energy limit of) the QCD S matrix, but we will also have a very powerful method for its construction. This is, in effect, what we do in this paper. By exploiting and developing

recent lattice gauge theory results on the analytic relation of the Higgs, and confining regimes in some theories, we are able to input the gauge theory structure into the S matrix framework in the perturbative Higgs regime, and then, analytically continue to pure QCD. Although our initial target is the Pomeron, it is clear that the method is powerful enough to answer many other questions, either directly or indirectly, about the QCD S matrix.

In fact, many of the qualitative features of the string picture emerge from our results and it is most easy to see how these results will extend to higher gauge groups when they are interpreted in terms of closed string exchange. As we have implied above, a complete, predictive description of gauge theories in terms of string operators may well prove elusive. Our approach may, therefore, complement, or even illuminate, the problem of string construction. However, the construction of non-local stringlike states from a local field theory perturbation expansion is a very complex multiparticle infra-red problem, and so it should not be surprising that we have to push the complicated multiparticle aspects of our general dispersion theoretic formalism to its present limits in order to even begin to discuss the problem.

Our starting point is the known perturbative results<sup>4),5)</sup> on the high-energy behaviour of spontaneously broken gauge theories (SBGT's). At first sight the possibility of a complete description of the high-energy behaviour of these theories looks very promising to a Regge theorist. Non-Abelian SBGT's have the remarkable property that all gauge vector mesons lie on Regge trajectories. Furthermore, it has been proven that (up to tenth order) in perturbation theory, the leading high-energy behaviour of all amplitudes can be described by multiple exchanges of the reggeized vectors. Therefore, we might anticipate that this would be the ideal situation to apply the general techniques of multi-Regge theory, and reggeon Field Theory (RFT) in particular, to study the complete asymptotic behaviour of the theory. For just this reason, Bartels<sup>6)</sup> has embarked on an extensive programme to derive the weak-coupling limit of the appropriate RFT by extending the dispersion theory calculations of Lipatov et al.<sup>4)</sup>.

Unfortunately, there is a, by now well-known, problem in making this a complete programme<sup>4)-7)</sup>. The Regge description of the high-energy behaviour of amplitudes depends on the transverse momentum of the theory being cut off. This is true perturbatively, order by order, in a non-Abelian SBGT, because of the renormalizability of the theory. But, in the leading-log approximation at least, the summation to infinite order produces a transverse momentum divergence in the vacuum channel. This divergence leads to a fixed-cut in the angular momentum

plane which violates the Froissart bound. A general SBT in which all vectors have mass and therefore reggeize is automatically non-asymptotically free. Consequently, the large transverse momentum region will be dominated by large renormalization contributions to the Higgs system in high orders of perturbation theory (renormalons) and is essentially uncalculable (if not meaningless) in this region<sup>8)</sup>. It seems that the perturbative starting point of reggeizing vector mesons with cut-off transverse momentum which, at first sight, seems so encouraging for SBT's, is completely overshadowed by the fundamental problem of the definition of the theory at short distances when we probe deeper into the high-energy behaviour.

It has been argued<sup>4)-6),9)-11)</sup> that this situation may nevertheless be useful for calculating the high-energy behaviour of unbroken gauge theories. Since the fixed-cut occurring in SBT's is due to a transverse momentum divergence, it is actually independent of the masses of the vector-mesons involved. A similar singularity may, it is argued, also occur in the corresponding (confining) unbroken gauge theory with the asymptotic freedom of the unbroken theory changing the fixed-cut to a moving Regge pole (still violating the Froissart bound)<sup>11)</sup>. However, the infra-red divergences of the (high-energy) perturbation expansion, arising in the massless limit, completely dominate the ultra-violet transverse momentum region (in gluon and quark scattering amplitudes at least), and when the leading infra-red singular behaviour is summed, the resulting high-energy behaviour is very different<sup>12),13)</sup>. In particular, there is no violation of the Froissart bound, in the sense that the amplitude does not increase with energy at fixed-momentum transfer. A priori therefore, there seems no reason to believe that the high-energy limit commutes with the massless limit. In fact, since we, in general, expect a phase-transition<sup>14)</sup> between the Higgs phase with massive vector mesons, and the confining phase of a gauge theory, we have no justification for expecting such a fundamental property of the theory as the high-energy behaviour to be preserved across the phase transition.

It is clear from the above discussion that there are many pitfalls in the way of extracting sensible high-energy results from gauge theories. It seems to us that we must initially have reggeizing massive vector mesons in the theory if we are to have a starting point for multi-Regge theory. We must also have asymptotic freedom if renormalization problems at large transverse momentum are not to dominate the calculations. If we want to study unbroken gauge theories we must have a limit into the unbroken theory in which the developing infra-red divergences do not destroy the high-energy behaviour. In effect, this means there must be no phase-transition from a Higgs to a confining phase in the limit

we consider. Most important of all perhaps, if we are to hope to handle the infrared divergences sensibly, we must also make sufficient contact with a confining (presumably stringlike) description of the physical states.

It might be thought that if we wish to satisfy all of the requirements of the last paragraph, then we will not find a theory that we can start to calculate. Fortunately, this is not the case, but our choice of theory is extremely restricted. If we wish to avoid the Higgs-confinement phase-transition, then recent lattice gauge theory calculations tell us that we should always use Higgs scalars in the fundamental representation of the gauge group<sup>15),16)</sup>. If we also want asymptotic freedom for the complete theory including the Higgs system then not only is the number of scalars we can add very restricted, but we must also have a large number of fermions present<sup>17),18)</sup>. In fact, the simplest theory to which we can add Higgs scalars and preserve asymptotic freedom is QCD with 16 flavours (QCD<sub>M</sub> - the asymptotic freedom constraint on the number of fermions is saturated). We can add just one complex triplet of scalars to QCD<sub>M</sub>. Applying the Higgs mechanism then breaks the gauge symmetry from SU(3) to SU(2) and gives a theory which we refer to as QCD<sub>MB</sub>.

For reasons that we shall elaborate it is likely that we can take a smooth limit from QCD<sub>MB</sub> into QCD<sub>M</sub> and that, in this limit, a reggeized vector becomes massless and decouples from the physical spectrum. QCD<sub>M</sub> is probably therefore the simplest continuum theory with the property that a small variation of the parameters of the theory can smoothly introduce a reggeized vector (with mass proportional to the parameter variation) into the theory. In recent papers we have argued that precisely this property is necessary to obtain the RFT critical Pomeron (that is a strong coupling, even signature, Regge pole with intercept one) as a limit from the RFT "super-critical phase"<sup>19)</sup>. This connection provides the central reason for our hope to be able to calculate precisely the high-energy behaviour of QCD<sub>M</sub>. In this and succeeding papers we hope to establish that the high-energy behaviour of QCD<sub>MB</sub> is that of "super-critical RFT" (the Pomeron intercept is formally above one), and that the limit from QCD<sub>MB</sub> into QCD<sub>M</sub> gives the RFT critical Pomeron<sup>20),21)</sup>. An additional general reason for believing that this limit gives the critical Pomeron is that in the version of RFT in which s channel unitarity is manifest (via the AGK cutting rules<sup>22)</sup>), the super-critical phase can be described as the spontaneous breakdown of a global SU(3) symmetry of the critical RFT to an SU(2) symmetry via a fundamental (complex triplet) representation of the SU(3) symmetry. Therefore, the symmetry breaking is the same as that involved in going from QCD<sub>M</sub> to QCD<sub>MB</sub>. If these symmetry patterns are indeed related, as we shall claim, then it implies a deep connection between the critical

Pomeron and the AGK cutting rules on the one hand, and  $SU(3)$  gauge symmetry on the other. We shall give a heuristic explanation of this connection in terms of Wilson loop operators in the last Section of this paper. We shall also return to the generalization to higher groups later in this introduction. First we discuss further the problems involved in finding the high-energy behaviour of  $QCD_{MB}$ .

We still have an unbroken  $SU(2)$  gauge symmetry to cope with in  $QCD_{MB}$  and so to begin our calculations we must also break this symmetry by adding a second  $SU(3)$  triplet of Higgs scalars. We keep the large transverse momentum behaviour under control at this stage by introducing a (transverse momentum) cut-off. We then have a theory which is, in principle, calculable from its perturbation expansion. [Since we have used fundamental representations of Higgs scalars, even the centre of the gauge group does not remain as a symmetry and, as a consequence, there are no non-perturbative classical configurations that we should consider in addition to the perturbation expansion.] In this situation therefore we can hope to extrapolate the perturbative high-energy calculations into a complete description of the (cut-off dependent) high-energy behaviour of all the multiparticle amplitudes of the theory. [The importance of constructing the multiparticle amplitudes is that, as we shall soon discuss, they are essential if we wish to follow the process of "string formation" as the  $SU(2)$  gauge symmetry is restored.] To carry out the desired extrapolation of the perturbative results we have to make maximum use of the multi-Regge theory developed in Ref. 3). In the past, this formalism has always been applied to justify the use of RFT for the even-signature (experimentally observed!) Pomeron. We show that it can be used equally well to derive a general diagram formalism for interacting reggeized vectors - "reggeons". Our multi-Regge theory is based on multiparticle dispersion relations<sup>3),23)</sup> which incorporate extensive  $S$  matrix unitarity analyses<sup>23)</sup> and also global analyticity domains which can be traced back to the primitive analyticity domains derived from axiomatic field theory<sup>24)</sup>. It also incorporates a complete analysis of multiparticle unitarity in the complex angular momentum plane. It is therefore a potentially very powerful formalism, and we feel that this is well demonstrated by its application to the "reggeon" problem.

Essentially, the general formalism enables us to iterate the perturbative Regge pole structure of multiparticle amplitudes through dispersion relations to obtain a "reggeon calculus" loop expansion for any multiparticle amplitude. In principle, one can then ask whether there is a simple RFT Lagrangian which generates this expansion for particular amplitudes; this is the question asked for elastic amplitudes by Bronzan and Sugar<sup>7)</sup>, and also Bartels<sup>6)</sup>, in the weak-coupling

limit. However, the most important problem for us is the infra-red singular behaviour of all amplitudes. We therefore concentrate on the general transverse momentum singularity structure of the formalism. In the previous weak-coupling RFT descriptions of elastic amplitudes<sup>6),7)</sup> it has appeared that both reggeon trajectory functions and all interactions have transverse momentum singularities whose structure could only be completely determined by impossibly laborious unitarity or Feynman diagram calculations. In fact, from our formalism we can show that all of the transverse momentum singularities found in the perturbation theory calculations have their origin in a regular triple reggeon interaction which simply contains a "nonsense zero" due to the odd-signature of the reggeons. This zero prevents the triple interaction from appearing in an RFT formulation of elastic amplitudes except as generating singularities in higher-order interactions. It will, however, appear in multiparticle amplitudes.

We extrapolate this last result by assuming that (in general) SGBT's can be described by non-singular reggeon interactions containing, when necessary, nonsense zeros and with all interactions related by Ward identities as an expression of the over-all gauge invariance of the theory<sup>25)</sup>. This extrapolation is sufficient to enable us to analyse and characterise the infra-red singular behaviour of all reggeon diagrams, in the limit that the SU(2) symmetry is restored to give QCD<sub>MB</sub>, provided we extract another important feature of the perturbative calculations<sup>4),6)</sup>. That is, the limit is best described by first undoing the reggeization of those gluons that are to be made massless, treating them essentially as elementary fixed-poles (in the angular momentum plane) having non-trivial transverse momentum interactions with properties we must generalize. The perturbation theory results show that these interactions lead to infra-red divergent diagrams except when the total SU(2) (t channel) colour is zero, with the result that all diagrams not carrying zero colour are suppressed. [This suppression is directly due to the "exponentiation" of reggeization which in turn is closely related to the "Sudakov form factor" exponentiation originally proposed by Cornwall and Tiktopoulos<sup>26)</sup> as a perturbative colour confinement mechanism.] The infra-red finiteness of the colour zero interactions in fact extends to all "off-shell" gluon or reggeon diagrams appearing in elastic amplitudes. Consequently, the only remaining infra-red divergences either occur when gluons or reggeons (or quarks) are taken on-shell to define particle amplitudes, or are generalizations of such singularities which appear in multiparticle reggeon amplitudes.

In fact, in colour zero elastic amplitudes, the leading "mass-shell" singularities also exponentiate to give finite results. We argue that this will be a general result as a consequence of the remaining infra-red singularity of the

colour zero interactions in non scale-invariant infra-red limits. However, because of the finiteness of the same interactions in scale-invariant infra-red limits, there is a class of mass-shell singularities in multiparticle amplitudes which do not exponentiate or cancel in any analogous way. The existence of these mass-shell singularities is closely tied to the breakdown of signature rules for reggeon diagrams in multiparticle amplitudes. They therefore imply that the states emerging from the infra-red limit are necessarily multiparticle gluon states. Indeed, it is this class of multiparticle mass-shell infra-red singularities which we argue are responsible for the formation of stringlike (that is, "flux-tube") physical states as the symmetry is restored. Let us discuss now why and how we believe we can make this identification. First we note that, since the high-energy limit giving the Pomeron is expected to be dominated by the exchange of low transverse momentum closed strings, it will not be surprising if we see only the structure of the large (in transverse distance) closed strings surrounding the zero-colour local physical states and do not see the short "linear" (presumably) string between constituent quarks.

Since our transverse momentum cut-off should be equivalent to a transverse lattice, we anticipate that the lattice arguments<sup>15),16)</sup> will apply and the restoration of the  $SU(2)$  gauge symmetry takes place smoothly. That is, as in the lattice theory, the stringlike states of the unbroken symmetry form continuously from multiparticle local states. In practice, this means that if we determine the infra-red singular reggeon diagrams we should find that the singularities can be absorbed into a re-definition of the external states as stringlike states, and that once this is done we have a smooth limit into the unbroken  $SU(2)$  gauge theory (with a transverse momentum cut-off). Since string states are complicated multiparticle states with a very special space-time structure, we anticipate that the most singular reggeon amplitudes will be those involving multiparticle external gluon (and quark) states, carrying zero total  $SU(2)$  colour, in particular momentum configurations associated with strings. The infra-red singularities that we find do have just this property. (We should perhaps emphasize that since all our formalism is based on  $S$  matrix elements, there is no problem with gauge invariance, and, in particular, our description of infra-red behaviour is gauge-invariant.)

The reggeon diagrams that we keep as the most infra-red singular all involve the massless  $SU(2)$  gluons only in a very particular way. They always occur as  $SU(2)$  singlet combinations attached to initial or final external particle interactions, all carrying zero transverse momentum, and having no self-interaction. The scale invariance property of the self-interactions referred to above, (which



actually produces the ultra-violet fixed-cut in the weak-coupling diagrams when there is no transverse momentum cut off<sup>7)</sup>, guarantees that they cannot cancel or enhance the infra-red divergence of the non-interacting diagrams as the transverse momenta of all gluons go uniformly to zero. We argue that this transverse momentum distribution is indeed that which would be produced by large (transverse) closed strings surrounding the (colour-zero) external particles. Also, as we discuss heuristically in Section 8, the negative charge parity and exchange degeneracy of the Regge singularity generated by the combination of gluons and a reggeon involved (which becomes our Pomeron), are just the properties that we would expect from the  $t$  channel exchange of a Wilson loop closed string propagating in transverse space. We feel confident, therefore, that we are recovering stringlike amplitudes from the infra-red singular reggeon diagrams as anticipated.

The additional properties of the singular diagrams which are important (apart from the simulation of string exchange) are, first, their independence of the cut-off region of transverse momentum in the  $SU(2)$  sector of the theory. This implies that there is no residual ultra-violet problem from the removal of the second Higgs triplet and that the asymptotic freedom of continuum  $QCD_{MB}$  can be safely used to remove the transverse momentum cut-off without introducing a fixed-cut in the angular momentum plane. Secondly, the resulting high-energy behaviour, after factorizing off the infra-red singularities, is given by an RFT formalism which simply replaces all the  $SU(2)$  particle poles in the original diagrams by two-dimensional  $\delta$  functions of transverse momentum. Consequently, there is no singularity at zero transverse momentum - we have complete confinement of  $SU(2)$  colour! Also, the leading high-energy behaviour is associated with an exchange degenerate Regge pole, the Pomeron in  $QCD_{MB}$ , which can be described as an  $SU(2)$  singlet reggeized gauge vector meson accompanied by an infinite number of non-interacting zero momentum  $SU(2)$  gluons (a closed string of  $SU(2)$  flux!) In addition to introducing the exchange degeneracy, the non-interacting gluons act like a "classical background Pomeron field" producing reggeons and Pomerons from the "vacuum" and also reabsorbing them. This produces precisely the situation in the super-critical RFT phase<sup>19)</sup>.

Thus it seems that the high-energy behaviour of  $QCD_{MB}$  is indeed that of super-critical RFT as we hoped from general arguments. We also show that the additional cancellation of infra-red divergences, which takes place as the  $SU(3)$  gauge symmetry is restored to give  $QCD_M$ , removes the vacuum production and absorption of Pomerons. Since the intercept of the exchange degenerate Pomeron also goes to one in this limit, we will have all the features of the critical Pomeron limit provided that the odd-signature trajectory (on which the  $SU(2)$

singlet gluon lies) decouples as it should [and restoration of the  $SU(3)$  symmetry implies it must], and we can identify a triple Pomeron interaction which remains finite in the limit. We shall show that quarks are essential for the triple Pomeron interaction, but the need to adequately incorporate reggeized quarks in our general formalism will prevent us from giving a complete description of the critical limit. However, the importance of quarks for the triple Pomeron interaction already hints at the connection of the chiral limit with the critical Pomeron limit. We actually outline several reasons why we believe it is the critical (and sub-critical) Pomeron which hides the parity-doublet hadron trajectories and is therefore responsible for the Nambu-Goldstone realization of chiral symmetry. The negative colour charge-parity of the Pomeron (which we have implied above is associated, at least heuristically, with an analogous property of Wilson loops) is certainly central. Unfortunately, while we believe that eventually all this part of the discussion can be made precise, this is certainly not the case at the moment. Apart from the need to incorporate quarks properly, we would like to carry out the infra-red analysis of  $QCD_{MB}$  in more detail before claiming to have proved beyond a doubt that the critical Pomeron occurs in  $QCD_M$ . We also intend to publish a better derivation of the super-critical Pomeron (from reggeon unitarity) than we have given previously, before attempting an exact comparison with  $QCD_{MB}$ . Nevertheless, we do believe that we have already derived all the essential ingredients to show that the critical Pomeron does indeed occur in  $QCD_M$ . Our confidence in the correctness of this result and an understanding of the underlying physics is enhanced once we consider the generalization of our results to higher groups and arbitrary numbers of fermions, and also their connection with the closed string structures of such theories<sup>14)</sup>. [The string picture actually shows us that the odd-signature trajectory will naturally decouple as we take the limit from  $QCD_{MB}$  into  $QCD_M$ .]

First we consider what we can say if we have less than 16 flavours in QCD. We can repeat all the arguments made for  $QCD_M$ , but keeping the transverse momentum cut off throughout. This means that we may formally define a transverse cut-off QCD which gives the critical Pomeron. However, it is straightforward to show that raising the cut-off lowers the Pomeron intercept. Consequently, the total cross-section ultimately falls asymptotically if there is less than the maximum number of fermions.

If the gauge group is larger than  $SU(3)$ , saturating the theory with fermions again enables us to break the gauge symmetry down to  $SU(2)$  and retain asymptotic freedom. Repeating the arguments made for  $QCD_{MB}$ , we obtain a similar "super-critical" phase, but with a more complicated "Pomeron" spectrum of trajectories. Thus restoring the full symmetry in higher gauge groups will produce a more

complicated critical phenomenon than the familiar "critical Pomeron". In particular, we argue that in  $SU(4)$  there will be an odd-signature Pomeron trajectory in addition to the usual even signature trajectory. In higher groups, there will presumably be increasing numbers of trajectories of both signatures, with many associated critical points as the number of fermions approaches the maximum. We emphasize, however, that all trajectories simultaneously have intercept one only when the asymptotic freedom constraint on the number of fermions in the theory is saturated, a situation far removed from the  $N \rightarrow \infty$  limit of  $SU(N)$  theories with a finite number of fermions.

The string formalism actually supports and illuminates this picture, if we assume that, to a first approximation, the  $t$  channel exchange of a Wilson loop composed of vectors gives an amplitude proportional to the total energy, with the stringlike structure appearing in the transverse space. We show that the well-known 't Hooft commutation rules<sup>14)</sup> for closed strings in a non-Abelian theory then imply that  $SU(2)$  cannot produce a pure imaginary Pomeron.  $SU(3)$  can, but cannot produce an odd-signature component.  $SU(4)$  can produce an odd-signature Pomeron trajectory and so on. From this point of view, it becomes clear that our method of calculation essentially involves breaking down the complicated closed strings of a large gauge group into  $SU(2)$  closed strings, plus whatever number of  $SU(2)$  singlet, massive, reggeized vectors is necessary to build up the complete gauge symmetry from  $SU(2)$ . The resulting critical phenomenon as the full symmetry is restored, then involves trajectories associated with all such vectors. Only in  $SU(3)$  is there just one trajectory.

A further physically attractive result emerges if we consider the  $s$  channel intermediate state structure associated with the closed string picture. We are then able to understand the association of  $SU(3)$  with the AGK cutting rules and the critical Pomeron. We show that if, in  $SU(N)$  theory, an initial Pomeron trajectory is defined from a multiperipheral approximation to events with close to the average multiplicity (the usual phenomenological Pomeron) then events with  $2, 3, \dots, N-2$  times the average multiplicity will give rise to new trajectories associated with the possible types of closed strings in the theory. The AGK cutting rules implicitly assume such a phenomenon is absent and so anticipate  $SU(3)$  closed strings.

Let us briefly comment on the relation of the above results to our previous paper<sup>27)</sup> in which we argued that an unbroken non-Abelian gauge symmetry was sufficient to produce the critical Pomeron, and that the supercritical phase occurred when the symmetry was broken to an Abelian symmetry. Clearly, two essential

elements of our present understanding were missing in that paper. That is the importance of maintaining asymptotic freedom during the restoration of the final symmetry and the importance of using Higgs scalars in the fundamental representation to avoid a phase transition. We also invoked a principle-value prescription in transverse momentum to produce artificially the kind of structures which appear directly from the infra-red singular part of the theory once the symmetry breaking is handled correctly. Therefore, we forced the right kind of mechanism to create the super-critical Pomeron to occur in a situation where it naturally does not occur when the theory is treated properly. Not surprisingly, this "unnatural" approach created almost hopeless problems of controlling all unwanted contributions, the unravelling of which led to our present (we hope) much better understanding.

Finally, we come to the lay-out of the paper. Clearly, this is a very long paper whose length, we believe, is justified by our development of a general formalism which we hope will eventually prove to be very powerful for studying a large part of hadronic QCD. Certainly, our initial target of diffraction scattering is sufficient justification in itself for the formalism. Unfortunately, almost all of our formalism is little known, especially to many people that we hope will be interested in this paper. In addition, we have to input many results from other areas of gauge theory calculations - lattice gauge theories, string formalisms, perturbative reggeization calculations, etc. Consequently, a large part of the paper is given over to the review and organization of both our previous work, and that of other authors from a coherent point of view required for the purpose of this paper. Also, in order to show how the formalism can be developed and brought to a conclusion in a finite length paper, much of the development is done in outline only. We hope nevertheless that the paper can be read in its entirety by a reader with very little previous specialized knowledge, and an appreciation of the potential power of our formalism gained. In succeeding papers we intend to give the kind of detailed development which would enable a reader to apply the formalism.

In Section 2 we review what general field theoretic properties of  $QCD_{MB}$  are known, and how we wish to interpret them and use them in our formalism. This Section also makes clear the specific problem we wish to consider before we go on to the succeeding general review Sections. In Section 3 we review the dispersion and multi-Regge theory results obtained in Ref. 3) and give what developments are needed for the rest of the paper. Section 4 reviews essentially all the needed perturbative results on reggeization, RFT in Yang-Mills theories, the ultra-violet fixed-cut of the leading-log calculations, and, finally, the analysis of infra-red singularities of RFT diagrams, with the resulting suppression of colour.

Section 5 contains the first really new formalism. We show how the multi-Regge "hexagraph" formalism described in Section 3 can be used to reproduce all the perturbative results from reggeon diagrams with non-singular reggeon interactions. We then describe how the formalism can be developed to give a complete high-energy description of all multiparticle amplitudes. In Section 6 we apply the general formalism specifically to the infra-red limit involved in defining  $\text{QCD}_{\text{MB}}$ . We show how the mass-shell singularities which necessarily accompany signature non-conserving reggeon diagrams in the multiparticle amplitudes lead naturally to a gauge-invariant string (or flux-tube) description of the states of  $\text{QCD}_{\text{MB}}$ , while at the same time developing all the vacuum production and absorption Pomeron diagrams which characterize super-critical RFT.

In Section 7 we discuss all aspects of our formalism in which quarks play a central role. This includes the control of the large transverse momentum region by asymptotic freedom as well as the triple Pomeron vertex. We discuss also the critical limit, its flux-tube interpretation and its relation to chiral symmetry breaking. Finally, in Section 8 we discuss the generalization of our results to higher groups and their connection with the Wilson loop structure, or closed string structure of such groups. We also discuss the connection of the AGK cutting rules with  $\text{SU}(3)$  gauge theory, and explain how the structure of a general gauge group would manifest itself in a conventional phenomenological analysis of diffraction scattering.

2. - QCD<sub>MB</sub> - A TOTAL SCREENING PHASE WITH ASYMPTOTIC FREEDOM

We write the Lagrangian density of the theory we call QCD<sub>MB</sub> as

$$\mathcal{L} = \mathcal{L}_G + \mathcal{L}_F + \mathcal{L}_H \quad (2.1)$$

where  $\mathcal{L}_G$  is the usual pure Yang-Mills Lagrangian for an SU(3) gauge field

$$\mathcal{L}_G = -\frac{1}{2} \text{Tr} \left\{ (\partial_\mu A_\nu - \partial_\nu A_\mu - g [A_\mu, A_\nu])^2 \right\} = -\frac{1}{2} \text{Tr} F_{\mu\nu}^2(A) \quad (2.2)$$

$\mathcal{L}_F$  is the fermionic part of the Lagrangian

$$\mathcal{L}_F = \sum_f \bar{\Psi}_f (i \not{\partial} - M_f - g \Lambda^f \not{A}) \Psi_f \quad (2.3)$$

and  $\sum_f$  is a sum over the "flavours" of the fermions [which may be in different representations of SU(3) - the  $\Lambda^f$  being the corresponding representation matrices - we shall discuss which representations, and how many, shortly.]

The Higgs part of the theory is given by

$$\mathcal{L}_H = |(\partial_\mu - ig A_\mu) \phi|^2 - \frac{1}{2} \lambda (\phi^* \phi)^2 + \mu^2 \phi^* \phi \quad (2.4)$$

where  $\phi$  is a triplet of complex scalar fields transforming under the fundamental (3) representation of SU(3).  $\phi^*$  obviously transforms under the  $\bar{3}^*$  representation.

We begin by discussing the possible asymptotic freedom of the theory. This has been investigated in the original paper of Gross and Wilczek<sup>17)</sup> and also by Cheng, Eichten and Li<sup>18)</sup>. Defining running coupling constants  $\bar{g}(t)$  and  $\bar{\lambda}(t)$  as usual, from the renormalization group equations, it is shown that :

$$\frac{d\bar{g}}{dt} = \beta_g(\bar{g}, \bar{\lambda}) \quad (2.5)$$

$$= -\frac{1}{2} b_0 \bar{g}^3 + \dots$$

(2.6)

where

$$b_0 = \frac{1}{8\pi^2} \left[ \frac{11}{3} \cdot 3 - \frac{4}{3} S_3(f) - \frac{1}{6} \right] \quad (2.7)$$

The  $\frac{1}{6}$  is due to the scalars  $\emptyset$  and  $\emptyset^*$  and  $S_3(f)$  depends on the fermion representations involved. Similarly

$$\begin{aligned} \frac{d\bar{\lambda}}{dt} &= \beta_\lambda(\bar{\lambda}, \bar{\vartheta}) \\ &= A\bar{\lambda}^2 + B'\bar{\lambda}\bar{\vartheta}^2 + C\bar{\vartheta}^4 + \dots \end{aligned} \quad (2.8)$$

where  $A = (7/8\pi^2)$ ,  $B' = -(1/\pi^2)$ ,  $C = (13/48\pi^2)$ . It is possible that  $\bar{\lambda} \rightarrow 0$  consistently in (2.8) if  $\bar{\lambda} = \alpha\bar{\vartheta}^2 + O(\bar{\vartheta}^3)$ . This gives the stability equation for  $\alpha$

$$\frac{d\alpha}{dt} = \bar{\vartheta}^2 (A\alpha^2 + B\alpha + C) \quad (2.9)$$

where  $B = B' + b_0$ . When the stability condition  $B^2 > 4AC$  is satisfied there are two fixed-points ( $\alpha_1$  and  $\alpha_2$ ) of (2.9) and the smaller is stable for  $t \rightarrow \infty$ . The stability condition is satisfied only if

$$\begin{aligned} (1 - \pi^2 b_0)^2 &> \frac{91}{96} \\ \sim \frac{5}{24} &> 8\pi^2 b_0 \end{aligned} \quad (2.10)$$

If all fermions are SU(3) triplets then

$$S_3(f) = N_f / 2 \quad (2.11)$$

where  $N_f$  is the number of flavours. Remarkably if  $N_f = 16$  then

$$8\pi^2 b_0 = \frac{1}{6} < \frac{5}{24} \quad (2.12)$$

whereas if  $N_f = 15$  then

$$8\pi^2 b_0 = \frac{5}{6} > \frac{5}{24} \quad (2.13)$$

and, of course, if  $N_f = 17$ ,  $b_0 < 0$  and even the gauge-coupling  $g$  is not asymptotically free. Therefore if the number of flavours just saturates the asymptotic freedom constraint on the gauge coupling the Higgs coupling  $\lambda$  can also be asymptotically free. By the end of the paper we will have attached great physical significance to this simple fact.

An important point for the following discussion is that, from the above, the Higgs coupling  $\bar{\lambda}$  must lie within a range of values proportional to  $\bar{g}^2$  as  $t$  approaches infinity. That is

$$\alpha_1 \bar{g}^2 < \bar{\lambda} < \alpha_2 \bar{g}^2 \quad t \rightarrow \infty \quad (2.14)$$

Therefore our choice of initial values for  $\lambda$  and  $g$  at some specified  $t_0$  must place us on a trajectory in the  $(\bar{\lambda}, \bar{g})$  plane which approaches the origin as  $t \rightarrow \infty$  as illustrated in Fig. 2.1. We shall return to this point shortly.

To complete our description of the asymptotic freedom constraints we quote further from Ref. 18). Firstly if we add another representation of Higgs scalars then asymptotic freedom is impossible without enlarging the gauge group. Secondly the only possible modifications of the fermion representation content, given the experimental observation of five flavours of triplets, are that we could have six flavours of triplets and two sextets, or eleven triplets and one sextet, or ten triplets and one adjoint.

We now begin a discussion which will eventually enable us to consider the possibility of taking a smooth limit from  $\text{QCD}_{\text{MB}}$  into  $\text{QCD}_M$ . To this end we first discuss the recent lattice gauge theory results of Fradkin and Shenker<sup>15)</sup> and Banks and Rabinovici<sup>16)</sup>. This will also enable us to discuss further breaking the symmetry of  $\text{QCD}_{\text{MB}}$  while keeping the transverse momentum cut-off.

Consider now the Lagrangian  $\mathcal{L}' = \mathcal{L}_G + \mathcal{L}_H$  where  $\mathcal{L}_H$  contains two (complex) triplets of Higgs scalars  $\phi_1$  and  $\phi_2$ . Making the non-unique decomposition (which is only possible strictly in the "Higgs régime" of parameter space - see below)

$$\phi_1(x) = \Omega(x) \begin{pmatrix} 0 \\ 0 \\ \rho_1(x) \end{pmatrix} \quad \phi_2(x) = \Omega(x) \begin{pmatrix} 0 \\ \rho_4(x) \\ \rho_2(x) + i\rho_3(x) \end{pmatrix} \quad (2.15)$$



where  $\Omega(x)$  is an SU(3) matrix and  $\rho_1 \dots \rho_4$  are real we can define

$$B_\mu = \Omega^\dagger \left( \frac{1}{g} \partial_\mu - A_\mu \right) \Omega \quad (2.16)$$

and write

$$\begin{aligned} \mathcal{L}' = & -\frac{1}{2} \text{Tr} F_{\mu\nu}^2(B) + \sum_i (\partial_\mu \rho_i)^2 + (\rho_1^2 + \rho_2^2 + \rho_3^2) g^2 [B_\mu^\dagger B_\mu]_{33} \\ & + \rho_4^2 g^2 [B_\mu^\dagger B_\mu]_{22} + g^2 \rho_4 (\rho_2 + i\rho_3) [B_\mu^\dagger B_\mu]_{23} + g^2 \rho_4 (\rho_2 - i\rho_3) [B_\mu^\dagger B_\mu]_{32} - V(\rho) \end{aligned} \quad (2.17)$$

where  $V(\rho)$  is the (gauge-invariant) potential for  $\phi_1$  and  $\phi_2$ .

The  $B_\mu$  and  $\rho_i$  are gauge-invariant local operators which are equal to the usual "physical" operators in the unitary gauge [which is defined by  $\Omega(x) = 1$ ]. When  $V(\rho)$  has a non-trivial minimum and the  $\rho_i$  acquire large expectation values we would conventionally say we are in the "Higgs phase" of the theory with the physical states defined perturbatively by the  $B_\mu$  (which all become massive) and the  $\rho_i$ . That is there will be eight massive vector mesons and four massive scalars.

Alternatively if the minimum of  $V(\rho)$  is at the origin and the gauge symmetry is "unbroken" we expect to be in the "confinement phase". In this phase we expect the most important "bare" states to be created by the "string operators"

$$\phi_i^*(x_1) P \exp \left[ -g \int_{x_1}^{x_2} dx_\mu A_\mu \right] \phi_j(x_2) \quad i, j = 1, 2 \quad (2.18)$$

where as usual  $P$  denotes path-ordering along some path joining  $x_1$  and  $x_2$ . The results of Refs. 15), 16) imply that on a lattice the states created by the operators of the form (2.18) and the local operators (2.16) are in fact analytically connected as the parameters of the potential are varied from the Higgs to the confinement region. There is no phase transition !

Heuristically we can understand that as the  $\phi$ 's acquire expectation values it is straightforward for a line integral of the form of (2.18) to "break-up" into a product of the  $B_\mu$  operators. Writing the line-integral formally as

$$\prod_i \left( \frac{\delta}{\delta x_i} - g A(x_i) \right) \delta x_i$$

$$= \dots \left( \frac{\delta}{\delta x_{i-1}} - g A(x_{i-1}) \right) \delta x_{i-1} \left( \frac{\delta}{\delta x_i} - g A(x_i) \right) \delta x_i \left( \frac{\delta}{\delta x_{i+1}} - g A(x_{i+1}) \right) \delta x_{i+1} \dots \quad (2.19)$$

$$\approx \dots \Omega(x_{i-2}) \Omega^+(x_{i-1}) \left( \frac{\delta}{\delta x_i} - g A(x_i) \right) \delta x_i \Omega(x_{i+1}) \Omega^+(x_{i+2}) \times$$

$$\times \left( \frac{\delta}{\delta x_i} - g A(x_i) \right) \delta x_i \Omega(x_i) \Omega^+(x_{i+1}) \left( \frac{\delta}{\delta x_{i+1}} - g A(x_{i+1}) \right) \delta x_{i+1} \dots \quad (2.20)$$

$$= \prod_i g B(x_i) \delta x_i \quad (2.21)$$

where the approximate equality follows from

$$\Omega(x_i) \Omega^+(x_{i+1}) \approx 1 \quad (2.22)$$

it is clear that a string state may be approximately described as a (bare) multi-particle state created by the gauge invariant local operators B. In fact in the case we are considering - two triplets of Higgs - there is essentially a 1-1 correspondence between the local vector operators (2.16) and the string-operators (2.18). Given  $x_1$  and  $x_2$  we have the eight orientated operators of the kind (2.18) shown in Fig. 2.2 (the arrow is directed from the point where the  $\phi^+$  field is).

By analogy with the dual string model we anticipate that the open string operators (2.18) will create states, all of which lie on Regge trajectories. Since (as we shall discuss further in Section 4) all the elementary vectors B reggeize in perturbation theory in the Higgs phase, we anticipate also that (provided we stay on a lattice or equivalently keeps a cut-off in the transverse momentum) the perturbative Regge trajectories go smoothly into those associated with the string operators as the confinement régime of parameter space is approached.

A vital point for the above discussion is clearly that the Higgs fields  $\phi_i$  must be in the fundamental representation of the gauge group to enable us to define the gauge invariant local operators (2.16). This also allows such operators to be defined for the fermions of the theory, e.g., for triplet fermions

$$\chi(x) = \Omega^+(x) \psi(x) \tag{2.23}$$

If the scalars are not in the fundamental representation then gauge-invariant local operators cannot be written for all the perturbative states of the "Higgs phase" and in general we have a transition from a magnetic confinement phase to an electric confinement phase as the parameters of the theory are varied. Banks and Rabinovici<sup>16)</sup> refer to the Higgs-confinement phase of a theory with fundamental scalars as a "total-screening phase". Note, however, that a difficulty is expected if we insist on the fermions being massless. Banks and Rabinovici<sup>16)</sup> anticipate that in this case there will in general be a phase-transition in which chiral symmetry is spontaneously broken. This will be important for our tentative discussion of chiral symmetry breaking in Section 7.

The next point we consider is whether the above results may extend to the continuum and in particular whether it is possible to take a limit into pure confining QCD. The most general form of the invariant potential  $V(\rho)$  in (2.17) is given by Cheng, Eichten and Li<sup>18)</sup> and involves five scalar couplings, which we refer to (loosely) in vector notation as  $\underline{\lambda}$ . There are also two mass terms for the two representations with masses which we refer to (again loosely) as  $\underline{\mu}$ . The limit  $L$  which in perturbation theory formally gives a pure gauge theory from a Higgs régime of parameter space always has the general form (all of our limits in the following will implicitly be of this form)

$$L: \quad \underline{\mu}^2 \rightarrow -\infty, \quad \frac{\underline{\lambda}}{\underline{\mu}^2} \rightarrow -\infty, \quad \frac{\underline{\lambda}}{\underline{\mu}^4} \rightarrow 0 \tag{2.24}$$

since this allows expectation values of the form  $\langle \rho \rangle \sim \mu^2/\lambda$  to go to zero simultaneously with the mass of the scalars becoming infinite sufficiently fast. That is since, for fixed external momenta, diagrams involving scalars are  $O(\lambda/\mu^4)^n$ , for some power  $n$ , the last condition in (2.24) ensures that all scalar diagrams go to zero in the perturbation expansion. The question is whether this limit which is clearly delicate even in its definition has any chance to succeed outside of perturbation theory ?

Since we necessarily have  $\underline{\lambda} \rightarrow \infty$  we can make direct contact with the explicit lattice models of Fradkin and Shenker<sup>15)</sup>. These models are always defined with the limit  $\underline{\lambda} \rightarrow \infty$  already taken. In a continuum theory this limit would give<sup>28)</sup> a

non-renormalizable massive Yang-Mills theory in the Higgs régime and so would be extremely dangerous. On the lattice it gives no problem. The resulting theories are then functions of  $g^2$  the gauge coupling constant and  $\rho \sim \mu^2/\lambda$ . The resulting phase diagram for a non-Abelian gauge symmetry where the Higgs scalars are in the fundamental representation is anticipated to have the general form shown in Fig. 2.3. From this diagram it is clear that the limit  $L$  that we need will give us a pure gauge theory as long as we stay on a lattice. [When the scalars are not in the fundamental representation the line  $AB$  becomes the Higgs confinement phase-transition and extends right across the diagram. There is then no chance to reach the confinement régime smoothly from the Higgs régime.] However, to define a continuum theory we must take the continuum limit<sup>29)</sup> by approaching a second-order critical point. That is either  $B$  or  $C$  in Fig. 2.3.

To define a Higgs régime continuum theory the best hope (although not proved to succeed because of the ultra-violet problems with a renormalizable non-asymptotically free theory) would be to approach  $B$  from the large  $\langle\rho\rangle$  direction with  $\lambda$  kept finite until  $B$  is reached (to avoid the non-renormalizable Yang-Mills theory). To define a confining theory including scalars we should approach  $B$  from the small  $\langle\rho\rangle$  direction. To define the pure gauge theory we should approach  $C$ . From this qualitative discussion it is clear that while the range of theories defined by approaching  $B$  from below may have a limit into that defined at  $C$  there is little hope that this is the case for a Higgs theory defined by approaching  $B$  from above. This argument applies as long as we are forced to define the continuum Higgs theory from the critical point which is at  $\lambda = \infty$  in terms of the bare parameters of the original Lagrangian  $\mathcal{L}'$ . The only possibility to avoid it is if there is a fixed-point at  $\lambda = 0$  which can define a continuum theory, or in other words if the theory is asymptotically free in  $\lambda$  as well as in  $g$ .

As we have already discussed for this we must remove one triplet of scalars, add 16 flavours of fermions and so arrive at  $\text{QCD}_{\text{MB}}$ . We can then consider the possibility of taking a limit of the form  $L$  from  $\text{QCD}_{\text{MB}}$  into  $\text{QCD}_{\text{M}}$ . Let us first consider whether the states formed by the relevant local and non-local operators can connect smoothly as previously. For this purpose we again initially ignore the fermions and consider  $\mathcal{L}' = \mathcal{L}_{\text{G}} + \mathcal{L}_{\text{H}}$  where now  $\mathcal{L}_{\text{H}}$  is given by (2.4). In (2.15)-(2.17) we set  $\rho_1 = \rho$ ,  $\rho_2 = \rho_3 = \rho_4 = 0$  and take

$$V(\rho) = \frac{1}{2} \lambda \rho^4 - \mu^2 \rho^2 \tag{2.25}$$

The "Higgs régime" is now  $\mu^2 \rightarrow +\infty$ , so that

$$\langle \rho \rangle^2 = \frac{\mu^2}{\lambda} \rightarrow \infty \quad (2.26)$$

If we take  $\Omega$  to be unity so that  $B$  is Hermitian we can write

$$B_\mu^i(x) = b_\mu^i(x) \lambda_i \quad i = 1, \dots, 8 \quad (2.27)$$

where the  $\lambda_i$  are the usual Hermitian  $SU(3)$  matrices, then since

$$[\lambda_i, \lambda_i]_{33} = 0 \quad i = 1, 2, 3 \quad (2.28)$$

$$= 1 \quad i = 4, \dots, 7 \quad (2.29)$$

$$= \frac{4}{3} \quad i = 8 \quad (2.30)$$

perturbation theory in the Higgs régime gives three massless vectors, four with a  $\text{mass}^2 = g^2 \langle \rho \rangle^2$  while a fifth acquires a  $\text{mass}^2 = \frac{4}{3} g^2 \langle \rho \rangle^2$ . However, although the operators  $B^i$  defined by (2.16) are gauge invariant with respect to the original  $SU(3)$  transformations on  $A$  (since such a transformation simply redefines  $\Omega$  by left multiplication of the corresponding gauge transformation) there is a new  $SU(2)$  gauge invariance when  $\theta_2 = 0$ . Equation (2.15) leaves  $\Omega(x)$  undefined up to right multiplication by an  $SU(2)$  matrix in the plane orthogonal to  $\rho$ . This arbitrariness means that the theory defined by  $\mathcal{L}'$  now has an  $SU(2)$  local gauge invariance.  $B^1, B^2, B^3$  are the gauge fields corresponding to this invariance and  $B^4, \dots, B^7$  form two (massive) vector doublets  $B^{\underline{1}}, B^{\underline{2}}$  under these transformations.  $B^8$  is a singlet.

The perturbative states will not now be the true states even in the "Higgs régime" but rather we expect that there will be confinement of the  $SU(2)$  symmetry. We anticipate therefore that the appropriate operators for discussing the states of the theory will be open  $SU(2)$  strings with the doublets  $B^{\underline{1}}$  and  $B^{\underline{2}}$  at the end, that is

$$B^i(x_1) \text{P exp} \left[ -g \int_{x_1}^{x_2} dx_\mu B_\mu \right] B^j(x_2) \quad i, j = 1, 2 \quad (2.31)$$

$B_\mu \in B^{\underline{1}}, B^{\underline{2}}, B^{\underline{3}}$

together with the singlet local operators

$$B_{\mu}^8(x), \rho(x) \quad (2.32)$$

If the Higgs régime is again smoothly connected to the confinement régime of parameter space (staying on a lattice for the moment) and there is no phase-transition then the operators (2.28) and (2.29) must create states which can analytically connect with those created by the operators of the "unbroken" theory defined by  $\langle \rho \rangle^2 \sim 0$  in (2.26). These are again oriented open strings of the form (2.18) with the Higgs triplet operator  $\emptyset$  at one end and  $\emptyset^*$  at the other end.

The process by which the operators (2.31) and (2.32) create the oriented strings of the unbroken theory is a bit more difficult to describe than the corresponding process when two triplets of Higgs are simultaneously involved. The essential point is again that we must contract the  $\Omega$ 's out of operators using the unitarity relation

$$\Omega^+ \Omega = 1 \quad (2.33)$$

leaving operators defined only in terms of the  $A$  fields. [This is the reverse of the process described by (2.19)-(2.20).] Now, however, we must combine the strings (2.31) and the local operators (2.32) in a complicated fashion, which is best described pictorially.

In Fig. 2.4 we have illustrated the integral (2.31) (on a lattice) by representing the fields  $B^1, B^2, B^3$  by circles and the massive vector fields  $B^i$  by short lines. The  $SU(2)$  singlet field  $B^8$  is represented by a star. If we add operators as indicated in Fig. 2.5 (considering the same lattice line throughout) then the unitarity of the  $\Omega$  matrices allows them to be removed on either side of the lattice point where  $B^8$  is located. The result is the introduction of the  $A$  field at one lattice point. This process has to be repeated over and over to convert a complete non-oriented  $SU(2)$  string to an oriented  $SU(3)$  string. Note that since

$$B_8 = \Omega_{3j}^+ \left( \frac{1}{3} \partial_{\mu} - A_{\mu} \right)_{jk} \Omega_{k3} \quad (2.34)$$

we must, in the above process, choose whether to combine  $\Omega_{3j}^+$  or  $\Omega_{k3}$  with the relevant  $\Omega$  or  $\Omega^+$  components on one neighbouring lattice point. This choice introduces a (local)  $SU(3)$  orientation of the string. Thus we can think of the

SU(3) orientation appearing pointwise as the SU(2) local singlet operator is added to the existing SU(2) string by the process of Fig. 2.5.

We have now argued that the SU(2) operators (2.31) and (2.32) can indeed create the same states as the SU(3) operators (2.18) and so we claim that on a lattice the results of Refs. 15), 16) apply and that there is no phase-transition in  $\text{QCD}_{\text{MB}}$ . We would like to combine this argument with the asymptotic freedom of the theory, as discussed earlier, and assume that  $\text{QCD}_{\text{MB}}$  can be defined as a continuum theory which in the limit  $L$  of (2.24) goes smoothly into continuum  $\text{QCD}_M$ . Although the argument against this that we discussed when the theory is defined through a phase-diagram of the form shown in Fig. 2.3, no longer applies, further discussion of this assumption is necessary.

Since we expect the gauge-coupling  $g^2$  to grow faster than the Higgs coupling  $\lambda$  in the infra-red region it is reasonable that the trajectory shown in Fig. 2.1 should approach or become parallel to the  $\bar{\lambda} = \infty$  line as  $t \rightarrow -\infty$ . Also the behaviour of perturbation theory when the limit  $L$  is taken at finite momenta indicates that there should be a sequence of trajectories at  $t$  finite approaching the  $\bar{\lambda} = \infty$  axis as illustrated in Fig. 2.6. The assumption we wish to make is really that this sequence of trajectories all drop down as  $t \rightarrow +\infty$  to satisfy the asymptotic freedom constraint. We can then argue that  $\text{QCD}_M$  can be reached as a limit through the sequence of trajectories shown in Fig. 2.6.

We finally consider how the mass of the singlet vector  $B_8^8$  must behave in the limit we require. This will be central for our discussion of the behaviour of closed strings, and more specifically the Pomeron, in  $\text{QCD}_{\text{MB}}$ . On the vertical part of the limiting trajectory in Fig. 2.6, we must have  $\bar{\lambda}$  finite while  $\mu^2 \rightarrow \infty$ . Consequently  $\langle \rho \rangle \rightarrow \infty$  and since  $\bar{g} \sim 0$  we have a purely perturbative situation in which  $M_{B_8^8}^2 \rightarrow \infty$ . This clearly is consistent with the departure of this part of the theory to  $t = +\infty$  in the limit we consider. For  $\bar{g} \sim 0$ ,  $\lambda \sim \infty$  we still have an essentially perturbative situation with now  $\langle \rho \rangle \rightarrow 0$  and so  $M_{B_8^8}^2 \rightarrow 0$ . Since  $B_8^8$  must disappear from the physical spectrum to restore the SU(3) symmetry we anticipate that either  $M_{B_8^8}^2 \rightarrow 0$  or  $M_{B_8^8}^2 \rightarrow \infty$  as  $t \rightarrow -\infty$  where the physical mass is defined. Since asymptotic freedom implies  $M_{B_8^8}^2$  must be exponentially small for finite  $t$  it seems very plausible that the symmetry can only be completely restored if indeed  $M_{B_8^8}^2 \rightarrow 0$  also for  $t \rightarrow -\infty$ , and this is what we shall take to be the case. It will be very important that in this case a description of the decoupling of this vector is naturally provided by supercritical RFT.

We believe it is also significant that the decoupling of the  $B^8$  vector has a natural description in a string picture. This is because as the confinement régime is approached the vector lies on a Regge trajectory associated with a closed string [rather than the open strings (2.18)]. To see this, note that process illustrated by Fig. 2.5 can be applied to closed  $SU(2)$  strings to show that  $B^8$  provides the necessary degree of freedom for the orientation of  $SU(3)$  closed strings. However, until the  $SU(3)$  symmetry limit is reached such strings can be thought of as essentially non-orientated but with local sections having an orientation dependence [cf. our remarks after (2.34)]. We anticipate that such strings will have signature properties similar to open strings and so have exchange degenerate Regge trajectories with the vector  $B^8$ , in particular, lying on the odd-signature partner of an exchange-degenerate pair of trajectories. As the symmetric limit is reached and the closed strings become pure  $SU(3)$ , they will also become purely even signature with the odd-signature trajectories, in particular that on which  $B^8$  lies, necessarily decoupling. We hope that this argument will be seen to acquire greater depth in succeeding sections.



### 3. - DISPERSION RELATIONS AND MULTI-REGGE THEORY

In the remainder of the paper we shall need to make extensive use of the multi-Regge theory developed in Ref. 3), applying it in particular to the high-energy behaviour of theories with reggeized vectors. This formalism is not generally well known and consequently it is not always appreciated that the use of Reggeon field theory<sup>30)</sup> to describe high-energy behaviour can be based directly on unitarity together with some global analyticity properties which can almost certainly be traced back to the assumptions of axiomatic field theory. However, it seems to us that to derive the high-energy behaviour of as difficult a theory as QCD, it is absolutely essential to make the maximum use of these powerful general results. We shall try, therefore, to summarize the results here as briefly as possible. We shall present and also develop them in a form which is most economical for the purpose of this paper.

The starting point for the formalism is the results on multiple discontinuity formulae for multiparticle amplitudes derived by Stapp and co-workers in S matrix theory<sup>23)</sup>. These results show that many (unphysical) boundary values onto the real axis of the analytically continued multiparticle S matrix have analyticity properties analogous to the physical S matrix. Remarkably these are the only boundary values involved in multi-Regge asymptotic limits (physical or unphysical). As a consequence multiple dispersion relations (which are generalized fixed-momentum transfer dispersion relations) can be shown to be valid asymptotically (that is up to non-leading powers of the asymptotic variables) which involve only multiple normal threshold discontinuities<sup>3),23)</sup>. There are no contributions from complex Landau singularities. The global analyticity needed to write the dispersion relations cannot be derived from S matrix theory (except as a maximal analyticity assumption !) but can very likely (certainly in the simplest cases) be shown to follow from the primitive analyticity domains<sup>24)</sup> of axiomatic field theory when the external masses are spacelike. This, together with an S matrix unitarity analysis showing the absence of complex singularities near the real axis, is essentially sufficient to derive the necessary mass-shell results.

Each dispersion relation is associated with a particular tree diagram for a multiparticle amplitude. The tree diagram contains only three-point vertices and is a purely kinematic concept to describe a set of (Toller) variables for an amplitude<sup>31),32)</sup>. We call it a Toller diagram. First momentum conservation at each vertex is used to allow four-momentum to flow through the diagram. Next a

set of standard (Lorentz) frames is defined at each vertex in which the momenta entering the vertex take a standard form. Frames at adjacent vertices joined by an internal line  $i$  can be related by a Lorentz transformation  $g_i$  in the little group of the four-momentum  $Q_i$  flowing along the line  $i$ . In this way we can write for a general  $N$  point amplitude (which should be a helicity amplitude if the external particles have spin)

$$M_N(p_1, \dots, p_N) \equiv M(m_1^2, \dots, m_N^2, Q_1^2, \dots, Q_{N-3}^2, g_1, \dots, g_{N-3}) \quad (3.1)$$

This is illustrated in Fig. 3.1. Taking all the  $Q_i^2$  spacelike the  $g_i$ 's can be taken to be elements of  $SO(2,1)$  and parametrized as

$$g_i = u(v_i) a(\beta_i) u(v_i') \quad (3.2)$$

where the  $u$ 's are rotations and the  $a$ 's are boosts. Writing  $z_i = \cosh \beta_i$  the conventional multi-Regge limit is  $z_i \rightarrow \infty$ ,  $v_i, v_i', Q_i^2$  fixed  $\forall_i$ . Correspondingly the dispersion relation is written regarding  $M_N$  as a function of the  $z_i$  with the  $v_i, v_i', Q_i^2$  kept fixed.

Some description of the full dispersion relation representation of  $M_N$  is given in Ref. 23) and we hope eventually to give a complete description in a future publication. Fortunately, however, we shall not need the exact form of the dispersion relation for the purposes of this paper, but instead we shall need only the general structure which we describe in the following. The dispersion relation enables us to write

$$M_N = \sum_S M_{NS} \quad (+ \text{subtraction terms}) \quad (3.3)$$

where each  $M_{NS}$  is a dispersion integral of a spectral function  $\rho_{NS}$ . Each  $\rho_{NS}$  could be taken to be an  $(N-3)$ -fold normal threshold multiple discontinuity consistent with the (generalized) Steinmann relations<sup>23)</sup>. However, for technical reasons that we shall elaborate to some extent later, it is better to initially group together certain multiple discontinuities into one spectral function. We can then develop a diagrammatic formalism for counting and describing the analytic and Regge properties of the  $M_{NS}$  contributing to each dispersion relation. We shall do this by means of two kinds of graphs. Hexagraphs, which are tree-like diagrams which will describe the angular-momentum or Regge-type properties of

each  $M_{NS}$  and flow-graphs, which resemble particular Landau graphs and will be used to describe analytic properties. To construct all the hexagrapghs and flow-graphs for a particular dispersion relation associated with a particular Toller diagram we proceed as follows (the construction is illustrated in Figs 3.2 - 3.6).

Given one Toller diagram we first associate with it a set of  $2^{N-3}$  "planar Toller diagrams", each one of which describes a particular scattering process in which  $Q_i^2 < 0 \forall_i$ . The planar diagram is obtained by projecting the original Toller diagram onto the plane of a page with the chosen incoming particles entering the diagram from the bottom direction of the page and the chosen outgoing particles exiting towards the top. We then distinguish an i vertex where two external particles enter and leave the tree diagram (connecting with an internal line  $i$ ), an i-j vertex where one external particle enters or leaves and an i-j-k vertex which is an internal vertex, where lines  $i, j$  and  $k$  meet.

A single Toller planar diagram generates a set of hexagrapghs in which all vertices are drawn with  $120^\circ$  angles. An  $i$  vertex is simply drawn with the  $i$  line horizontal. An  $i-j$  vertex generates two vertices (each of which appears in a distinct hexagrapgh) in one of which the  $i$  line is horizontal and one of which the  $j$  line is horizontal. Finally an  $i-j-k$  vertex generates three vertices in distinct hexagrapghs in which the  $i, j$  and  $k$  lines are respectively horizontal. In this way one planar Toller diagram gives rise to

$$2^{n_{ij}} \cdot 3^{n_{ijk}}$$

hexagrapghs, where  $n_{ij}(n_{ijk})$  is the number of  $ij$ -( $ijk$ -) vertices.

The set of hexagrapghs is already in (1-1) correspondence with the spectral components  $M_{NS}$ . However, an essential feature of the  $M_{NS}$  is that they have only certain normal threshold branch cuts and this is described by the flow-graphs which are constructed from the hexagrapghs as follows. Each vertex of the hexagrapgh is replaced by a structure which we call a "polygraph" and which is illustrated in Fig. 3.5. [For our purposes it will be more convenient to represent an  $i-j-k$  vertex by the planar polygraph shown, and not the non-planar polygraph of Ref. 3).] If the horizontal lines of the hexagrapgh are now contracted and the remaining adjacent sides of the polygraphs are sewn together a unique flow-graph results as shown in Fig. 3.6.

The flow-graph represents the analytic structure of an  $M_{NS}$  in that the  $M_{NS}$  has normal threshold cuts in all those invariant variables in which the flow-graph regarded as a Feynman graph would have cuts. The set of such cuts can be shown to be the complete set of asymptotic cuts. Each  $M_{NS}$  can therefore be defined as a dispersion integral of the sum of all  $(N-3)$  fold multiple normal threshold discontinuities which correspond to a set of  $(N-3)$  distinct cuts through the flow-graph. (With the qualification that there will be no contribution from a set of cuts which are not asymptotically equivalent to a set of cuts allowed by the generalized Steinmann relations.) The possible cuts associated with some simple flow-graphs are illustrated in Fig. 3.7 (as well as a set of cuts that does not contribute).

In summary then the dispersion relations provide the enormous simplification of analytic structure that (asymptotically) an  $N$  point amplitude can be written as a sum of terms  $(\sim(3 \times 2)^N)$  each of which has much simpler analyticity properties than the complete  $M_N$ . In fact it is possible to show within the axiomatic field theory framework<sup>24)</sup> of Bros, Epstein and Glaser that the decomposition (3.3) is closely related to the decomposition of a complete Green's function into a sum of generalized retarded functions. [Actually we believe there are potentially very many beautiful results that could be derived basing the "asymptotic dispersion" relations, that we utilize here, directly on the axiomatic field theory formalism. The Toller variables described above appear to be ideally suited to describe the primitive analyticity domains of field theory and the boundary values needed for the dispersion relations are just those reachable from the "cells" of the axiomatic formalism and hence describable by the generalized retarded functions. In the distant future it may be that a complete (even rigorous !) formalism can be derived this way. Unfortunately our present priorities demand that we do not dwell on this subject here, it is certainly a long way from the purpose of this paper.]

For us the point of the decomposition (3.3) is that each  $M_{NS}$  has a generalized Sommerfeld-Watson (SW) representation giving its Regge asymptotic behaviour. Fortunately this can be constructed knowing only which normal threshold cuts are present in each  $M_{NS}$ , since this enables us to construct generalized Froissart-Gribov (FG) continuations of the relevant partial wave amplitudes into complex angular momentum and helicity planes. This is why, as we noted earlier, we can bypass the precise form of the dispersion relation. The construction of FG amplitudes is described in detail in Ref. 3) and here we simply quote the result.

For each  $M_{NS}$  we can introduce, via its hexagraph, an analytically continued partial wave amplitude  $a_H$  as follows. The hexagraph consists of internal horizontal and sloping lines and it will be useful to distinguish three kinds of horizontal lines.

- a T line joins directly two vertices
- a D line joins directly one vertex to one sloping line
- a V line joins directly two sloping lines.

The kinds of line are illustrated in Fig. 3.8 and the notation is explained in Ref. 3). We next use the fact that some of the combinations of  $v_i$  and  $v_i'$  variables of (3.2) are redundant to associate each line of the hexagraph with a group variable. Each horizontal line  $i$  we associate with the corresponding  $z_i$ . Each sloping line  $j$  is attached to a vertex at which a horizontal line  $i$  enters and we associate with it  $u_{ij} = e^{i(v_i - v_j)}$  where  $v_i$  and  $v_j$  enter in  $g_i$  and  $g_j$  as given by (3.2). The  $z_i$  and  $u_{ij}$  (together with the  $Q_i^2 = t_i$ ) constitute a complete set of group variables for describing amplitudes and the group theoretic partial wave analysis<sup>3)</sup> of  $M_{NS}$  is essentially a Fourier analysis with respect to  $u_{ij}$  and a Legendre (or Jacobi) polynomial projection with respect to  $z_i$ . Thus an angular momentum  $\ell_i$  is associated with each horizontal line of the hexagraph and a helicity  $n_{ij}$  with each sloping line. An FG continuation to complex  $\ell_i$  and  $n_{ij}$  can be made with the constraint that for each D-line the angular momentum is kept differing by an integer from the helicity of the sloping line to which it is attached, and for each V line the angular momentum differs only by an integer from each of the helicities of the lines to which it is attached, which also therefore differ only by an integer.

The rules for writing a complete SW representation of each  $M_{NS}$  are given in Ref. 3). The representations are made particularly cumbersome by all the sums over integer differences of angular momenta and helicities that are involved. Since we shall ultimately only be interested in Regge pole contributions to many particle amplitudes in phase space regions of unitarity integrals where Regge cuts are generated, we can in fact consider the following simplified kinematic situation which will also simplify the SW representations.

We consider the  $M_{NS}$  in a generalized "helicity pole" limit which is defined differently for each  $M_{NS}$  and is defined from its hexagraph. Each  $z_i$  associated with a T line is taken large and all the  $u_{ij}$  are taken large but with the ratio of  $u$ 's associated with sloping lines attached to the same V line kept fixed. We can then define generalized rapidity variables which absorb all the kinematic singularities in the asymptotic relation between the invariant variables and the group variables and give us simple expressions for those invariants corresponding to cuts of the flow-graph representing the particular  $M_{NS}$ .

For each T line we simply define

$$\exp [\psi_i] \sim z_i \quad (3.4)$$

for each D line (j) whose attached sloping line connects to a vertex at which a T line (i) enters we define (see Fig. 3.8 for notation)

$$\exp [\psi_j] \sim (z_j^2 - 1)^{\frac{1}{2}} u_{ij} \quad (3.5)$$

for each D line (j) whose attached sloping line connects to a vertex at which a D line (i) enters we define

$$\exp [\psi_j] \sim \left[ \frac{z_i + 1}{z_i - 1} \right]^{\frac{1}{2}} (z_j^2 - 1)^{\frac{1}{2}} u_{ij} \quad (3.6)$$

for each V line (k) whose two attached sloping lines are connected to vertices where T lines (i and j) enter we define (again see Fig. 3.8)

$$\exp [\psi_k] \sim u_{ik} (z_k + 1) u_{kj} \quad (3.7)$$

for each V line (k) with one attached sloping line attached to a vertex where a D line (j) enters we define

$$\exp [\psi_k] \sim u_{ik} (z_k + 1) u_{kj} \left[ \frac{z_j + 1}{z_j - 1} \right]^{\frac{1}{2}} \quad (3.8)$$

and finally for each V line (k) with attached sloping lines connected to vertices with D lines (i and j) entering we define

$$\exp [\psi_k] \sim \left[ \frac{z_i + 1}{z_i - 1} \right]^{\frac{1}{2}} u_{ik} (z_k + 1) u_{kj} \left[ \frac{z_j + 1}{z_j - 1} \right]^{\frac{1}{2}} \quad (3.9)$$

The (flow-graph) cuts of an  $M_{NS}$  are all in invariant variables asymptotically (in the helicity pole limit) equivalent to invariants of the form

$$S_{mn} = (R_m + R_n)^2 \quad (3.10)$$

where each of  $R_m$  and  $R_n$  may be either external momenta  $P_1, P_2, \dots$  or the internal momenta  $Q_1, Q_2, \dots$ .  $R_m$  and  $R_n$  can therefore be associated with lines of the Toller diagram and there is a unique path through the tree diagram connecting them - passing along lines  $i_1, i_2 \dots i_\nu$  for example. The asymptotic expression for  $S_{mn}$  is then

$$S_{mn} \sim \exp [y_{i_1} + y_{i_2} + \dots + y_{i_\nu}] \quad (3.11)$$

where the constant of proportionality is a function of the  $Q_i^2$  and the masses only. Note that (3.11) only holds for invariants corresponding to cuts through the flow-graph.

In its helicity pole limit each  $M_{NS}$  becomes independent of the angular variables kept finite (the  $z_j$  and the  $u_{ik}/u_{ij}$ ) and becomes a function of the rapidity variables only, which could actually be defined directly by (3.11). The independence of the finite angular variables follows from the fact that the leading term in the SW representation is that in which all integer differences of angular momenta and helicities are set to zero. Having absorbed all kinematic singularities by (3.5)-(3.10), the SW representation can then be written in terms of the rapidity variables only.

To write the SW representation we first conform with the usual RFT notation by introducing energy variables  $E_i$  for each horizontal line of the hexagraph as follows

$$\begin{aligned} \text{for each T line we write} \quad E_i &= 1 - l_i \\ \text{for each D line we write} \quad E_j &= 1 - l_j = 1 - m_{ij} \\ \text{for each V line we write} \quad E_k &= 1 - l_k = 1 - n_{ik} = 1 - n_{jk} \end{aligned} \quad (3.12)$$

To include signature properties in the SW representation we add together all  $M_{NS}$  whose hexagraphs differ only by a twist of one part of the graph relative to the other part about some horizontal line. We can then write (in the helicity pole limit only)

$$\sum M_{NS}(\underline{y}, \underline{E}) = \sum_{\underline{\tau}} \left( \prod_i dE_i e^{-E_i y_i} a_H^{\underline{\tau}}(\underline{E}, \underline{E}) T_H^{\underline{\tau}}(\underline{E}) \right) \quad (3.13)$$

where  $\underline{\tau}$  denotes a signature label ( $\tau_i = \pm 1$ ) for each horizontal line of the hexagraph, and  $T_H^{\underline{\tau}}(\underline{E})$  is a generalized signature factor, which plays a central role in the following and can in principle be read off from the hexagraph by rules which we now describe.

To give a complete discussion of signature factors we should take into account the complication that distinct partial wave continuations are defined for each possible ordering in which the helicities of a hexagraph can be taken complex<sup>3)</sup>. This complication is directly related to the signature properties of multiparticle amplitudes which form the core of the analysis of the latter half of the paper, and so in principle we should analyze it fully. However, this would lead to an impossibly cumbersome formalism and so in this paper we shall consistently bypass the general problem making only qualitative references to its implications, and illustrating them in more detail when we come to the reggeon problem in Section 5. For the moment we note only that the distinct partial wave amplitudes associated with the helicity orderings allow us to separate the different combinations of cuts appearing in the same flow-graph. For example, consider the simplest multiparticle hexagraph containing one internal T line, that of Fig. 3.9 which also shows the corresponding flow-graph. There are six possible combinations of five cuts through the flow-graph as illustrated in Fig. 3.10. There are four relevant helicities, that is the two pairs associated with each of the pairs of sloping lines attached to the T line,  $-n_{ij}, n_{ik}$  and  $n_{il}, n_{im}$  with the notation of Fig. 3.9. The possible orderings are

$$n_{ij} \geq n_{ik}, \quad n_{ij} + n_{ik} \geq n_{il} + n_{im}, \quad n_{il} \geq n_{im} \quad (3.14)$$

that is six in all. So the number of possible orderings matches the possible combinations of cuts. This is generally the case. To represent the complete analytic structure of an  $M_{NS}$ , therefore, we should write (3.13) including a sum over the  $a_H^{\underline{\tau}}$  and  $T_H^{\underline{\tau}}$  associated with each relevant helicity ordering. In general  $T_H^{\underline{\tau}}$  would have a complicated structure dependent on the whole hexagraph and not factorizing into substructures. If, however, we consider only pole contributions in each E-plane, then the factorization of Regge pole residues<sup>3)</sup>



implies the equality of all the possible partial wave amplitudes. In this case the complicated signature factors for different helicity orderings can be combined to give a much simpler signature factor which does factorize for  $E_i \sim 0, \forall E_i$ . Since Regge pole amplitudes will be the starting point for our construction of reggeon diagrams such signature factors will be adequate for our purposes.

The above discussion partly describes the "technical reasons" alluded to earlier for grouping several combinations of cuts into one flow-graph - that is the helicity orderings which distinguish such combinations are irrelevant for Regge pole amplitudes. There is also a more complicated reason, associated with the writing of the initial dispersion relation in terms of discontinuities which satisfy the generalized Steinmann relations<sup>23)</sup>, but this we shall not discuss at all here. For Regge pole amplitudes, the following signature factor rules are adequate.

For each V line we write a conventional signature factor

$$T_V = \frac{\tau_k - e^{-i\pi E_k}}{\sin \pi E_k} \underset{E_k \sim 0}{\sim} \frac{\tau_k - 1}{\pi E_k} + i \quad (3.15)$$

For each D line, attached to other lines as indicated in Fig. 3.11a

$$T_D = \frac{\tau_i \tau_j \tau_k - e^{-i\pi(E_j - E_i - E_k)}}{\sin \pi(E_i - E_j - E_k)} \underset{\forall E \sim 0}{\sim} \frac{\tau_i \tau_j \tau_k - 1}{\pi(E_i - E_j - E_k)} + i \quad (3.16)$$

For each T line attached to other lines as indicated in Fig. 3.11b

$$T_T \underset{\forall E \sim 0}{\sim} \frac{E_j + E_k}{E_j + E_k - E_j' - E_k'} \left[ \frac{\tau_i \tau_j \tau_k - 1}{\pi(E_i - E_j - E_k)} + i \right] + \frac{E_j' + E_k'}{E_j' + E_k' - E_j - E_k} \left[ \frac{\tau_i \tau_j' \tau_k' - 1}{\pi(E_i - E_j' - E_k')} + i \right] \quad (3.17)$$

The two terms here reflect only the orderings of the helicity sums in (3.14). Note that if all  $\tau$ 's are negative so that  $E \rightarrow 0$  gives a particle pole, then

$$T_T \xrightarrow{E_j, E_k \rightarrow 0} T_D \xrightarrow{E_j, E_k \rightarrow 0} T_V \quad (3.18)$$

The above discussion implies clearly that the phase structure of the SW representation reflects directly the cut structure of each  $M_{NS}$ . This means that in principle it should be straightforward to evaluate discontinuities (asymptotically) from the representation. In practice this is a complicated project which requires initially identifying explicitly the correspondence between cuts and helicity orderings referred to above. Since we are trying to avoid this problem we shall not attempt to give a general formalism for discontinuities. Instead we shall give only a subset of a potential general set of rules, which will be sufficient for the purpose of this paper.

To illustrate the general procedure consider first a simple hexagraph with only one possible combination of cuts through the flow-graph. It is straightforward to use (3.11) to write

$$\prod_i e^{-E_i y_i} \sim S_{i_1 j_1}^{\sum_1 \pm E_i} S_{i_2 j_2}^{\sum_2 \pm E_i} \dots \quad (3.19)$$

where  $\sum_r \pm E_i$   $r = 1, 2 \dots$  are sums over some subset of the  $E_i$ 's (with some specific choice of signs) and  $S_{i_r j_r}$   $r = 1, 2, \dots$  are the invariants associated with the cuts through the flow-graph. Substituting (3.19) into (3.13) the discontinuity in  $S_{i_r j_r}$ , say, can easily be evaluated. Applying this same procedure to more complicated hexagraphs, where we can still apply (3.19) unambiguously, we can derive the following subset of rules for discontinuities of Regge pole amplitudes which will be sufficient for our purposes.

We associate a discontinuity with the path through the hexagraph associated with the invariant involved. Then

- 3A if the path passes through a  $V$  line and exits from the graph at the earliest opportunity, the discontinuity necessarily removes the pole term in  $T_V$

3B if the path passes through a sequence of D lines after passing through the minimum of additional lines the discontinuity removes the pole in the  $T_D$  associated with the D line attached to the vertex through which the line exists

3C if the path passes through a T line only, the discontinuity removes both poles in the square brackets in (3.16).

Clearly if all signatures are positive and  $E_i \sim 0 \forall_i$ , all the poles in (3.14) - (3.16) are absent anyway and taking a discontinuity leaves the SW representation essentially unchanged. This can be regarded as the general basis for the well-known Abramovski, Gribov and Kanchelli cutting rules<sup>22)</sup> as we shall explain shortly. When odd signature amplitudes are involved, however, taking a discontinuity is clearly an important operation on the SW representation of an  $M_{NS}$ .

The final aspect of general multi-Regge theory that we require is the Regge-cut discontinuity formulae<sup>3),33)</sup> that follow from "t channel" unitarity. The FG amplitudes described earlier can be used to carry out a complete analysis of the cross-channel unitarity equation for each  $M_{NS}$  in each of its "t channels" - that is each channel where one  $Q_i^2$  is positive and is the total invariant energy. Near all phase space boundaries, the full multiparticle unitarity equations can be diagonalized and continued into the complex angular momenta and helicity planes. To analyze the 2N particle intermediate state in a channel which splits the hexagraph H into two subgraphs  $H_1$  and  $H_2$  as illustrated in Fig. 3.12, we use the hexagraph partial wave amplitudes shown. It will be important in the following that it does not matter precisely how the initial i line splits to form the 2N particle state. This is because the associated flow-graphs actually have the same cut structure. Consequently any  $M_{NS}$  corresponding to a hexagraph of the form shown has an FG continuation corresponding to an alternative hexagraph of the same form. A general argument is given in Ref. 3) that only  $M_{NS}$ 's corresponding to hexagraphs (flow-graphs) of this form can possibly generate (via the unitarity equation) Regge singularities in the  $Q_i^2$  channel.

The essential result of the t channel analysis, for our purposes, is that if the theory contains a Regge pole with trajectory  $E = \Delta(Q^2)$ , then there must be an infinite sequence of Regge cuts with trajectories

$$E_M = \Delta_M(Q^2) = M \Delta\left(\frac{Q^2}{M^2}\right) \quad M=2,3,\dots \quad (3.20)$$

If Regge poles with distinct trajectories are involved the corresponding trajectory formulae are more complicated. The conventional signature rule for Regge cuts is that the signature  $\tau_M$  of the  $M^{\text{th}}$  cut is

$$\tau_M = \prod_{i=1}^M \tau_i' \quad (3.21)$$

where  $\tau_i'$   $i = 1, \dots, M$  are the signatures of the Regge poles involved. It will be central in the following that this rule does not hold in general in multi-particle amplitudes. Before discussing this in detail we give the general discontinuity formulae for Regge cuts. These formulae are particularly simple if we consider only the partial wave amplitudes  $a_H^{\tau}(E, \underline{1})$  which appear in (3.13). That is we consider only amplitudes in which all helicities are set equal to the angular momenta to which they are coupled, and normalize the amplitudes as implied by (3.13), (3.15) and (3.17). The cuts then appear in each  $E_i$  plane  $i = 1, 2, \dots$  consistent with the signature rules which we shall discuss (and also group selection rules which we shall discuss in later sections) and satisfy the following discontinuity formulae - usually referred to as "Reggeon unitarity" -

$$\begin{aligned} \text{disc}_{E_i = \Delta_m(Q_i^2)} a_H^{\tau}(\underline{E}, \underline{E}) &= \int d\rho_m(t_i, \underline{t}') \delta(E_i - \Delta(t_i) - \dots - \Delta(t_m)) \times \\ &\times \frac{1}{T_{\tau_i}^{\tau_i'}} R_{H_1 \Delta}^{\tau_i, \tau_i'}(E_i, t_1, E_i^+) R_{H_2 \Delta}^{\tau_i', \tau_i'}(E_i^-, E_2, t_2) \end{aligned} \quad (3.22)$$

where the  $R_{H_1, 2\Delta}^{\tau_1, 2\tau_1'}$  are multiple residues of hexagraph partial wave amplitudes  $a_{H_1, 2}^{\tau_1, 2\tau_1'}$  at the Regge poles  $E_1 = \Delta(t_1'), \dots, E_M = \Delta(t_M')$  (after factorizing off two particle/Regge pole residues). The primed variables refer to the internal variables (as illustrated in Fig. 3.12). The variables  $E_1, t_1, E_2, t_2$ , are associated with the hexagraphs  $H_1$  and  $H_2$  respectively. The + and - superscripts for  $E_i$  indicate that the amplitude should be evaluated above or below its cut in the  $E_i$  plane. The phase space integration implied by  $d\rho_m$  is best described by introducing the usual RFT two-dimensional transverse momentum<sup>30)</sup> (timelike if  $Q_i^2 > 0$ ) so that

$$t_i = \underline{k}_i^2, \dots, t_j = \underline{k}_j^2 \quad \forall j \quad (3.23)$$

and we can write

$$\int d\rho_m(t_i, \xi') = \int \prod_{j=1}^M d^2 k_j \delta^2 \left( k_i - \sum_{j=1}^M k_j \right) \quad (3.24)$$

We shall distinguish two contributing factors to the signature factor  $\tilde{T}_{t_i}^{\xi'}$ . That is we write

$$\tilde{T}_{t_i}^{\xi'} = \tilde{T}^{\xi'} \tilde{T}_{u t_i}^{\xi'} \quad (3.25)$$

where  $\tilde{T}^{\xi'}$  originates simply from the signature factor poles associated with each internal Regge pole and has the form

$$\tilde{T}^{\xi'} = \frac{1}{\sin \frac{\pi}{2} \left[ -\Delta(t'_1) + \frac{\alpha'_1 + 1}{2} \right] \dots \sin \frac{\pi}{2} \left[ -\Delta(t'_m) + \frac{\alpha'_{m+1}}{2} \right]} \quad (3.26)$$

$\tilde{T}_{u t_i}^{\xi'}$  contains the signature factors from the analytic continuation of the  $t$  channel unitarity integral and to discuss this we must distinguish whether  $H$  describes a four-particle amplitude (and is therefore the simplest hexagraph of Fig. 3.13) or a higher multiparticle amplitude.

In fact the treatment of the unitarity integral that we have given in Refs 3) and 34) is really only adequate for the four-particle case. In this special case the only complex helicities involved are those associated with the internal Regge poles generating the Regge cut. As a result the helicity ordering problem can be avoided (since only one ordering of the internal helicity variables is relevant). Correspondingly the flow-graphs associated with either of the hexagraphs shown in Fig. 3.12 all have the form shown in Fig. 3.14 and so have only one possible combination of cuts through them as shown. It then follows that the "on energy-shell" amplitudes in (3.22) (which can be regarded as generalized "fixed pole residues") have a simple dispersion integral representation. That is

$$R_{H_i \Delta}^{\tau_i \tau'_i} (E_i = \sum_{j=1}^M \Delta(\tau'_j)) \sim \int_{C_1} \dots \int_{C_{N-1}} ds_1 \dots ds_{N-1} \text{disc}_{s_1} \dots \text{disc}_{s_{N-1}} M_{H_i \Delta} (s_1, \dots, s_{N-1}) \quad (3.27)$$

where as indicated the integrand is a multiple discontinuity of a rapidity space Regge pole amplitude  $M_{H_i \Delta}$  defined analogously to  $R_{H_i \Delta}$  by factorizing off the Regge pole contributions to the full hexagraph amplitude. The invariant variables  $s_1, \dots, s_{N-1}$  can be described as the cuts of the flow-graph corresponding to the hexagraph obtained by removing the Regge pole lines of  $H_i$  as illustrated in Fig. 3.15. The integration is over all combinations of right- and left-hand cuts in  $s_1, \dots, s_{N-1}$  with a sign for each contribution which depends on the signatures of  $a_{H_i}^{\tau_i \tau'_i}$ .

When (3.21) is not satisfied it is always possible to find one of  $s_1, \dots, s_{N-1}$  for which the signs allow the integration contour in (3.27) to be closed to zero (provided that  $M_{H_i \Delta_1, \dots, \Delta_N}$  is Regge-behaved in that variable). Also it is straightforward to show from four (external) particle unitarity integrals that  $\tilde{T}_{UT_i}^{\tau_i \tau'_i}$  can be written as a sum of terms each one of which is a product of factors of the form

$$\tilde{T}_{ijk} = \frac{\sin \frac{\pi}{2} \left( \frac{1 + \tau'_i}{2} - E_i \right)}{\sin \frac{\pi}{4} (\tau'_i - \tau'_j - \tau'_k - 1)} \quad (3.28)$$

for each combination of Regge trajectories (poles or cuts) with signatures  $\tau'_j$  and  $\tau'_k$  in a channel with signature  $\tau'_i$  and energy  $E_i$ .  $\tilde{T}_{UT_i}^{\tau_i \tau'_i}$  then gives the well-known sign rules for Regge cut discontinuities involving all possible combinations of odd and even signature Regge poles.

If one is interested only in Regge cuts in four-particle amplitudes, (3.21) - (3.28) give a complete basis for the development of a signature conserving RFT formalism. In particular, the usual RFT formalism<sup>30)</sup> for the Pomeron can be regarded simply as constructing the most general solution of (3.22) for a single even signature Pomeron pole, assuming only the existence of a triple Pomeron vertex and that Pomeron amplitudes are non-singular as functions of transverse momenta. The solution is constructed in the form of a Feynman graph loop expansion by replacing the "on energy-shell" integration of (3.22) by an off-shell integration, that is we write

$$\delta(E_i - \Delta(t'_1) - \dots - \Delta(t'_m)) \rightarrow \left( dE_1 \dots dE_m \delta(E_i - \sum_{j=1}^m E_j) \right) \times \prod_{j=1}^m \frac{1}{E_j - \Delta(t'_j)} \quad (3.29)$$

Energy is still conserved but a propagator is introduced for each Regge pole. Energy conserving multi-Pomeron amplitudes are then constructed by starting with a pole approximation for each hexagraph partial wave amplitude with "energy conservation" imposed on the vertices (that is angular momenta for lines meeting at a vertex are summed to one). Iterating (3.22) with the substitution (3.29) and taking into account cross products of hexagraphs as illustrated in Fig. 3.16 we obtain the usual RFT Pomeron graphs, as illustrated in Fig. 3.17, in the rapidity (or "time") ordered form - that is the Rayleigh-Schrödinger form of the RFT perturbation expansion. Finally the energy conserving Pomeron amplitudes are coupled to external particles by couplings shown in Fig. 3.18.

As soon as the hexagraph  $H$ , for which (3.22) is written, involves more than four external particles we meet the complication that the hexagraphs involved in the unitarity integral contain at least one internal  $T$  line, i.e., the  $i$  line of Fig. 3.12. Consequently the associated flow-graphs have at least the structure of those shown in Fig. 3.19, the simplest example of which is the graph of Fig. 3.9. These are of course, typical graphs with many combinations of cuts for which the helicity ordering problem must be faced if the unitarity integral is to be properly analyzed. Again we shall avoid the problem here, but there are several qualitative features that we can say follow from the flow-graph complication and which we shall see borne out in the reggeon analysis of Section 5.

The general form of the reggeon unitarity Eq. (3.22) will still hold but the signature factor  $\tilde{T}_{UT_1}^{I'}$  will be more complicated although we cannot give a precise form for  $\tilde{T}_{UT_1}^{I'}$  without the detailed analysis. The simple dispersion representation (3.27) for  $R_{H_1}$  and  $R_{H_2}$  will not hold since the different possible combinations of cuts in the flow-graphs will give distinct contributions to the  $R_{H_i}$ . In fact some combinations of cuts will appear as subtractions in such a dispersion relation. For example, the hexagraph of Fig. 3.9 appears in the analysis of the two-Regge pole cut in the eight-particle amplitude as illustrated in Fig. 3.20. The dispersion representation analogous to (3.27) would be an integral over the invariant  $s_1$  depicted in Fig. 3.21. However, this invariant cut does not appear at all in the combinations (5) and (6) of cuts in Fig. 3.10.

Consequently such combinations would appear as subtractions in such a relation. Therefore we anticipate that these contributions will destroy contour closing arguments and hence violate the signature rule (3.21) in multiparticle amplitudes. This is indeed what we shall find.

Multiparticle hexagraph amplitudes also involve independent external energies (that is angular momenta) and this must be built into any loop expansion for the multiparticle hexagraphs. The general form of the reggeon unitarity equation implies that this can be done by first introducing energy non-conserving vertices at the initial Regge pole approximation stage. [These will, of course, simply be the vertices automatically present in multiparticle Regge pole amplitudes.] The Pomeron loop expansion can, for example, then be built up using the same diagrams as appear in energy conserving Pomeron amplitudes but always containing just the number of energy non-conserving vertices to give the right number of external energy variables. These vertices actually have a unique location in the diagram as we shall explain in Section 5. For this it is important that (helicity pole limit) hexagraphs can simply be regarded as representing rapidity ordered interactions, with the result that the multiparticle loop expansion also appears as a Rayleigh-Schrödinger type perturbation expansion. A formalism of this kind for the triple Pomeron amplitudes appearing in the one-particle inclusive cross-section was derived directly from reggeon unitarity in Ref. 35) and confirmed by extensive hybrid Feynman diagram calculations<sup>36)</sup>.

In general, signature non-conservation and energy non-conservation will go together in multiparticle amplitudes. In particular the reggeon interactions containing "nonsense-zeros" which we referred to in the Introduction and which we utilize in Section 5 are simply signature non-conserving interactions which vanish when energy is conserved - to give consistency with the corresponding vanishing of (3.27). Since signature factors play a relatively minor role for the even signature Pomeron the signature properties of multiparticle hexagraph loops are not very significant. However, they are present and in particular the energy non-conserving four-Pomeron graph of Fig. 3.22 which appears in the eight-particle amplitude and corresponds to the hexagraph shown, should not be expected to conserve signature in the channel corresponding to the central T line. (That is the graph will contribute to an amplitude with odd-signature for the T line.) This is because the coupling functions for the two-Pomeron cut in this channel naturally have the cut structure of the (5) and (6) combinations in Fig. 3.10. This is of no importance experimentally for the Pomeron but theoretically it is significant when the graphs for the super critical Pomeron (similar to that of Fig. 3.22) are interpreted as arising from a redefinition of the physical external particle states of the theory.



Finally we note that (at least in the restricted kinematic region of the helicity pole limit) we can apparently construct the complete hexagraph solution of reggeon unitarity for the Pomeron (with a triple Pomeron vertex) without reference to  $s$  channel unitarity. Equivalently, we have not asked whether our expressions for hexagraph amplitudes are consistent with the unitarity derived multiple discontinuity formulae<sup>23)</sup> which define them via the initial dispersion relation. Actually, we can "derive" the unitarity relation (formally) to the extent that the discontinuity properties of hexagraph amplitudes allow the following interpretation of the Pomeron graphs. Introducing a rapidity variable for each vertex the graphs can be transformed to rapidity space and regarded as loops formed from hexagraph amplitudes in rapidity space of the form (3.10). The rapidities of all energy conserving vertices are integrated over to produce the energy conservation. Knowing the discontinuity properties of hexagraphs a meaning can be given to discontinuities denoted by any line passing along an internal path of the graph. If such discontinuities are interpreted as terms in the  $s$  channel unitarity equation as in the usual AGK formalism and as illustrated in Fig. 3.23 we claim that we obtain uniquely the AGK cutting rules. Thus we obtain the familiar (formal) solution of unitarity (also the multiple discontinuity formulae for hexagraph amplitudes - although we shall not attempt to demonstrate this property).

The above brief description illustrates how the usual RFT Pomeron formalism<sup>30)</sup> can in principle be derived completely from our general multi-Regge theory with no appeal to any underlying models. We have not attempted a complete treatment partly because we would need a more complete discussion of the helicity ordering problem and the resulting discontinuity rules and partly because it would not be appropriate for this paper. Our purpose here being to extract a comparable treatment of interacting odd signature reggeons from the general formalism. For this clearly the general hexagraph structure will be very important and the  $s$ -channel unitarity properties "derived" for the Pomeron will have to be used to complement the reggeon unitarity Eq. (3.22). Actually the results of Section 5 will illustrate clearly that the derivation of the "AGK solution of  $s$  channel unitarity" for the Pomeron from  $t$  channel unitarity is only possible because of the absence of transverse momentum singularities in the formalism, which in turn is directly related to the insensitivity of multiparticle hexagraphs to the process of taking a discontinuity.

Before discussing the general formalism for odd signature reggeons we first briefly describe the existing perturbative Yang-Mills calculations, in order to have a starting point for the abstract formalism.

4. - PERTURBATION THEORY CALCULATIONS - INFRA-RED FINITENESS AND  
PERTURBATIVE CONFINEMENT

There now exist many perturbation theory calculations of Yang-Mills theories in the Regge limit. With some exceptions<sup>37)</sup> almost all calculations are done after the Higgs mechanism has been used to give all gauge vector mesons a mass. The most general group-theoretic results are those recently obtained by Grisaru and Schnitzer<sup>38)</sup>. From the unitarity point of view these calculations are the most elementary since only two-particle  $t$  channel unitarity [or equivalently lowest (non-trivial) order perturbation theory] is used. However, the conclusions drawn from such analyses have always, in the past, been confirmed by more extensive higher-order calculations. We therefore first state the conclusions of Grisaru and Schnitzer.

The central result is that in an arbitrary, renormalizable non-Abelian gauge theory with arbitrary scalar and fermion representation structure, if the Higgs mechanism can be (and is) invoked to give all elementary vector mesons mass, then all the vectors will lie on Regge trajectories if and only if the gauge group is semi-simple - that is there are no proper Abelian subgroups. To lowest order in the gauge coupling  $g$  the trajectory function ( $= 1-\Delta$  in the notation of the last section) for a vector meson  $V_i$  is given by the two-dimensional transverse momentum integral :

$$d_i(q^2) = 1 + g^2 (q^2 - M^2) \sum_{j,\ell} \bar{f}_{ij\ell}^2 \frac{1}{\pi^2} \int \frac{d^2 k}{(k^2 - M_j^2)(q-k)^2 - M_\ell^2} \quad (4.1)$$

where the  $\bar{f}_{ij\ell}$  are the structure constants of the group in a basis which diagonalizes the vector-meson mass matrix. The sum over  $j$  and  $\ell$  is therefore over those two-particle vector states that couple directly to  $V_i$ . This result holds for any set of vector masses  $M_i$  given by an arbitrary symmetry breaking scheme. However, for the particular case of  $QCD_{MB}$  that we are interested in, the presence of the three massless gluons associated with the unbroken  $SU(2)$  symmetry will give rise to infra-red divergences in many of the trajectory functions. This is our first encounter with the infra-red divergences of transverse momentum integrals which will concern us extensively in the rest of this section. For the moment we carry on our description of existing perturbative calculations assuming all vectors have masses.

Having argued that all vector mesons lie on Regge trajectories the next question is whether the high energy behaviour (Regge limit) of all amplitudes can be described by the exchange of such "reggeons". We know from the general arguments of the last section that whenever quantum numbers and signature rules allow it there will be distinct Regge cuts associated with the  $t$ -channel exchange of any number of reggeons. There may, however, be additional Regge singularities not directly associated with such exchanges. This has been investigated up to at least tenth order in perturbation theory by many different calculations in the leading-log approximation. The most general group structure and symmetry breaking schemes considered by Grisaru and Schnitzer have not been calculated but it is evident from the nature of the results that the conclusions should be general. (This seems to be the universal expectation of all authors.).

The somewhat remarkable result of the higher-order calculations<sup>4)-6)</sup> is that the reggeized vector trajectories are the only high energy Regge singularities that appear and up to the orders calculated all amplitudes can be described by the exchange of reggeons. The remaining question is therefore, what is the nature of the Regge cut discontinuities, or in RFT language, how do the reggeons interact? The answer to this question in terms of the gradual appearance of an RFT description of the reggeons can be presented in various ways.

The simplest (but least illuminating) presentation is probably that of Bronzan and Sugar<sup>7)</sup>. They write down the leading logarithmic results of Cheng and Lo<sup>5)</sup> [in the case where an  $SU(2)$  gauge symmetry is broken to an  $SU(2)$  global symmetry] in the form

$$T_0 = i s g^4 \sum_n a_{0n}(q^2) (g^2 \ln s)^n \quad (4.2)$$

$$T_1 = s g^2 \sum_n a_{1n}(q^2) (g^2 \ln s)^n \quad (4.3)$$

$$T_2 = i s g^4 \sum_n a_{2n}(q^2) (g^2 \ln s)^n \quad (4.4)$$

where  $T_0$ ,  $T_1$  and  $T_2$  are four-particle amplitudes with  $t$  channel "isospin" 0, 1 and 2, respectively. Bronzan and Sugar simply observe that the series for  $T_1$  contains only the expansion of the Regge pole behaviour given by the trajectory of (4.1), and that the only signature conserving RFT diagrams that can contribute to  $T_0$  and  $T_2$  are those shown in Fig. 4.1. These diagrams contain only two RFT

couplings, that is those shown in Fig. 4.2, which must be highly over-determined by the series for  $T_0$  and  $T_2$ . That these series can be completely reproduced by the RFT diagrams therefore appears as a striking confirmation of the RFT formalism.

A much more illuminating description of the same result follows from the unitarity dispersion relation approach initiated by Lipatov and collaborators<sup>4)</sup> and further developed by Bartels<sup>6)</sup>. In this approach we observe that the weak coupling leading logarithms can only come from the multi-Regge regions of phase space in the unitarity integral. Also strictly  $T_0$  and  $T_2$  are zero to leading order in  $g^2$  for a fixed power of  $g^2$  lns. The central result to understand the emergence of RFT is then that for all  $m$ - $n$  production amplitudes the leading logarithm result in the multi-Regge limit is that amplitudes that can exchange reggeons in each  $t$  channel do so and all other amplitudes are zero. In addition there is a bootstrap property, valid at the leading log level, which we shall refer to later. Unitarity is satisfied identically in the sense illustrated in Fig. 4.3.

It follows then that the "next-to-leading-log" results for  $T_0$  and  $T_2$  must necessarily come from inserting the leading-log reggeized production amplitudes in the multi-Regge region of phase space in the unitarity integral. At finite order this process can only possibly generate the two-reggeon RFT diagrams of Fig. 4.1. Further the four-reggeon interaction of Fig. 4.2 is necessarily given by squaring the two-reggeon/particle vertex and summing over particle states as illustrated in Fig. 4.4. The resulting vertex has two terms

$$V_I(q, k, k', M^2) = R_I(q^2, M^2) + S_I(q, k, k', M^2) \quad (4.5)$$

where  $R_I$  is regular and has the form

$$R_I = a_I(q^2 - 3M^2) + b_I M^2, \quad a_0 = 2g^2, \quad a_2 = -g^2 \quad (4.6)$$

The  $a_I$  term arises directly from gluon particle intermediate states, while the  $b_I$  term arises from the Higgs scalars in the intermediate state sum and therefore depends on the representation used for the scalars.  $S_I$  is singular as a function of the transverse momenta. It can be shown to arise from transversely polarized (in a  $t$  channel sense) vectors in the intermediate state sum. It has the form :

$$S_I = -\frac{\alpha_I}{2} \left[ \frac{(\underline{k}^2 + M^2)((q - \underline{k}')^2 + M^2) + (\underline{k}'^2 + M^2)((q - \underline{k})^2 + M^2)}{(\underline{k} - \underline{k}')^2 + M^2} + \frac{(\underline{k}^2 + M^2)(\underline{k}'^2 + M^2) + ((q - \underline{k}')^2 + M^2)((q - \underline{k})^2 + M^2)}{(q - \underline{k} - \underline{k}')^2 + M^2} \right] \quad (4.7)$$

where  $M^2$  is the common vector meson mass. In the next section we shall show that the numerator zeros in (4.7) can be interpreted as "nonsense zeros" and this will be a central feature in our generalization of the leading log results.

If the vertex  $V_I$ , together with the reggeon propagator

$$M(E, \underline{k}^2) = \left[ (E + d(\underline{k}^2) - 1) (\underline{k}^2 - M^2) \right]^{-1} \quad (4.8)$$

is used to evaluate the RFT diagrams of Fig. 4.1 with the usual RFT prescription<sup>30)</sup> to impose energy and momentum conservation at vertices and to integrate over transverse momenta  $\underline{k}$  and energies  $E$  then the (S-W or Mellin transforms of the) series (4.2) and (4.4) are reproduced.

The above results are expected to generalize to any symmetry breaking scheme with obvious minor changes when there are many vector mesons with different masses. In particular they should apply to the initial problem we shall consider that is  $QCD_M$  with the  $SU(3)$  gauge symmetry completely broken by two triplets of Higgs scalars. However, the theory we really wish to study is  $QCD_{MB}$  and for this we must restore an  $SU(2)$  gauge symmetry. In addition to the trajectory function divergence referred to earlier this produces further infra-red divergences from the singularities in the reggeon interaction and the particle poles in the reggeon propagators. Before studying the particular problem of  $QCD_{MB}$  we review what is known in general about the infra-red behaviour of reggeon diagrams.

The main results come from the work of Fadin, Kuraev and Lipatov<sup>4)</sup> with some extensions due to Bartels<sup>6)</sup> and also Kwiecinski and Praszalowicz<sup>39)</sup>. We consider the  $SU(2)$  theory discussed above, in which the leading log reggeon diagrams depend only on the vector meson mass  $M$  and are independent of the parameters of the Higgs system. Consider first the trajectory function divergence. From (4.1) we obtain

$$\alpha(q^2) \underset{M^2 \rightarrow 0}{\sim} q^2 \int \frac{d^2 k}{(k^2 - M^2)((q-k)^2 - M^2)} \quad (4.9)$$

$$\sim -2 \ln [q^2/M^2] \quad (4.10)$$

$$\sim \ln M^2 \left[ q^2 \int \frac{d^2 k \delta^2(k)}{(q-k)^2} + q^2 \int \frac{d^2 k \delta^2(q-k)}{k^2} \right] \quad (4.11)$$

At first sight this divergence is sufficient, through (4.8), to send every reggeon diagram to zero as  $M^2 \rightarrow 0$ . Equivalently in rapidity space factors of the form

$$S \alpha(q^2) \underset{M^2 \rightarrow 0}{\sim} \exp [-\ln s \ln q^2/M^2] \quad (4.12)$$

are sufficient to send diagrams to zero. This "exponential damping" associated with the reggeization of massive gluons is very closely related [as is clear from the explicit calculations of Ref. 12)] to the Sudakov form factor exponentiation originally proposed by Cornwall and Tiktopoulos<sup>26)</sup> as a confinement mechanism in the zero-mass limit. In fact (4.12) is responsible for the suppression of colour as  $M^2 \rightarrow 0$ , but to show this we have to consider first the other sources of infra-red divergence since they may cancel the trajectory divergence (and actually do so in the colour-zero channel). Note first that the coefficient of the  $\ln M^2$  divergence of  $\alpha(q^2)$  is simply obtained by the rule that we replace in turn every potentially singular pole factor in (4.9) by  $\delta^2(k)$  and sum the resulting expressions as in (4.11). This simple rule for infra-red divergences will be exploited extensively in the following.

To exhibit the infra-red cancellation that takes place in the colour-zero channel we first "undo" the reggeization by expanding  $S^{\alpha(q^2)}$  in powers of  $g^2$ . The gluon can then be treated as a fixed singularity with a propagator of the form (4.8) with  $\alpha = 1$ , and the reggeization effect represented by an interaction written in the form

$$\begin{aligned} \hat{V}_I(q, k, k') &= d_I \left[ \delta^2(k-k') \left[ (k^2 \cdot (q-k)^2 + k'^2 (q-k')^2) \ln M^2 \right. \right. \\ &\quad \left. \left. + O(\ln k^2) \right] + \delta^2(q-k-k') \left[ (k^2 \cdot k'^2 \right. \right. \\ &\quad \left. \left. + (q-k)^2 (q-k'^2) \right) \ln M^2 + O(\ln (q-k)^2) \right] \end{aligned} \quad (4.13)$$

Now, when  $S_I$  is inserted in integrations it will give divergences of precisely the form (4.13) [in analogy with (4.11)] and there will be a cancellation provided  $d_I = a_I/2$ . This is true only for  $I = 0$ . For  $I \neq 0$   $d_I$  dominates and the exponentiation of the reggeization is sufficient to send all reggeon diagrams to zero. Consequently we have suppression of colour in the sense that all amplitudes with non-zero colour in the t channel vanish when  $M^2 \rightarrow 0$ .

Therefore if we write diagrams directly for elementary gluons with propagators in which  $\alpha = 1$  we can use the "infra-red finite" colour-zero interaction

$$\tilde{V}_0(q, k, k') = V_0(q, k, k', M^2=0) + \hat{V}_0(q, k, k') \quad (4.14)$$

There remains the potential divergences associated with the particle pole in the propagator (4.8). However, if we evaluate  $\tilde{V}_0$  as  $k \rightarrow 0$  with  $q, k'$  fixed then  $\hat{V}_0$  is zero and from (4.7) we obtain

$$V_0 \underset{k^2 \rightarrow 0}{\sim} -g^2 \left[ -4q + \frac{2q^2 k'}{k^2} + \frac{2q^2 (q-k')}{(q-k')^2} \right] \cdot k \quad (4.15)$$

This linear zero is sufficient to cancel the  $(k^2)^{-1}$  divergence from propagators and leave only integrable  $(k^2)^{-\frac{1}{2}}$  singularities. Since the remaining singularity of  $\tilde{V}_0$  as  $(k-k') \rightarrow 0$  is similarly integrable it immediately follows that all one-loop gluon diagrams are finite provided that all combinations of external transverse momenta are non-zero. When the external momenta vanish the integrable singularities may coincide and produce logarithmic singularities. However, when the one-loop diagrams are used to build up higher diagrams such logarithmic singularities cannot transform the basic integrable singularities to non-integrable

singularities. Consequently multi-loop diagrams are also finite provided that all combinations of external transverse momenta are non-zero. Since we are discussing massless gluons, this is equivalent to saying all "off-mass-shell" gluon diagrams are finite. [Note that the "mass-shell" is  $\underline{k}^2 = M^2$ , whereas the "energy-shell" is  $E = \Delta(\underline{k}^2) = 1 - \alpha(\underline{k}^2)$ .]

In summary, the "off-mass-shell" finiteness of the gluon diagrams of Fig. 4.5 is due to two distinct cancellations. The first involves the trajectory divergence and the singular interaction and requires zero (t channel) colour. It is embodied in (4.14). The second is a cancellation between the  $R_I$  and  $S_I$  terms in (4.5), and does not require zero colour. It is embodied in (4.15).

The central question for our discussion of infra-red behaviour is, however, the infra-red finiteness of on-mass-shell scattering amplitudes. As we emphasized in the introduction we expect the infra-red divergences of such amplitudes to lead us to stringlike external states in the infra-red limit we consider. It is vital therefore that we investigate the mass-shell infra-red divergences of gluon amplitudes systematically. This requires that we first set the external transverse momenta, of the gluon diagrams that we are discussing, on-shell; before taking  $M^2 \rightarrow 0$ . This implies that at all external gluon vertices the  $S_I$  term will be missing from  $V_I$  so that (4.15) will not hold. [ $V_I$  will in fact reduce to  $(a_I + b_I)$  since the  $M^2$  factor is cancelled by scale factors for external rapidity variables as we go on shell.] Consequently, since the internal vertices are able to cancel only the initial or final propagator divergences attached to external vertices, but not both, the diagrams are divergent. Such mass-shell divergences are clearly of a kind that may possibly be absorbed by a redefinition of the external states. This is the point of view adopted by several authors as we now describe (afterwards we shall contest this point of view).

We consider explicitly the work of Lipatov et al.<sup>4)</sup> and its development by Bartels<sup>6)</sup> (essentially the same point of view is, however, also implied in the work of Cheng et al.<sup>9)</sup> and Yeung<sup>10)</sup> which derives equivalent results). It is argued that we should consider the gluon diagrams coupled to external states by couplings with similar zeros to those of the gluon interaction. In particular quark bound states do have just this property. In this case all diagrams are finite as  $M^2 \rightarrow 0$  and the high energy behaviour of the "constructed" amplitudes is obtained by summing all the massless gluon diagrams. The following "scale-invariance" property of the gluon interaction then becomes central. The effect of each transverse momentum integration with the interaction (4.14) is best represented by absorbing the pole factors of the propagators symmetrically into a kernel which we can write formally as



$$K(q, k) [f(k', q)] = \frac{1}{E} \int d^2 k' \frac{\tilde{V}(q, k, k') f(k', q)}{[(q-k)^2 (q+k)^2 (q-k')^2 (q+k')^2]^{\frac{1}{2}}} \quad (4.16)$$

Clearly  $K$  is scale-invariant in that

$$K(\lambda q, \lambda k) = K(q, k) \quad (4.17)$$

Further, the effective Hilbert-Schmidt norm for this kernel is

$$\|K\|^2 \sim \int d^2 q d^2 k K(q, k) \quad (4.18)$$

which has an ultra-violet divergence because of (4.17). Consequently the integral equation representing the sum of gluon diagrams of Fig. 4.1 is non-Fredholm and the solution has a fixed-cut in the  $E$  plane<sup>4),7)</sup> arising from the ultra-violet divergence. Of course, if (4.14) is finite  $K$  must be scale-invariant since there is no scale left when  $M^2 \rightarrow 0$ . We can say therefore that the infra-red finiteness of the colour-zero interaction and the fixed-cut in the  $E$  plane are unavoidably related.

There are several criticisms of the above analysis if it is used to argue that the ultra-violet divergence of  $K$  is the dynamical mechanism generating the Pomeron in massless Yang-Mills theories. Firstly since the fixed-cut resulting from the diagrams of (4.1) violates the Froissart bound one must assume that summing higher-order diagrams will restore the Froissart bound. This is argued for by Bartels in a recent paper<sup>6)</sup>. Even so it remains a problem to argue that the renormalization mass scale of the massless theory (which should ultimately appear in the ultra-violet region) can enter the formalism to allow the Pomeron to become a  $q^2$  dependent singularity, while maintaining the ultra-violet divergence of the theory as the dynamically dominant effect. On a more fundamental level the large transverse momentum region of a Higgs theory with massive vectors, which is not asymptotically free, is a region where perturbation theory is anticipated to be completely unreliable. Specifically renormalization contributions to the Higgs system will grow uncontrollably (the renormalon problem<sup>8)</sup> of a just renormalizable theory) and it is an open problem at the moment whether the theory can be given a

meaning in this region. In the language of Section 2 a continuum Higgs theory, if it exists, must be defined from a fixed-point of the lattice theory which gives it no chance to be related smoothly to the pure gauge asymptotically-free theory. A property not evident from perturbation theory.

The lattice theory tells us that to relate the Higgs theory to massless Yang-Mills we must work with a lattice or equivalently a transverse momentum cut-off. In fact it is clear from the Feynman diagram calculations<sup>5)</sup> leading to reggeon diagrams that, since renormalizability plays a fundamental rôle in giving the finite order perturbative transverse momentum cut-off, the growth of renormalization contributions and the resulting ambiguity of the theory will manifest itself directly in the large transverse momentum region of the reggeon diagrams. Consequently the theory really is well-defined only with a transverse momentum cut-off and this eliminates the fixed-cut associated with (4.17) and (4.18).

A further point of principle, closely related to our emphasis of the importance of the mass-shell singularities for determining the correct external states, is that the choice of simple quark bound states as external states, while eliminating infra-red divergences, does not remove all effects of the massless gluons. That is the amplitudes produced still have a finite singularity at zero momentum transfer and so cannot represent completely the high energy behaviour of a confining theory. As we argued in the introduction we believe the mass-shell infra-red singularities must be investigated more completely before determining the correct external states.

The leading mass-shell singularities of the reggeon diagrams which generate the fixed-cut can actually be studied systematically by going to the double leading log approximation. That is we keep only leading powers of  $\log(q^2/M^2)$  as well as  $\log s$ . The work of Carruthers, Fishbane and Zachariasen<sup>12)</sup> in this approximation has been cast into our language by Bronzan and Sugar<sup>7)</sup> by calculating the diagrams of Fig. 4.1 in the same approximation. The result is

$$[K^N] = \frac{1}{E^N} \int \frac{d^2 \underline{k}_1 V(q, \underline{k}_1, \underline{k}'_1)}{[\dots]^{1/2}} \int \frac{d^2 \underline{k}_2 V(q, \underline{k}'_1, \underline{k}_2)}{[\dots]^{1/2}} \dots \int \frac{d^2 \underline{k}_N V(q, \underline{k}'_{N-1}, \underline{k}_N)}{[\dots]^{1/2}} \quad (4.19)$$

$$\sim \frac{1}{E^N} \left[ \ln q^2 / \frac{1}{2} \right]^N \quad (4.20)$$

which demonstrates explicitly the infra-red finiteness and scale-invariance properties of  $K$ . To obtain gluon (or quark) scattering amplitudes we must calculate the partial-wave amplitude

$$T_0(E, q^2) = \lim_{M^2 \rightarrow 0} \sum_{N=0}^{\infty} \frac{1}{E} \int \frac{d^2 k [K^N]}{(k^2 - M^2)((q-k)^2 - M^2)} \quad (4.21)$$

which in the same approximation we should take to be

$$T_0(E, q^2) \sim \frac{1}{q^2} \int_0^{q^2} \frac{dk^2}{k^2 [E + \ln q^2/k^2]} \quad (4.22)$$

This result displays two important features. First there is a remaining mass-shell divergence at  $k^2 = 0$ , but from this region we obtain

$$T_0(E, q^2) \sim \frac{1}{q^2} \int_0^{q^2} \frac{dk^2}{k^2 \ln k^2} \quad (4.23)$$

which is independent of  $E$ . Secondly the only singularity in  $E$  comes from the region  $k^2 \sim q^2$  where the kernel  $K$  is finite and gives

$$T_0(E, q^2) \underset{E \rightarrow 0}{\sim} \frac{1}{q^2} \int_0^{q^2} \frac{dk^2}{[E + q^2 - k^2]} \quad (4.24)$$

$$\sim \frac{1}{q^2} \ln E \quad (4.25)$$

Consequently the large rapidity amplitude - which is determined by the  $E$  plane singularities - is given by

$$T_0(E, \ln s) \underset{\ln s \rightarrow \infty}{\sim} \frac{1}{q^2 \ln s} \quad (4.26)$$

which is the result obtained in Ref. 12). So although each term in the sum (4.21) is infra-red singular, in rapidity space the infra-red singularities sum (they actually exponentiate) to give an infra-red finite answer.

That the above features can be expected in general can be seen by writing the integral equation formalism of Refs. 4)-6) in the following form. We write

$$T_0(E, q^2) = \frac{1}{E} \int \frac{d^2 k}{k^2 (q-k)^2} \phi(q, k, E) \quad (4.27)$$

where  $\phi$  satisfies an integral equation which we can write formally as

$$\phi = K_0 + \frac{K}{E} \phi \quad (4.28)$$

The (mass-shell) divergences of (4.27) arise from the regions where  $\underline{k}^2 \rightarrow 0$  or  $(\underline{q}-\underline{k})^2 \rightarrow 0$ , but not both. Since such a region is not scale-invariant the infra-red finiteness of  $K$  breaks down and  $K \rightarrow \infty$ . Consequently from (4.28) we have formally

$$\phi \sim -\frac{EK_0}{K} \quad (4.29)$$

and

$$T_0 \sim \int \frac{d^2 k}{k^2 (q-k)^2} \frac{K_0}{K} \quad (4.30)$$

which is independent of  $E$ . Clearly the above argument could equally well be applied to the full two-gluon/two-particle amplitude  $\phi$  which will satisfy (4.28) with  $K$  defined as the full two-gluon irreducible kernel. Since we also expect the full  $K$  to be infra-red finite but singular in non-scale invariant limits we will obtain from (4.30) the general conclusion that the leading  $E$  dependence of  $T_0$  for  $E \sim 0$  is eliminated from the potentially singular infra-red regions. [Note that the infra-red singularity of (4.30) will also be softened by  $K$ .]

We further expect the above analysis to extend to a general massless gluon state. The key point was the breakdown of the infra-red finiteness of the off-shell four-gluon vertex on-shell. The natural generalization would be to expect off-mass-shell infra-red finite vertices for arbitrary numbers of gluons in which the infra-red finiteness is guaranteed by Ward identities between different local vertices (many results in this direction have already been derived by Jaroszewicz<sup>25)</sup>). The off-shell finiteness will break down as some gluons are taken on-shell to

define particle amplitudes. We will then have the above pattern repeated. For the contribution to  $T_0$  of the  $N$  gluon state (actually for reasons discussed in Section 6,  $N$  will always be even) we will write, in analogy with (4.27)

$$T_{0N}(E, q^2) = \left( \frac{d^2 k_1 \dots d^2 k_{N-1}}{k_1^2 \dots k_{N-1}^2 (q - \sum k_i)^2} \right) \frac{1}{E} \phi_N(q, k_1, \dots, k_{N-1}, E) \quad (4.31)$$

where formally

$$\phi_N = K_{0N} + \frac{K_N}{E} \phi_N \quad (4.32)$$

$K_N$  is the full  $N$  gluon irreducible vertex and (4.32) sums the diagrams shown in Fig. 4.6. The mass-shell infra-red divergences of (4.31) will arise from regions where some subset of  $k_1, \dots, k_{N-1}, q - \sum k_i$ , go to zero, but not all since  $q \neq 0$ . We anticipate that  $K_N$  will be infra-red finite and scale-invariant for non-zero  $k$ 's, but singular in such regions. The structure of (4.31) and (4.32) will therefore again, as in (4.30), remove the  $E$  dependence from the infra-red singular regions.

The leading  $E$  dependent singularity of  $T_0(E, q^2)$  will naturally arise from (4.28) or (4.31) in a region of phase-space where the kernel  $K$  is finite. If this is to be an infra-red region it must be approachable in a scale-invariant way. But this is impossible in (4.28) or (4.31) except if we take  $k_1, \dots, k_{N-1}, q - \sum k_i$ , all to zero simultaneously, which is only possible at  $q^2 = 0$ . For finite  $q^2$  therefore we conclude that the mass-shell infra-red singularities of elastic amplitudes (including those diagrams that generate the fixed-cut) will sum to give finite large rapidity amplitudes without a redefinition of the external states. (The large rapidity amplitudes necessarily come from the leading  $E$  plane singularities via the S-W transform and so the absence of infra-red divergences in the contribution of such  $E$  plane singularities implies the finiteness of such amplitudes.) Further the resulting amplitudes have, in the leading log approximation at least, no negative  $E$  singularity (that is no angular momentum plane singularity above one) and so do not violate the Froissart bound at finite  $q^2$ . A singularity remains at  $q^2 = 0$  [as is evident from (4.26)] and so such amplitudes still cannot represent a confining theory.

To produce infra-red singularities which survive in the large rapidity amplitudes and therefore force us to redefine the external states we must find singularities which occur in regions of phase space where the kernels  $K_N$  for interacting massless gluons remain finite because of their scale invariance. This we shall do, in the limit that the  $SU(2)$  gauge symmetry is restored to give  $QCD_{MB}$ , in Section 6.

## 5. - MULTI-REGGE THEORY OF ODD SIGNATURE REGGEONS

From the point of view of the general multi-Regge theory of Section 3 it is clear that the existing perturbative calculations in Yang-Mills theories have only opposed an extremely small subset of the full reggeon structure which from the general arguments must be present. We should like to use the general formalism to reliably extrapolate the perturbative results to the complete structure, particularly the multiparticle amplitudes which we shall need in the following sections. In the first instance, at least, we shall not ask for as much detail as appears in the weak coupling perturbative calculations. Instead we would like a formalism where the general features are sufficiently under control for us to discuss reliably the infra-red and critical limits, that will concern us, in a manner comparable with the usual "critical phenomenon" treatment of the Pomeron. As is well-known the Pomeron formalism has the very attractive feature that we need to know only the existence of an even signature Regge pole with intercept  $\alpha(0)$  near unity and a finite, non-singular triple Pomeron interaction. We can then<sup>3)</sup> justify the neglect of non-singular higher order interactions and (in effect) use the reggeon unitarity relations alone to predict the dominant scaling behaviour of the diffraction peak in the limit  $\alpha(0) \rightarrow 1$ .

In analogy with the Pomeron formalism, therefore, it is important to ask how much of the structure found in the perturbative Yang-Mills calculations described in the last section can we reproduce from the general formalism of Section 3, knowing only the existence of odd signature reggeons, with a particular group structure, together with low order non-singular interactions. At first sight it would appear that the answer is very little, since we could not predict the singular four-reggeon interaction. Further from its derivation it is clear that analogous but more complicated unitarity (or Feynman diagram) calculations will lead to singular interactions of arbitrarily high order. Not only would it be anticipated that we could not predict the structure of such interactions but also any approach based on an extrapolation of the form of low order interactions would seem to be futile.

Fortunately we shall be able to argue in the following that the singularity of the interactions, and even the singularity of the trajectory function (4.1), can be viewed as an effect of formulating an RFT with only these interactions which satisfy the signature conservation rules for four-particle amplitudes. As we discussed in Section 3 we expect to find in multiparticle amplitudes, signature non-conserving interactions which contain nonsense-zeros and so vanish in energy (angular momentum) conserving amplitudes. We shall see in the following that the effect of such interactions is to generate transverse momentum singularities in the signature conserving interactions of four-particle amplitudes. Therefore we

shall find that if we generate reggeon diagrams by a hexagraph loop formalism, as we briefly outlined for the Pomeron in Section 3, we shall be able to reproduce all of the perturbative results of the last section with non-singular reggeon interactions.

Our starting point can be stated as follows. We begin with Yang-Mills multi-Regge pole hexagraph amplitudes obtained by keeping only the Regge poles in each  $E_i$  plane in (3.10). The (factorized) residue functions can in principle be computed perturbatively by extending the calculations described in the last section along the lines followed by Bartels<sup>6)</sup>. The group structure will manifest itself in the tensor structure of the various multi-Regge pole couplings (the effects of quarks on this structure will be important in Section 7) and the underlying gauge invariance presumably implies that in the limit of zero reggeon masses all couplings are related<sup>25)</sup> by Ward identities. For the moment we concentrate on details of our construction that are independent of such relations and also of the group involved.

In principle we would next like to simply iterate the reggeon hexagraphs through the reggeon unitarity Eq. (3.22) and form hexagraph loops in such a way that we count all possible contributions to the loops in the  $s$  channel unitarity equation (or the multiple discontinuity formulae for hexagraphs) compatible with the discontinuity rules of Section 3. This would be the analogue of the AGK formalism for the Pomeron. While this may eventually be possible when the full formalism is developed, at the moment it is simply too complicated. Instead we concentrate on the most singular part in transverse momentum of each reggeon loop. The discontinuity rules of Section 3 show that cutting a reggeon line always removes some singular real part so the contributions we shall construct will in general cut the minimum number of reggeons forming a particular loop. (The analogue of the "multiperipheral" cut of the two reggeon diagram.) Such contributions will allow us to make contact with the perturbative infra-red singularities and be the most important in the following sections.

Before discussing the general iteration process we consider first the construction of some simple reggeon diagrams involving the triple reggeon vertex. We assume that this vertex has a nonsense-zero. That is every triple Regge coupling in a hexagraph has a zero at

$$E_i = \Delta_j + \Delta_k \quad (\Delta_{j,k} = 1 - \alpha_{j,k}) \quad (5.1)$$



where  $E_i$  is the energy of the horizontal line entering the vertex and  $\alpha_j$  and  $\alpha_k$  are the trajectories associated with the remaining lines. We begin with the simplest loop diagram of all shown in Fig. 5.1. Taking the multiperipheral cut through the diagram implies that we are evaluating a particular partial cross-section as illustrated. Fixing the rapidity differences  $(y_1 - y_2)$  and  $(y_3 - y_4)$  implies that we are fixing the masses of the produced particle states. In this situation we can in principle apply the  $t$  channel analysis to the reggeon loop (by inserting  $t$  channel intermediate states into the reggeons) and deduce that the phase-space integration is the normal two-reggeon integration. The diagram also involves two discontinuities of triple Regge vertices which appear in six particle hexagraphs (say) - or one particle inclusive cross-sections as illustrated in Fig. 5.2. According to the discontinuity rule 3C, for the hexagraphs involved, such a discontinuity simply removes the signature factor for the cut reggeon line. Therefore, the only signature factors we must keep are those of the two internal reggeons which are  $V$  lines and therefore have simple signature factors

$$\frac{1}{\sin \pi \alpha(t)} \sim_{t \sim M^2} \frac{1}{\pi \alpha'(t - M^2)} \quad (5.2)$$

where  $M^2$  is the vector mass (which for the moment we take to be common to all vectors) and  $\alpha'$  is the slope defined at  $t = M^2$  (which we also take to be common). Using the notation of Fig. 5.3 we write for the triple reggeon vertex (using timelike transverse momenta)

$$\Gamma_{1,2}^0 = r_0 \left[ E + \alpha'(k_1^2 - M^2) + \alpha'(k_2^2 - M^2) \right] \quad (5.3)$$

where  $r_0$  will also carry group indices, which, for the moment, we suppress. For each reggeon propagator (which we do not define to include the signature factor pole) we write

$$\Gamma_{1,1}^0 = \frac{1}{E + \alpha'(t - M^2)} \quad (5.4)$$

We take the transverse momentum cut-off to be  $\Lambda$  and to keep  $r_0$  dimensionless we scale the transverse momentum integration by  $\alpha'$ . The vertices and propagators of Fig. 5.1 are now determined by (5.3) and (5.4) and the discontinuity rules and so we obtain for the full imaginary part

$$\begin{aligned}
 I(y_1, y_2, y_3, y_4) &= \frac{\gamma_0^2}{\pi^2 \alpha'^2} \int_{i=1}^4 dE_i \int_{|k^2| < \Lambda} d^2 k \frac{e^{-E_1(y_2-y_1) - E_2(y_4-y_3) - (E_3+E_4)(y_3-y_2)}}{[k^2 - M^2][(\underline{q}-k)^2 - M^2]} \\
 &\times \frac{[E_1 + \alpha'(k^2 - M^2) + \alpha'((\underline{q}-k)^2 - M^2)][E_2 + \alpha'(k^2 - M^2) + \alpha'((\underline{q}-k)^2 - M^2)]}{[E_1 + \alpha'(q^2 - M^2)][E_2 + \alpha'(q^2 - M^2)][E_3 + \alpha'(k^2 - M^2)][E_4 + \alpha'((\underline{q}-k)^2 - M^2)]} \quad (5.5)
 \end{aligned}$$

We now integrate over the internal rapidities  $y_2$  and  $y_3$ . The upper end points give poles at  $E_1 = E_3 + E_4$  and  $E_3 + E_4 = E_2$  respectively. These poles pinch to give a pole at  $E_1 = E_2$  which can be used to perform the  $E_1$  integration by closing the contour in the left-half plane. The result is

$$\begin{aligned}
 I(y_4 - y_1) &= \frac{\gamma_0^2}{\pi \alpha'} \int \frac{dE_2 e^{-E_2(y_4 - y_1)}}{[E_2 + \alpha'(q^2 - M^2)]^2} \int_{|k^2| < \Lambda} d^2 k \frac{[E_2 + \alpha'(k^2 - M^2) + \alpha'((\underline{q}-k)^2 - M^2)]^2}{[k^2 - M^2][(\underline{q}-k)^2 - M^2]} \quad (5.6)
 \end{aligned}$$

$$\times \int dE_3 \frac{1}{[E_3 + \alpha'(k^2 - M^2)][E_2 - E_3 + \alpha'(k^2 - M^2)]}$$

Performing the  $E_3$  integration gives a two-reggeon denominator which cancels one of the nonsense-zeros so that we can write

$$I(y_4 - y_1) = \int dE e^{-E(y_4 - y_1)} F(E) \quad (5.7)$$

where

$$F(E) = \frac{\gamma_0^2}{\pi^2 \alpha' [E + \alpha'(q^2 - M^2)]} \int_{|k^2| < \Lambda} d^2 k \frac{[E + \alpha'(k^2 - M^2) + \alpha'((\underline{q}-k)^2 - M^2)]}{[k^2 - M^2][(\underline{q}-k)^2 - M^2]} \quad (5.8)$$

As we discussed above the multiperipheral cut of Fig. 5.1, which we have calculated here, can be distinguished from other possible cuts (shown in Fig. 5.4) in that both internal propagators remain uncut and so both signature factor poles remain. This implies that (5.8) is necessarily the dominant contribution to the complete diagram near the two-particle threshold at  $q^2 \sim 4M^2$ , which is dominated by  $k^2 \sim M^2$ ,  $(q - k)^2 \sim M^2$ . There we can take

$$F(E) \sim \frac{\gamma_0^2 E K_\Lambda^{(2)}(q^2)^2}{\pi^2 \alpha' [E - \alpha'(q^2 - M^2)]^2} \quad (5.9)$$

where

$$K_\Lambda^{(2)}(q^2) = \int_{|k^2 < \Lambda|} \frac{d^2 k}{(k^2 - M^2)((q - k)^2 - M^2)} \quad (5.10)$$

Considering the infinite series of diagrams shown in Fig. 5.5 all of which contribute to the same (four-particle amplitude) imaginary part, we obtain a simple renormalization of the reggeon propagator

$$[M_{1,1}^R]^{-1} \sim E + \alpha'(q^2 - M^2) + \frac{\gamma_0^2}{\pi^2 \alpha'} K_\Lambda^{(2)}(q^2) \quad (5.11)$$

which to  $O(r_0^2)$  gives a pole at

$$E = -\alpha'(q^2 - M^2) + \frac{\gamma_0^2}{\pi^2} (q^2 - M^2) K_\Lambda^{(2)}(q^2) \quad (5.12)$$

$$\underset{q^2 \sim 4M^2}{\sim} \frac{\gamma_0^2}{\pi^2} (q^2 - M^2) K^{(2)}(q^2) \quad (5.13)$$

where  $K^{(2)}(q^2) = \lim_{\Lambda \rightarrow \infty} K_\Lambda^{(2)}(q^2)$ . So comparing with the perturbative trajectory function (4.1) we see that we reproduce the perturbative result precisely if we make the identification

$$r_0 \sim ig \bar{f}_{ijk} \quad (5.14)$$

which is just what we would expect to get for  $r_0$  from direct calculation.

We can regard  $\alpha'$  as originating from  $k^2 \geq \Lambda$ , so if we extend the perturbative calculation into that region to define  $\alpha'$ ; we can essentially equate (5.12) and (5.13) although, of course, we have made it clear that we believe perturbative calculations are meaningless for  $k^2 > \Lambda$ . (In fact the perturbative calculation is probably only reliable for  $q^2 \sim 4M^2$  !) The point we wish to emphasize is that the singularity in transverse momentum of (4.1) is reproduced by reggeon diagrams with a regular triple reggeon vertex. The reggeization of the gluon near this threshold being directly due to the nonsense-zero of the vertex. So although the Regge cut of the reggeon diagram is cancelled the same region of phase space generates the transverse momentum singularity. It must originate from the same region of phase space, otherwise we could not use the helicity pole limit of hexagraph amplitudes to reproduce it. The leading log results described in the last section do, as we noted, arise from the multi-Regge region of phase space, so this is consistent with our results. (Actually the reggeization of those gluons producing the transverse momentum threshold, in the multi-Regge region, is not important, only that the discontinuity of a single (t-channel) helicity amplitude - with maximal helicities - is isolated in this region of phase space.)

Next we consider the triple reggeon diagram of Fig. 5.6 which, as we shall see, gives a renormalization of the triple reggeon vertex. Since the diagram gives a contribution to the triple reggeon hexagraph shown, we evaluate it as a triple discontinuity with respect to the cuts 1, 2 and 3 shown. To obtain the maximum degree of singularity in the transverse momenta we evaluate cut 3 as a "multiperipheral cut" of the reggeon loop. Again if we initially evaluate the diagram with the rapidity differences  $y_2 - y_1$ ,  $y_5 - y_3$  and  $y_6 - y_4$  finite we can use t channel unitarity to determine that the phase space integration is the usual reggeon phase space. According to the discontinuity rule 3B, cuts 1 and 2 remove the signature factors associated with reggeons d and b respectively, while rule 3C gives that cut 3 removes the signature factors associated with reggeons a and f. There are three external energies  $E_a$ ,  $E_d$ ,  $E_f$  and there is no over-all energy conservation. This implies that there is no energy conservation at one of the internal vertices, or equivalently that one of the

internal rapidities is not integrated over. To determine which vertex we look at the structure of the reggeon states as indicated by the vertical lines in Fig. 5.7. It is clear that all states to the left of the  $y_3$  vertex are associated with the  $E_a$  channel, while those to the right are associated with either  $E_d$  or  $E_f$ . Therefore reggeon unitarity will still be satisfied in each channel if the  $y_3$  vertex is energy non-conserving, or equivalently we integrate over rapidities  $y_2$  and  $y_4$  to reproduce energy conservation poles at the upper end points as in our evaluation of Fig. 5.1. Using the energy conservation to perform the  $E_e$  and  $E_c$  integrations we obtain

$$\begin{aligned} & r_0^3 \int dE_a dE_d dE_f e^{-E_a(y_3-y_1) - E_d(y_5-y_3) - E_f(y_6-y_4)} \\ & \times \int_{|k^2| < \Lambda} \alpha' d^2k \int dE_b \frac{[E_a - \Delta_b - \Delta_c][E_b - \Delta_e - \Delta_d][E_f - \Delta_e - \Delta_f]}{\sin \pi \Delta_c \sin \pi \Delta_e [E_a - \Delta_a][E_b - \Delta_b][E_d - \Delta_d][E_f - \Delta_f]} \quad (5.15) \\ & \times [E_a - E_b - \Delta_c]^{-1} [E_f - E_a + E_b - \Delta_e]^{-1} \end{aligned}$$

where

$$\begin{aligned} \Delta_a &= \Delta(q_a^2) = -\alpha'(q_a^2 - M^2), \quad \Delta_b = \Delta(k^2), \quad \Delta_c = \Delta((q_c - k)^2) \\ \Delta_d &= \Delta(q_d^2), \quad \Delta_e = \Delta((k - q_d)^2), \quad \Delta_f = \Delta((q_a - q_d)^2) \quad (5.16) \end{aligned}$$

Performing the  $E_b$  integration by closing in the left-half plane and picking up the pole at  $E_b = E_a - \Delta_c$  we obtain

$$\begin{aligned} & r_0^3 \int dE_a dE_d dE_f \frac{e^{-E_a(y_3-y_1) - E_d(y_5-y_3) - E_f(y_6-y_4)}}{(E_a - \Delta_a)(E_d - \Delta_d)(E_f - \Delta_f)} \quad (5.17) \\ & \times \left[ \alpha' \int_{|k^2| < \Lambda} d^2k \frac{(E_a - \Delta_c - \Delta_e - \Delta_d)}{\sin \pi \Delta_c \sin \pi \Delta_e} \right] \end{aligned}$$

so the reggeon loop gives no Regge cuts but instead gives only a renormalization of the triple reggeon vertex, introducing a transverse momentum singularity in  $q_f \equiv q_a - q_d$ . Note that if we evaluate the vertex appearing in the square brackets in (5.17) on energy shell, that is set  $E_a = E_d + E_f$  and also take  $E_a = \Delta_a$ ,  $E_d = \Delta_d$ ,  $E_f = \Delta_f$ , then making the approximation (5.2) and keeping only the singular part of the transverse momentum loop we obtain a renormalization of the triple reggeon vertex

$$S_{1,2}^M = - \frac{\tau_0^3}{\pi^2} \left( q_f^2 - M^2 \right) K_{\Lambda}^{(2)} \left( q_f^2 \right) \quad (5.18)$$

Clearly if we add this, together with the analogous diagram in which  $E_d \leftrightarrow E_f$  to the original triple reggeon vertex (5.3) we obtain

$$M_{1,2}^R = \tau_0 \left[ E - \Delta_R(k_1^2) - \Delta_R(k_2^2) \right] \quad (5.19)$$

where

$$\Delta_R(k^2) = - \alpha'(k^2 - M^2) + \frac{\tau_0^2}{\pi^2} \left( q^2 - M^2 \right) K_{\Lambda}^{(2)} \left( q^2 \right) \quad (5.20)$$

Comparing with (5.12) we see that the triple reggeon diagrams of Fig. 5.6 simply renormalize the triple reggeon vertex by shifting the nonsense-zero to match the shift of the trajectory produced by the diagrams of Fig. 5.5. That is the vertex acquires the two-particle threshold in each of its transverse momenta. Again our calculation keeping only the multiperipheral contribution to the 3 cut of Fig. 5.6 is only accurate near this threshold.

Consider now the insertion of the diagrams of Fig. 5.6 into diagrams for the elastic amplitude. In this case we necessarily integrate over  $y_3$  and so keep only the energy conserving part of the diagrams. For example, the "renormalized propagator" contains the diagram of Fig. 5.8 for which we consider the cut shown. This can be evaluated by repeating (5.5) - (5.8) with one triple reggeon vertex replaced by (5.18). In this case there is only one nonsense zero to cancel the two reggeon denominator and the result for the partial wave amplitude is a two loop transverse momentum integral multiplying the square of the original Regge pole propagator, that is

$$\frac{\tau_0^5 K_{\Lambda}^{(3)}(q^2)}{\alpha' \pi^4 \left[ E + \alpha'(q^2 - M^2) \right]^2} \quad (5.21)$$

where

$$K_N^{(3)}(q^2) = \int_{|k_i| < \Lambda} \frac{d^2 k_1, d^2 k_2}{[k_1^2 - M^2][k_2^2 - M^2][(q - k_1 - k_2)^2 - M^2]} \quad (5.22)$$

Summing an infinite set of similar diagrams again renormalizes the propagator pole and so introduces a three-particle threshold into the trajectory function. At first sight it also destroys the reggeization. However, we clearly must add all the diagrams shown in Fig. 5.9, so that the sum can be written in the renormalized form illustrated in Fig. 5.10 with the full vertex (5.19) and trajectory function (5.12). The manipulations (5.5) - (5.12) can then be repeated to demonstrate that the reggeization persists.

Note that the sum of diagrams implied by Figs 5.9 and 5.10, gives a trajectory function with three and four-particle thresholds, but no Regge cut is generated, even though signature conservation would allow a three reggeon cut in Fig. 5.8, for example. The simplest diagram which actually generates a three reggeon cut is that shown in Fig. 5.11, since there is no nonsense-zero capable of cancelling the propagator associated with the central three reggeon state.

At this point it is straightforward to illustrate how signature is violated in the multiparticle amplitudes but restored in elastic amplitudes. First we note that there is no signature conservation in the triple reggeon diagram of Fig. 5.6. The obvious reason for this is that there is no energy conservation at the  $y_4$  vertex and so there is no over-all energy conservation. Hence we would not expect any potential nonsense-zero to be operative. However, from (5.18) - (5.20) we see that even when energy is conserved we must add the diagram of Fig. 5.6 to other diagrams to produce a renormalized vertex before signature conservation operates in the full set of diagrams of Figs 5.9 and 5.10. Therefore we should not be surprised that the diagram for the eight point function shown in Fig. 5.12 gives no signature rule for the central two reggeon cut - the cut will be exchange degenerate - even if there is energy conservation at the non-conserving vertices  $V_N$  (this is the diagram discussed for Pomerons in Section 3). Even if the external reggeon lines are joined to form an energy conserving amplitude as in Fig. 5.13 it is still necessary to add additional diagrams as illustrated to obtain signature conservation.

From this analysis we can immediately locate some more complicated multi-particle vertices which will necessarily involve signature non-conservation. The vertex of Fig. 5.14 will be non-conserving because there is no suitable vertex to which it can be added to produce a renormalized nonsense-zero. Similarly the vertex of Fig. 5.15 will be non-conserving. These particular examples will suffice for our later discussions although clearly they are only a small subset of the kinds of amplitudes which, from their analyticity properties, we anticipated in Section 3, would lead to signature non-conservation. Although a general analysis of such amplitudes is essential as we have emphasized, we shall, in the following, simply generalize the above brief discussion of how the conservation is brought about in particular sets of diagrams.

Consider now diagrams generated by a vertex coupling two reggeons to two external particles in an even signature amplitude. This vertex could be the on-shell limit of a local four reggeon coupling. We use the notation for this vertex shown in Fig. 5.16 where we have also shown some of the even signature diagrams the presence of the vertex generates. The multiperipheral cut of the single reggeon loop diagram of Fig. 5.16 is easily evaluated. The four reggeon vertex will be unchanged by cutting and so we will simply obtain the usual two reggeon cut diagram with signature factors. That is for the partial wave amplitude we obtain

$$\frac{1}{\alpha'} \int_{|k^2| < \Lambda} \frac{d^2 k' \lambda_0^2}{[k'^2 - M^2][(q-k')^2 - M^2][E + \alpha'(k'^2 - M^2) + \alpha'((q-k')^2 - M^2)]} \quad (5.23)$$

To evaluate the next diagram of Fig. 5.16 we must first evaluate the hexagraph loop of Fig. 5.17 which involves  $\lambda_0$ . Again this is a triple discontinuity and we evaluate it analogously to Fig. 5.6 using the cuts shown. The only difference from the evaluation of Fig. 5.6 will be that in the  $E_a$  channel there will be no Regge pole, but instead the two reggeon propagator will not be cancelled by a nonsense-zero. Consequently we obtain, by comparison with (5.17), the partial wave amplitude

$$\frac{\lambda_0 r_0^2}{(E_d - \Delta_d)(E_f - \Delta_f)} \int \frac{\alpha' d^2 k [E_a - \Delta_c - \Delta_e - \Delta_d]}{\sin \pi \Delta_c \sin \pi \Delta_e [E_a - \Delta_b - \Delta_c]} \quad (5.24)$$



Substituting this result for one factor of  $\lambda_0$  in (5.23) to obtain Fig. 5.18 with the cut shown, and making analogous approximations to those made in obtaining (3.22), we are led to

$$\frac{\lambda_0^2 r_0^2}{\alpha'} \int d^2k d^2k' \left[ (k^2 - M^2)(k'^2 - M^2)((q+k-k')^2 - M^2) \right]^{-1} \quad (5.25)$$

$$\times \left[ (E - \alpha'(k^2 - M^2) - \alpha((q-k)^2 - M^2))(E - \alpha'(k'^2 - M^2) - \alpha((q-k')^2 - M^2)) \right]^{-1}$$

Again the approximations made imply that this result is only necessarily valid near the transverse momentum singularity of the diagram. That is when all particle poles are close to their mass-shell, which in this case implies that we should be near the three particle threshold at  $q^2 \approx 9M^2$ . This is sufficient, however, to make the major point we wish to emphasize since in this form (5.25) compares exactly with the perturbative reggeon diagram of Fig. 4.2, with the internal four reggeon interaction given by the singular term  $S_I$  in (4.7), if we again make the identification (5.14) and identify  $\lambda_0$  appropriately. Consequently our claims, that the transverse momentum singularities resulting from the singular part of the four reggeon interaction should really be viewed as originating from triple reggeon diagrams, is borne out. Of course, we also have to construct the full set of diagrams of Fig. 4.1 but such diagrams will arise automatically from the general iteration procedure giving the complete class of reggeon diagrams which we now outline.

We begin by noting that since hexagraphs are drawn in the plane of a page with vertices joined by horizontal lines, if we associate a rapidity variable with each vertex (defining the rapidity variables associated with horizontal lines as differences of such rapidities) then there is an automatic rapidity ordering of many of the vertices if we define rapidity as increasing from left to right horizontally. When forming loops it will be important to resolve the remaining rapidity ordering ambiguity precisely. With this in mind and also because in the helicity pole limit hexagraph amplitudes depend on rapidity variables only (not on the finite angular variables) it will be convenient to simplify the hexagraph diagrams to the usual old-fashioned (time ordered) perturbation theory diagrams used in RFT. This can be done by removing the D- and V- horizontal lines and joining smoothly the sloping lines attached to V- lines. This is illustrated in Fig. 5.16. D; V- and T- lines can still be distinguished by the nature of the vertices they join as we shall describe below.

By joining together the hexagraph trees in all topologically distinct ways we form a set of loop diagrams. We then project this set of diagrams onto a plane and look at the rapidity ordering (left to right) of all vertices. We count as distinct diagrams, all possible orderings obtained from one original loop diagram and refer to such rapidity ordered diagrams as hexagraph loops. Each vertical line cutting a maximal set of internal lines which are all connected to the same sets of external particles by all paths lying entirely to the right or to the left of the vertical line, distinguishes an "intermediate state". Defining the "channel" of the intermediate state by the external particles to which the internal lines cut are linked, the evolution of channels with rapidity maps the hexagraph loop diagram uniquely onto a hexagraph tree diagram. This is illustrated in Fig. 5.20. We can easily enlarge the set of all diagrams by allowing point vertices which couple any number of internal (and external) lines. This will also generate all the non-singular parts of the perturbative reggeon diagrams that the triple reggeon diagrams either do not produce or else produce incorrectly.

The complete set of reggeon diagrams for a particular hexagraph can now be constructed in  $E$  space as follows (we omit the rapidity space integrations included in the simple examples). First we construct the set of hexagraph loops which maps uniquely onto the hexagraph tree by the above process. The hexagraph tree corresponds to a particular multiple discontinuity (or more generally a sum of multiple discontinuities). If we consider again only the most singular part in transverse momentum of each loop then it will be sufficient to denote discontinuities by a single path through a loop diagram. (That is we neglect all discontinuities which are analogous to the doubly multiperipheral cut of Fig. 5.4 in that they pass through more than one reggeon in the same rapidity interval.) Each hexagraph loop diagram for a particular hexagraph tree is then written as a sum of diagrams in which the multiple discontinuity (or discontinuities) associated with the tree diagram is taken in all possible ways by paths through the loop diagram. Again we keep only those diagrams in which the maximum number of loops are cut "multiperipherally" by paths, or equivalently the maximum number of lines are uncut by paths. Each diagram is then "broken open", to give a diagram or diagrams, with a smaller number of loops, by breaking each uncut line. The complete process is illustrated in Fig. 5.21.

If the resulting diagrams are tree diagrams (as in Fig. 5.21) the discontinuities involved can be computed by the rules of Section 3 and the full diagram assembled as described below. If not the resulting diagrams must again be considered as multiple discontinuities and the process repeated.

To form a loop from tree amplitudes we write the amplitudes in terms of reggeon propagators (5.4), vertices containing nonsense-zeros or not, depending on whether an odd or even number of reggeons are coupled, and signature factors not removed by the discontinuities taken. The loop is then formed by first imposing transverse momentum conservation at each vertex and integrating over the remaining loop momentum. Secondly energy conservation is imposed at all vertices, except those where the vertex produces a change in the intermediate state channels propagating in rapidity - these are energy non-conserving vertices. There will initially be distinct energy integrations for each internal line of the loop, some of which can clearly be performed using energy conservation at vertices. However, the internal energy integrations will not necessarily reduce to a single energy loop integration because of the non-conserving vertices. The full amplitude corresponding to the loop can be formed by using the SW transform to reconstitute it from (the sum of) its multiple discontinuity(ies).

Having formed one loop from tree diagrams the loop amplitude can be treated as the tree diagram on to which it maps in order to form a new loop. The needed discontinuities of the first loop being taken using the SW transform. Proceeding in this way general multiloop diagrams can be built up. The diagrams can be written with the internal energies integrated over, or alternatively these integrations can be performed by picking up the poles of some reggeon propagators. Adding diagrams which differ only by the rapidity ordering of some interactions will then allow us to write the complete set of reggeon diagrams for a particular hexagraph as a set of "Rayleigh-Schrödinger" diagrams with "energy denominators" for each intermediate state, but with distinct energies for each channel.

As in the simple examples, many energy denominators will be cancelled by nonsense-zeros, leaving only transverse momentum singularities as evidence of the original reggeon states. The following rules describe this process in a large class of energy conserving diagrams

5A An energy denominator of a multi reggeon state is cancelled whenever there is at least one nonsense-zero capable of cancelling either the full denominator or the energy denominator of any substate.

5B The signature factor of a V line remains, that of a D-line is cancelled and that of a T line is replaced by the corresponding zero.

This last rule applies also to generalizations of V, T and D lines defined as follows

a T line joins two nonsense vertices with no additional production of reggeons at the earlier vertex and no additional absorption of reggeons at the final vertex.

a D line joins two vertices only one of which has the property of the T line vertices.

a V line joins two vertices, neither of which has this property.

The above rules clearly reproduce all the reggeon diagrams of Fig. 4.1 as desired. Rule 5B does not apply directly to any diagrams which give only renormalization of vertices appearing in simpler diagrams after 5A is applied. Rather 5B applies only to sums of diagrams in which all trajectory functions and vertices are renormalized in the same way (that is one-loop, two-loop, etc.).

Rule 5A applies also in multiparticle amplitudes. However, 5B applies straightforwardly only within energy conserving subparts of the multiparticle diagrams. The cancellation of signature factors and production of zeros leading to 5B is a consequence both of taking discontinuities and of the presence of nonsense-zeroes. Therefore we can expect a modification of these rules where the breakdown of signature conservation is associated with the absence of nonsense-zeroes. To illustrate this we note that the rules 5A and 5B can be easily understood for the subset of diagrams of Fig. 4.1 involving only T and V lines by taking the discontinuity shown in Fig. 5.22, which cuts every loop multiperipherally. This discontinuity removes all T line signature factors leaving simply a nonsense-zero for each vertex. For each T line we can associate one vertex zero with the removal of the adjacent three reggeon propagator leaving the second vertex zero to provide the zero of 5B.

Consider now the diagram of Fig. 5.23 where two vertices of the form of Fig. 5.15 are coupled. In this case the three reggeon propagators shown will be cancelled but the nonsense-zeros of the T line vertices are the only zeros available to do this. In contrast to the elastic amplitude case illustrated in Fig. 5.23 the (external) states adjacent to the three reggeon states produce no zeros. Hence the zeros of the T line vertices are totally absorbed by the cancellation of the propagators for the three reggeon states. Consequently while the discontinuity procedure involved in defining the diagram will still remove the T line signature factor, there will be no zero.

Perhaps the most logical procedure at this point would be to investigate rules of the above form comprehensively and at the same time look for a detailed formalism which would easily reproduce diagrams without the full labour of the

above iteration process - particularly for adding diagrams which differ only by the cuts through them. Unfortunately the general formalism of Section 3 with the helicity ordering problem properly treated is essential for this. Alternatively we could try to write a simple RFT Lagrangian to reproduce the signature conserving elastic amplitudes since this would bypass the helicity ordering problem. In fact although our results show that elastic amplitudes (like all others) can be reproduced by a set of rapidity ordered old-fashioned perturbation theory diagrams containing non-singular reggeon interactions it seems unlikely that the complicated nonsense-zero signature factor structure could be reproduced by a simple Feynman diagram Lagrangian formalism containing only such interactions (in contrast to the energy conserving Pomeron amplitudes briefly described in Section 3). It may well be that if we insist on writing an RFT Lagrangian to reproduce elastic amplitudes, then this can only be done with the signature conserving singular interactions formulated by other authors.

At first sight it even appears that our formalism could break the signature conservation rules in elastic amplitudes. Consider the diagram shown in Fig. 5.24 which we would generate in an even signature amplitude. The two reggeon states marked will, of course, appear but so also will the three reggeon state marked since there are no nonsense-zeros able to cancel it (all other states will in fact be cancelled by nonsense-zeros). The resolution of this apparent signature non-conservation involves the bootstrap equation illustrated in Fig. 4.3. This tells us that signature conservation in elastic amplitudes can sometimes appear only after summing an infinite set of diagrams. Our discussion of analyticity properties of amplitudes in Section 3 tells us that a nonsense-zero should indeed cancel the three reggeon cut of Fig. 5.24 but choosing a simple form for the initial vertices that we iterate to produce reggeon diagrams may in this and many other cases require an infinite sum to produce the zero. In this case the bootstrap equation tells us that the infinite sum of Fig. 5.25 will be sufficient to produce the zero.

Such cancellations are also important in multiparticle amplitudes for ensuring that signature non-conservation does not occur within energy conserving subparts of multiparticle reggeon diagrams. On the other hand, for the signature non-conservation illustrated in Figs 5.14 and 5.15, to be not cancelled by such sums, it is essential that transitions of states propagating past an energy non-conserving vertex are involved.

Our reason for not pursuing the detailed questions posed above is that we believe the most important and exciting question to be asked within the above formalism, is how the infra-red singularity analysis of perturbation theory, discussed in the last section, generalizes, both to the restoration of an  $SU(2)$  symmetry which is a subgroup of a larger broken symmetry, as in  $QCD_{MB}$ , and also to multiparticle amplitudes. This we shall discuss in the next section. We would clearly prefer the above rules to be more completely formulated. However, we shall be able to go quite far by applying the rules (and their violation) where we believe them. The most important result of this section is perhaps that the complete set of reggeon diagrams for all hexagraph amplitudes can be generated by an iteration process which begins with only the set of all possible local reggeon interactions which, taken on-shell, also give the particle reggeon couplings. We shall assume only that these interactions satisfy group selection rules and that they are related in zero mass limits (by Ward identities<sup>25</sup>) in such a way that the infra-red finiteness results of perturbation theory generalize.

6. - THE INFRA-RED LIMIT DEFINING  $QCD_{MB}$

We now consider the specific problem of the reggeon diagrams describing the high-energy behaviour of spontaneously broken QCD in which the Higgs mechanism is applied using two complex triplets of scalars. In this Section we ignore the quarks and so the Lagrangian can be written as in (2.17), with  $V(\rho)$  possessing a non-trivial minimum which gives expectation values to  $\phi_1(\equiv \rho_1)$  and  $\phi_2(\equiv \rho_2, \rho_3, \rho_4)$ . These expectation values give two mass scales  $M_1^2$  and  $M_2^2$  for the massive vectors originating from the Higgs mechanism. Although giving few details, we shall implicitly construct reggeon diagrams by the general formalism of the previous Section. Since we are interested in infra-red divergences only, we can eliminate any ultra-violet problems by imposing a transverse momentum cut-off.

The form (2.17) for the Lagrangian hides a global SU(2) symmetry that remains in the theory after the Higgs mechanism is applied. The symmetry results from the choice of an SU(2) direction implied by placing the  $\rho_4$  component of  $\phi$  along the two-axis in (2.15). This global symmetry plays a central role in the following. Firstly, the massive vectors form SU(2) representations. In the notation of Section 2,  $B^1, B^2, B^3$  form an SU(2) triplet with mass  $M_2$ .  $B^4-B^7$  form two SU(2) multiplets  $B^1$  and  $B^2$  with a mass which, as implied by (2.29), goes to  $M_1$  as  $M_2 \rightarrow 0$ .  $B^8$  is an SU(2) singlet whose mass similarly goes to  $2/\sqrt{3} M_1$  as  $M_2 \rightarrow 0$ . In addition, we can define a charge conjugation transformation which will classify SU(2) singlets. To exploit the underlying SU(3) symmetry we parametrize the  $B^i$  in terms of SU(3) generators as in (2.27). The charge conjugation operation can then be defined on the vectors by

$$C B_{\alpha\beta}^i C^{-1} = C [b^i \lambda_{\alpha\beta}] C^{-1} = -b^i \lambda_{\beta\alpha} = -B_{\beta\alpha}^i \quad (6.1)$$

which implies

$$B^i \rightarrow -B^i \quad i=1,3,4,6,8 \quad B^i \rightarrow B^i \quad i=2,5,7 \quad (6.2)$$

So all vector fields (and the associated reggeons) carry positive or negative charge parity. The transformation is easily extended to Higgs fields as complex conjugation, so that (when  $\Omega = 1$ ) in (2.15)  $\rho_1 \rightarrow \rho_1$ ,  $\rho_2 \rightarrow \rho_2$ ,  $\rho_3 \rightarrow -\rho_3$  and  $\rho_4 \rightarrow \rho_4$ .

In the limit that the SU(3) gauge symmetry is restored, C becomes the usual colour charge conjugation operation<sup>40)</sup>. It plays a central role in the

following. Note that the SU(2) singlets we can form, which are eigenstates of C, are the following

$$S_1 = \delta_{ij} B^i B^j \quad i, j = 1, 2, 3 \quad (6.3)$$

$$S_2 = \epsilon_{ijk} B^i B^j B^k \quad i, j, k = 1, 2, 3 \quad (6.4)$$

$$S_3 = f_{\alpha\beta\gamma} B^\alpha B^\beta B^\gamma \quad \alpha, \beta, \gamma = 4, 5, 6, 7 \quad (6.5)$$

$$S_4 = d_{\alpha\beta\gamma} B^\alpha B^\beta B^\gamma \quad \alpha, \beta, \gamma = 4, 5, 6, 7 \quad (6.6)$$

$$S_5 = B^8 \quad (6.7)$$

where the f and d symbols are the usual SU(3) tensors. From (6.2) we have

$$C S_i C^{-1} = +S_i \quad i=1, 2, 4 \quad C S_j C^{-1} = -S_j \quad j=3, 5 \quad (6.8)$$

After the Higgs symmetry breaking, all eight vectors will lie on Regge trajectories which are given in the leading log approximation by (4.1). We introduce a diagrammatic notation which will distinguish the vectors in reggeon diagrams. As illustrated in Fig. 6.1, we use a dotted line for the triplet  $B^1, B^2, B^3$ , a solid line for the two doublets  $B^4$  and  $B^5$ , and a wavy line for the singlet  $B^8$ . The triple gluon coupling in  $\mathcal{L}$  can be represented diagrammatically as in Fig. 6.2. The global SU(2) symmetry implies that the full triple reggeon couplings must have the same structure, provided that charge parity is conserved by the vertices. Since it is conserved (with or without quarks), only even numbers of d tensors are generated by gluon or Higgs loops. Consequently, the triple reggeon couplings have the structure of Fig. 6.2.



The leading log trajectory functions of (4.1), or in the language of the last Section, the one reggeon loop renormalization of the trajectory, can be represented as in Fig. 6.3. From this figure we see immediately that if we let  $M_2^2 \rightarrow 0$ , so that  $B^1, B^2, B^3$  become massless, then in the one-loop approximation the  $B^8$  trajectory function remains infra-red finite. From Section 4 we also know that the other trajectory function divergences can be absorbed into effective finite interactions as illustrated in Fig. 6.4. It is straightforward to check that the divergent parts of the diagrams of Fig. 6.4 cancel only when the (t channel) SU(2) colour is zero.

For our purposes, it will be convenient to separate the singular loop diagram in the  $B^1$  trajectory function into a singular and finite part by noting that the relevant loop integral is

$$K^{(2)}(M_1^2, M_2^2, q^2) = \int \frac{d^2 k}{[(q-k)^2 - M_1^2][k^2 - M_2^2]} \quad (6.9)$$

$$= \frac{1}{2\sqrt{Q}} \ln \left[ \frac{(q^2 + \Delta + \sqrt{Q})(q^2 - \Delta + \sqrt{Q})}{(q^2 + \Delta - \sqrt{Q})(q^2 - \Delta - \sqrt{Q})} \right] \quad (6.10)$$

where

$$Q = [q^2 - (M_1 - M_2)^2][q^2 - (M_1 + M_2)^2] \quad (6.11)$$

and

$$\Delta = M_1^2 - M_2^2 \quad (6.12)$$

The logarithmic divergence of (6.9) as  $M_2^2 \rightarrow 0$  arises in (6.10) from the factor  $(q^2 - \Delta - \sqrt{Q})$  in the logarithm, while the divergence as  $M_1^2 \rightarrow 0$  arises from the  $(q^2 + \Delta - \sqrt{Q})$  factor. We shall separate these divergences by writing

$$K^{(2)} = K_1^{(2)} + K_2^{(2)} \quad (6.13)$$

where

$$K_1^{(2)} = \frac{1}{2\sqrt{Q}} \ln \left[ \frac{q^2 + \Delta + \sqrt{Q}}{q^2 + \Delta - \sqrt{Q}} \right] \quad (6.14)$$

$$\xrightarrow{M_2^2 \rightarrow 0} \frac{-1}{2(q^2 - M_1^2)} \ln \left[ \frac{q^2}{M_1^2} \right] \quad (6.15)$$

and  $K_2^{(2)}$  is defined by  $+\Delta \rightarrow -\Delta$  in (6.14). We represent the same split in the trajectory function formally by Fig. 6.5. We then absorb only the  $K_1$  factor into the interaction, replacing the diagrams of Figs. 6.3 by the complete set of finite trajectories of Fig. 6.6. The SU(2) invariant interaction will still be infra-red finite, however the trajectory for the  $B_1^1$  and  $B_2^2$  doublets will now be

$$\tilde{\alpha}_i(q^2) \underset{M_2^2 \rightarrow 0}{\sim} 1 + \frac{3g^2}{2\pi^2} (q^2 - M_1^2) \left[ K_1^{(2)}(M_1^2, M_2^2) + K^{(2)}(M_1^2, \frac{4}{3}M_1^2) \right] \quad (6.16)$$

$$\rightarrow 1 - \frac{3g^2}{4\pi^2} \ln \left[ \frac{q^2}{M_1^2} \right] + \frac{3g^2}{2\pi^2} (q^2 - M_1^2) K^{(2)}(M_1^2, \frac{4}{3}M_1^2) \quad (6.17)$$

so that

$$\tilde{\alpha}_i(q^2) \xrightarrow{q^2 \rightarrow 0} -\infty \quad (6.18)$$

So if we absorb only the infra-red divergent part of the trajectory into the effective interaction, we have an effective trajectory which implies that near  $q^2 = 0$  we can ignore the high-energy behaviour associated with the doublet trajectories, although they do still generate SU(2) singlet particle states with mass  $\sim M_1^2$ . If we assume that this is the correct way to organize the  $M_2^2 \rightarrow 0$  limit, we will have an adequate description, for our purposes, of the confined status of the doublet vectors as the SU(2) gauge symmetry is restored.

We are now in a position to analyse the infra-red singularities as  $M_2^2 \rightarrow 0$  by extrapolating the results of Section 4. Consider first the set of energy-conserving reggeon amplitudes obtained by drawing all possible diagrams involving the reggeons of Fig. 6.1 with the triple reggeon interactions of Fig. 6.2. The infra-red finiteness results of Section 4 will generalize if we organize the diagrams as follows. We write the diagrams in terms of the infra-red finite trajectories of Fig. 6.6 (that the massless gluon\*) lies on a finite slope trajectory will not change the infra-red analysis). As we made clear, there are two kinds of cancellation central in the infra-red analysis. The first kind, analogous to (4.14), is already described in Fig. 6.4. The second cancellation (4.15) will be obtained by adding the necessary local four-reggeon interactions (which we assume here are correctly determined by the gauge-invariance of the theory). The complete set of SU(2) colour-zero, infra-red finite, energy-conserving, four-reggeon interactions will therefore be those given by Fig. 6.7 in which are embodied all the infra-red cancellations, together with all those generated by finite triple and quartic reggeon interactions amongst the massive reggeons. With this set of interactions, and the infra-red finite trajectories, we will obtain a complete set of colour-zero, infra-red finite, "off-shell", energy-conserving reggeon diagrams.

Consider next the coupling of the energy-conserving diagrams to particles to define elastic amplitudes. In principle, there could be couplings to external particles of all combinations of even and odd numbers of reggeons carrying SU(2) colour-zero which would appear respectively in even and odd signature amplitudes. However, to lowest order (or in the SU(3) limit) for all couplings and exactly for couplings involving just gluons, the couplings arise from the  $t$  channel exchange of a gauge-invariant vector. Consequently, in elastic scattering,  $s$  channel helicities are conserved<sup>41)</sup>. This implies there is no parity transformation from the initial to the final state. In this case, the signature of a  $t$ -channel reggeon state must coincide with its charge parity (more generally<sup>32),42)</sup> signature involves TCP). From (6.3) - (6.8) we see that all colour singlet combinations of gluons (that is  $B^1, B^2, B^3$  have even charge parity. Consequently, amplitudes involving only colour-zero combinations of gluons must all have even signature, and so contain an even number of gluons. All additional allowed couplings must have the correct combination of signature (determined by an odd or even number of reggeons) and charge parity [determined by (6.3) - (6.8)] for the coupled reggeons. Allowed couplings are illustrated in Fig. 6.8. [Since we are ultimately interested in restoration of the SU(3) symmetry, we need only such couplings.] Actually,

---

\*) We consistently refer to massless gauge vector particles as "gluons". The context should make it clear whether "gluons" are also considered as reggeons in the following.

the results of Refs. 39) and 43) imply that not all allowed couplings are present, in particular, the even signature combination of two doublet vectors or two singlet vectors seems to be absent. [This is almost certainly important for the comparison with super-critical RFT although at present we have no general explanation for it.]

We can, of course, regard the two-particle/many reggeon couplings as just on-shell limits of local two-reggeon/many reggeon couplings. We therefore enlarge the reggeon diagram framework to its most general structure by first allowing all signature-conserving local couplings of arbitrary numbers of reggeons in colour-zero combinations having identical signature and charge parity. We also allow signature non-conserving couplings which conserve charge parity and carry nonsense-zeros as described in the last Section. We assume that all couplings of non-zero colour reggeon states are either removed by the infra-red limit, or are absorbed into infra-red finite, but non-local signature conserving interactions as generalizations of Fig. 6.7. It seems safe to assume that with this general set of couplings we can produce all the mass-shell infra-red singular part of  $\text{QCD}_{\text{MB}}$  elastic amplitudes. If, in addition, we allow diagrams with the same vertices, but at some of which there is no energy conservation, then, as discussed in the last Section, we can also reproduce all the infra-red singular part of the multiparticle amplitudes. The question now is how does the mass-shell singularity analysis of Section 4 generalize to this full set of  $\text{QCD}_{\text{MB}}$  amplitudes?

As we discussed in Section 4, the central element in the analysis of mass-shell infra-red singularities is that when some reggeons of a reggeon coupling involving non-local contributions are taken on-shell, the cancellation (4.15) between local and non-local couplings breaks down. This is because the non-local part decouples in the mass-shell limit. This situation clearly generalizes so that we will have mass-shell singularities whenever some number of gluons couples to an external state, carrying finite transverse momentum, as illustrated in Fig. 6.9. Suppose first there are no accompanying massive reggeons in the gluon state, then not all gluons can carry zero transverse momentum. Consequently, their self-interaction will be described by a singular kernel which will remove the infra-red singularity as a generalization of (4.19)-(4.32), as illustrated in Fig. 6.10..

Next suppose that there are accompanying massive reggeons. The existence of the external particle coupling implies that the reggeons plus gluons have the correct charge-conjugation to allow a local self-interaction. Summing the diagrams with this self-interaction, as illustrated in Fig. 6.11, leads to an infra-red finite result of the form

$$S d\Omega / 1 + I S d\Omega \tag{6.19}$$

where  $Sd\Omega$  is the divergent phase-space and  $I$  is the self-interaction. Since there exists one set of diagrams in which the divergence cancels, we assume that it is cancelled in the complete set of diagrams.

To avoid the above arguments, we need to find a combination of reggeons and gluons with a charge conjugation which prevents their self-interaction and in which the gluons all carry zero transverse momentum so that the scale-invariance of the gluon self-interaction will allow some infra-red singularity to remain after the interaction. The simplest possibility is the combination of a singlet reggeon with a triplet of gluons as illustrated in Fig. 6.12. This carries negative charge conjugation (from the reggeon), but is an even signature combination. However, this property which prevents the interaction between the reggeon and the gluons, also prevents the coupling to a local external particle state. Therefore, the combination of Fig. 6.12 does not appear in elastic amplitudes. In fact, our present analysis implies that all colour-zero elastic amplitudes will actually be infra-red finite (at large rapidity).

To find the potentially infra-red singular combination of Fig. 6.12 we must go to a multiparticle amplitude. The simplest amplitude which does not violate any of the above constraints is that shown in Fig. 6.13. Since this diagram is our prototype for the generation of the Pomeron in  $QCD_{MB}$ , we shall discuss it in some detail. First we note that it is a hexagraph loop diagram whose essential structure is that shown in Fig. 6.14, and so is just of the kind that we have anticipated from the previous Sections will not obey the elastic signature rules, and will, in fact, give an exchange degenerate four-reggeon cut in the central  $t$  channel. This central state involves an integration over three transverse momenta  $\underline{k}_1, \underline{k}_2, \underline{k}_3$ . Interactions of the scale-invariant kernel  $K(\underline{k}_1, \underline{k}_2, \underline{k}_3)$  illustrated in Fig. 6.15 will cancel the infra-red divergences from the regions

$$\underline{k}_i^2 \sim 0 \quad i=1,2,3 \quad \underline{k}_i^2, \underline{k}_j^2 \sim 0 \quad (i,j)=(1,2),(2,3),(3,2) \quad (6.20)$$

and we will be left only with the divergence as

$$\underline{k}_1 \sim \underline{k}_2 \sim \underline{k}_3 \rightarrow 0 \quad (6.21)$$

Since the kernel  $K(\underline{k}_1, \underline{k}_2, \underline{k}_3)$  will be finite in this limit due to its scale invariance property, this divergence will occur in the same way in all the interacting diagrams. Therefore, the leading divergence (in the sense that the minimum

number of gluons is involved) is the non-interacting diagram of Fig. 6.13. If we simply cut out the region of phase-space (6.20), keeping only the divergence from (6.21), then since the reggeon plus gluons propagator gives

$$\frac{1}{E - \Delta_0(k_1^2) - \Delta_0(k_2^2) - \Delta_0(k_3^2) - \Delta_8(q_1 - k_1 - k_2 - k_3)^2} \rightarrow \frac{1}{E - \Delta_8(q^2)} \quad (6.22)$$

and the gluon signature factors combine to give an over-all logarithmic divergence

$$\int \frac{d^2 k_1 d^2 k_2 d^2 k_3}{k_1^2 k_2^2 k_3^2} \rightarrow \int \frac{k^5 dk}{k^6} \sim \int \frac{dk}{k} \quad (6.23)$$

we obtain from Fig. 6.13

$$\sim \lim_{M_2^2 \rightarrow 0} M_2^2 \left[ \beta(E_1, E_2, q_1, q_2) \frac{1}{E - \Delta_8(q^2)} \beta(E_3, E_4, q_3, q_4) \right] \quad (6.24)$$

where  $\beta$  contains a two reggeon transverse momentum loop and propagator, and also contains all the ambiguity associated with the removal of the phase-space (6.20). There is no signature factor because the reggeon line of Fig. 6.13 is a generalized T line as defined in the last Section. There will also be no T line zero since the couplings are non-energy conserving and their nonsense zeros are not operative.

The obvious (and unambiguous) feature of (6.24) is the occurrence of the Regge pole propagator to give an exchange degenerate singularity. That is, the exchange degenerate Regge cut in Fig. 6.13 becomes a Regge pole in the limit  $M_2^2 \rightarrow 0$ . [Note that it is important that the region of phase-space (6.21) is that from which the Regge cut is generated, whereas (6.20) is not. Since the Regge cut gives the leading asymptotic behaviour of Fig. 6.13 for  $M_2^2 \neq 0$ , if the infra-red divergence from the regions of phase-space of (6.20) survived, the high-energy behaviour of the reggeon diagrams could not have a smooth limit as  $M_2^2 \rightarrow 0$ , and the whole approach of this paper would be unlikely to succeed.] As we have anticipated, the  $M_2^2$  singularity can, in principle, be absorbed into a definition of the residue functions and consequently into a redefinition of the external states.

We believe it is significant that we can interpret this redefinition of the external states as a "closed string" renormalization of the local vector states.

We do this as follows. Interpreting Fig. 6.13 as a high-energy scattering process with  $q^2$  spacelike, but  $q_1^2, \dots, q_4^2$  taken timelike, the "initial" ( $C = +1$ ) local vector states scatter into ( $C = -1$ ) local vector states accompanied by a "flux" of zero colour gluons in the transverse momentum configuration of (6.21). In the conjugate (transverse) co-ordinate space, multiple gluon states with transverse momenta uniformly taken to zero will be conjugate to states with the same gluons initially randomly placed and then uniformly moved out to infinity. When an infinite number of gluons is involved in this process (as will soon be the case), this is just the configuration of gluons that we would expect to appear as the large distance limit (in reality, the zero transverse momentum limit) of a "closed string" (tube) of flux surrounding the massive vector state as in Fig. 6.16. In Section 8 we will argue that the charge conjugation property of the "flux-tubes" we are producing is consistent with their qualitative identification as "approximate" Wilson loops of flux.

Since the flux tube is also exchanged between the scattering vector states, our initial picture of the  $QCD_{MB}$  Pomeron is as a singlet reggeized vector  $B^8$  propagating inside a large  $SU(2)$  flux tube which gives it an even signature component. Note, however, that this Pomeron is odd under the charge conjugation operation of (6.1). Assuming that it couples to physical particle/antiparticle  $t$ -channel states with even signature (implying even angular momentum), then such physical states must also be odd under colour charge conjugation. The vacuum quantum numbers of the Pomeron therefore suggest the physical interpretation of this result that the QCD vacuum is odd under colour charge conjugation. We shall return to this point in the next Section when discussing chiral symmetry breaking.

Of course, it is consistent with our general aims that we are not concerned with obtaining a precise description of the physical states which are formed by the process of restoring the  $SU(2)$  symmetry. We need only to be confident that they are truly confined hadron-like states to be sure that we are identifying the correct "physical" Pomeron. Nevertheless, we can argue that our approximate identification of the states as above, and in the following, together with their confining properties, is actually a demonstration of confinement as the  $SU(2)$  symmetry is restored.

We do, however, wish to describe the Pomeron precisely and here we exploit the fact that all the ambiguity in identifying the infra-red divergent part of Fig. 6.13 can be absorbed by the residue functions of (6.22). The Pomeron propagator is unambiguously

$$\Gamma_{\mathbb{P}}^{(1,1)} = \frac{1}{E - \Delta_g(q^2)} \quad (6.23)$$

and we can extract this from the reggeon plus gluon state of Fig. 6.12 by the simple prescription of writing for each massless gluon

$$\int \frac{d^2 k_i}{k^2} \rightarrow \int d^2 \underline{k}_i \delta^2(k_i) \quad (6.24)$$

Since  $\Delta_0(\underline{k}^2) = 0$ , the massless gluons then automatically contribute zero energy to the energy denominator which simply becomes (6.23).

We now look for additional diagrams that will be singular, for analogous reasons, to that of Fig. 6.13. Clearly, we can simply add even numbers of gluons, in colour singlet combinations, produced and absorbed at the same points as the triplet in Fig. 6.13. The total number of gluons will again have disparate signature and charge conjugation and so be prevented from interacting with the reggeon. However, any even number, colour-zero subset will have a local interaction with the reggeon, producing diagrams which will sum to cancel the additional divergence associated with this subset in the original diagram as in (6.19), and illustrated in Fig. 6.17. Therefore, only the single divergence produced as the transverse momentum of all gluons goes uniformly to zero is present in such diagrams, there is no enhancement of the degree of singularity. As a result, the effect of these diagrams is to add gluons to the surrounding flux tube of Fig. 6.16. Since vertices with the same external particles and reggeons, but different numbers of gluons, will be related<sup>25)</sup> by Ward identities as a consequence of gauge invariance, the effect of the additional gluons in the flux tube will be simply to produce what we shall call a gauge-invariant flux tube, containing (after adding all similar diagrams) an infinite number of massless gluons. The description of the resulting Pomeron will still be as in (6.23) and (6.24).

To find diagrams with additional degrees of divergence, we have to exploit a fundamental property of the energy non-conserving vertices. All the cancellations, which we are assuming exist as generalizations of (4.15), are between signature-conserving local and non-local vertices; the non-local vertices arising from the cancellation of a signature-violating reggeon intermediate state by a nonsense zero. In multiparticle amplitudes the existence of the energy non-conservation vertices allows non-local vertices which also arise from the cancellation of a



reggeon state by a nonsense zero, but which (over-all) are signature non-conserving (or, as in the next Section, charge conjugation non-conserving). For such non-local vertices, local vertices cannot possibly exist to provide infra-red cancellations. A potential non-local vertex of this kind is illustrated in Fig. 6.18. Both local vertices in the Figure are charge conjugation preserving, but while the top vertex is signature conserving, the bottom is non-conserving. The consequent nonsense zero leads to the cancellation of the reggeon intermediate state involving the exchanged reggeon. [In elastic amplitudes, the resulting non-local vertex combines with other vertices as discussed in the last Section and is eliminated.] Since the exchanged reggeon is actually taken on mass-shell in defining the non-local vertex, the top local vertex effectively becomes an on mass-shell vertex coupling directly to massless gluons which will have no zero to cancel the gluon infra-red divergence. The only possibility for cancellation would be the existence of a local vertex of the form shown in Fig. 6.19. Since such a vertex would be signature non-conserving and itself have a nonsense zero, it could not cancel the non-vanishing vertex produced by Fig. 6.18.

Vertices of the form of Fig. 6.18 can only occur accompanying energy non-conservation vertices as in Fig. 6.20. The presence of the energy non-conserving vertex means that we again have the situation of Fig. 5.14 where signature rules break down. According to the construction process outlined in the last Section, the main loop of Fig. 6.20 is constructed as an integral over the energy  $E$  illustrated in Fig. 6.21. This figure shows that singularities in the right-half  $E$  plane come either from the massless gluon channel or from the exchanged reggeon channel ( $E-E_c$  in Fig. 6.21). The second possibility corresponds to the rapidity-ordering of Fig. 6.22 and gives only an energy non-conserving vertex for production of the three reggeon state as indicated. The rapidity ordering which interests us is that obtained by picking up the massless gluon in the  $E$  integration. The infra-red divergence of this contribution, which is not cancelled by interactions, will again be that in which the transverse momenta of all the gluons are taken uniformly to zero, at which point the gluon state has  $E = 0$ . Consequently, if the resulting logarithmic mass divergence is absorbed into the external state as before, the residue will be a singular reggeon transition as illustrated in Fig. 6.23, with the vertex  $V$  given by

$$V = \frac{A(E=0, \underline{k}=0, \underline{k}')}{\Delta(\underline{k}'^2)} V_L \quad (6.25)$$

where  $V_L$  is the original local vertex (with nonsense-zero removed),  $\Delta(\underline{k}^2)$  originates from the signature factor of the exchanged reggeon, and  $A$  is the

amplitude for production by zero colour, zero energy, zero momentum transfer, gluons, of the combination of produced and exchanged reggeons. On dimensional grounds alone we must have  $A \sim M_1^2$ , as is easily checked on examples. As in our discussion of Fig. 6.13, the pair of gluons could be replaced by any colour zero, even signature combination. Summing all such diagrams will again produce a "gauge-invariant" flux tube.

Generalizing this last discussion, we will generate additional infra-red divergences in all diagrams having the general form illustrated in Fig. 6.24. The hatched lines can be replaced by any combination of reggeons that is consistent with the local vertices shown. In all such diagrams, we shall obtain the correct form for the propagating reggeon states, after removing infra-red divergences, if we make the replacement (6.24) for each massless gluon and if each massless colour singlet which produces or absorbs massive reggeons is initially allowed to carry separate energy, which is then set to zero. That is, for each such (even signature) colour singlet we effectively write

$$\int dE \delta(E) \int d^2k \delta^2(k) \quad (6.26)$$

Consequently, we have "vacuum production and absorption" of all even signature combinations of massive reggeons exactly as in super-critical RFT<sup>19)</sup>. Clearly, this production and absorption can include the combination of reggeons and gluons that we would identify as two Pomerons (by the vertex illustrated in Fig. 6.25). As above, we add together all diagrams of the form of Fig. 6.24, but differing only by the number of gluons involved in one or more of the even signature vacuum production or absorption combinations. Ward identities for the vertices involved<sup>25)</sup> imply then that each vacuum production or absorption involves an independent "gauge-invariant" large transverse flux tube producing an additional logarithmic divergence factor to be absorbed into the definition of the external states.

From our infra-red analysis of  $QCD_{MB}$ , we can so far tentatively conclude that

- 6.1) the Pomeron is a Regge pole, exchange degenerate with the singlet reggeon trajectory - both trajectories have  $C = -1$ .
- 6.2) there is vacuum production and absorption of even signature states of reggeons and Pomerons which vanishes as  $M_1^2 \rightarrow 0$ , or as the  $SU(3)$  symmetry is restored.

Since these are essentially the defining features of super critical RFT as we

have defined it in previous papers<sup>19)</sup>, we feel confident that a precise comparison can be made. However, there is so far a missing element which we shall discuss further in the next Section, and that is the triple Pomeron vertex. For this, quarks are essential, and we defer all discussion of quarks until the next Section. We shall also indicate that all the external states can be treated symmetrically in terms of the production and absorption of massless gluons, once quarks are included. This is not the case for Fig. 6.24 and clearly indicates that we do not yet have a satisfactory definition of external states - a minimum requirement being that there is elastic scattering!

7. - QUARKS, ASYMPTOTIC FREEDOM, CHIRAL SYMMETRY BREAKING  
AND THE CRITICAL LIMIT

This section is devoted to those parts of our arguments that depend strongly on the presence of quarks in  $\text{QCD}_{\text{MB}}$ . As we shall see the quarks are an essential dynamical ingredient in the whole argument that the limit  $\text{QCD}_{\text{MB}} \rightarrow \text{QCD}_{\text{M}}$  gives the critical Pomeron. Nevertheless some work is needed to adequately incorporate fermion reggeons<sup>44),45)</sup> into our multi-Regge formalism and this must be done before the arguments outlined below can be made more precise.

We consider first the significance of asymptotic freedom for our constructions. As we discussed in Section 2 it is necessary to saturate asymptotically free QCD with quarks in order to break the gauge symmetry to  $\text{SU}(2)$  and retain asymptotic freedom. On general grounds it is likely that asymptotic freedom is essential to even define a four-dimensional continuum theory (the renormalon problem<sup>8)</sup> being one of many ways of seeing the probably insuperable difficulty of constructing a just-renormalizable, non-asymptotically free theory, outside of perturbation theory). Since we want the mass of the singlet vector  $B^8$  to be a well-defined S matrix concept (independent of any cut-off) defining precisely the critical limit for the Pomeron, as we shall discuss shortly, we need to define  $\text{QCD}_{\text{MB}}$  as a continuum theory. For this reason alone it is probably essential for us to have asymptotic freedom. However, as we implied in the Introduction we would also like to see specifically that asymptotic freedom provides sufficient transverse momentum cut-off to eliminate the possibility of fixed singularities in the angular momentum plane such as the fixed-cut of the leading logarithm diagrams discussed in Section 4. [Actually it has recently been shown<sup>46)</sup> that the fixed cut suffers from precisely the ambiguity that we expect of a just-renormalizable theory in the ultra-violet region, that is its presence or absence depends on the method of regularization employed - it is absent when dimensional regularization is used. The importance of asymptotic freedom is, of course, that it eliminates this ambiguity.]

In fact it is almost orthogonal to the construction of the theory by reggeon unitarity to try to construct the theory perturbatively at large transverse momentum. The unitarity and dispersion relation formalism really only makes sense at low transverse momentum (strictly when all reggeons are on-shell). It is therefore reliable precisely when all the arguments made are of an infra-red or critical phenomenon kind where a transverse momentum cut-off can as well be kept throughout. It suffices then to know that the parameter which defines a critical limit (for us this will be the singlet mass) is a well-defined physical (S matrix) concept and there is no need to analyze the theory in detail away from the infra-red region.

Nevertheless it is interesting to ask whether asymptotic freedom can be used to define a reggeon theory perturbatively (and convergently) at large transverse momentum, which smoothly joins with our infra-red analysis. This would in principle provide a mechanism to see the connection between perturbation theory and the confining (flux-tube) Pomeron which emerges from our analysis without the symmetry breaking that we have used.

Bronzan and Sugar<sup>7)</sup> have discussed how to apply the renormalization group to the transverse momentum dependence of the high energy formalism and so introduce the running coupling constant as a function of transverse momentum. This work shows that the full gluon kernels  $K_N$  of Section 4 will satisfy

$$K_N(q, q, \underline{k}_i, E) \xrightarrow{k_i \rightarrow \infty} K_{\text{perturbative}}\left(q\left(\frac{k^2}{\lambda^2}\right), \frac{q}{|k|}, \frac{k_i}{|k|}\right) \quad (7.1)$$

$$\sim \frac{1}{[\ln(b^2/\lambda^2)]^N} K_{\text{perturbative}}\left(q_0, \frac{q}{|k|}, \frac{k_i}{|k|}\right) \quad (7.2)$$

where  $\lambda$  is the renormalization group scale. This logarithmic damping is sufficient to break the ultra-violet scale invariance of the  $K_N$ , giving ultra-violet convergence and eliminating the possibility of a fixed cut. (The infra-red scale invariance which we have exploited in previous sections will be unaltered.) However, the Bronzan and Sugar analysis also shows that if the perturbative kernels are used for all values of  $\underline{k}_i$ , then the renormalization group transformation simply replaces the ultra-violet divergence by an infra-red divergence.

Since we have learnt how the infra-red divergences of reggeon diagrams are absorbed into external states leaving infra-red finite results we should now be able to adapt the Bronzan and Sugar formalism to show that asymptotic freedom does indeed provide sufficient damping to remove the transverse momentum cut-off in our formalism. In the last section we stated that we had cut off the transverse momentum in all diagrams without specifying precisely how this was to be done. It is important that all of the massless gluons in the diagrams we kept (and which we shall describe a little more fully shortly) carried zero transverse momentum so that no (ambiguous) relic of the full cut-off remains in the SU(2) sector of the theory. The remaining part of the theory is precisely that which can be cut off by asymptotic freedom (when we have sixteen flavours of quarks).

Next we come to the problem of finding the triple Pomeron vertex in QCD<sub>MB</sub>. If the Pomeron is composed (in a first approximation, of course) of a reggeon plus gluons as in Fig. 6.12, then we need a vertex of the form of Fig. 7.1a, or,

since any even number of gluons is essentially equivalent, at least a vertex of the form of Fig. 7.1b. However, such vertices do not conserve charge parity and so certainly cannot be constructed from the triple reggeon vertices of Fig. 6.2. Equivalently we require a coupling constructed from an odd number of  $SU(3)$   $d$  tensors. A  $d$  tensor would allow the additional triple reggeon tensor couplings shown in Fig. 7.2. The simplest tensor structure for the vertices of Fig. 7.1 would then be that shown in Fig. 7.3.

The charge conjugation transformation can be extended to quarks as usual with the result that the  $QCD_{MB}$  Lagrangian is still invariant under the transformation. Since the  $B$  fields carry definite charge conjugation it follows from the path-integral representation for their Green's functions that these Green's functions must conserve charge conjugation. (In particular even in the presence of quarks the full triple gluon vertex must have the tensor structure of Fig. 6.2.) This implies we must look for the Pomeron interaction diagrams within charge conjugation conserving multi-gluon amplitudes (this is clearly related to and potentially in conflict with our asymmetric treatment of the external states in the previous section). An additional requirement is that we want to identify the Pomeron with an internal  $T$  line reggeon (plus gluons) but we do not want a  $T$  line zero (cf. rule 5B). Therefore the  $T$  line must be connected back to external energy non-conserving vertices. Thirdly we want to couple the positive charge parity gluon triplets into the vertex using quarks (to produce the transformation of charge parity) in an essential way. However, the triplet needs to couple essentially like an axial vector in that it carries odd signature but positive charge-parity. This implies it does not couple to on-shell quarks for the same reasons that we have noted earlier for the absence of local couplings for the triplet (helicity is preserved in elastic scattering). It must therefore couple to off-shell (that is reggeized) quarks only and therefore must couple in a nonsense state. For infra-red finiteness, the reggeized quarks must also propagate in colour-zero combinations. Finally we also want the quark loops involved to produce a  $d$  tensor coupling.

Although this is a large list of requirements they are clearly inter-related and we anticipate they have a simultaneous solution. The simplest possible coupling seems to us to be that shown in Fig. 7.4 where we have used a double solid line to indicate a (reggeized) quark. The nonsense couplings shown firstly allow the gluon triplets to couple and secondly allow the reggeons to be  $T$  lines which because of the coupling of the gluon triplets back to the external states will carry no  $T$  line zero (analogously to the diagram of Fig. 5.23). Also since we have a quark-loop with an odd number of "axial vectors" coupling we should

generate a  $d$  tensor coupling in analogy with the familiar axial vector anomaly - the tensor structure of Fig. 7.3a seems the most likely. Clearly only a more complete analysis including reggeized quarks in our formalism can properly determine whether the diagram of Fig. 7.4 will indeed contribute to the triple Pomeron vertex. For the moment we assume that it does although our following discussion will generalize to a more complicated vertex.

Firstly we note that the gluon triplets absorbed by the quark loop must be accompanied by additional triplets (to couple locally to external states) which must be absorbed somewhere. In fact the most obvious possibility for this absorption is at the initial and final vertices so that the external states can be symmetrized (with respect to charge conjugation) as we require. In this case our triple Pomeron diagrams will now have the structure illustrated in Fig. 7.5, where we have used a single dotted line to indicate a gluon triplet. Every single Pomeron state is accompanied by an odd number of ("axial vector") gluon triplets while each two Pomeron state is accompanied by an even number. The exact number is immaterial as Fig. 7.5 implies. The triplet coupling into the quark-loop has the form of the signature violating non-local vertex of 5.15 which we concluded in the previous section would generate additional infra-red divergences. We anticipate therefore that there will be an additional logarithmic divergence for each such coupling and that adding diagrams with additional gluons, but the same degree of divergence, will simply convert each combination of gluons involved into a gauge-invariant transverse flux-tube as for the vacuum production diagrams of the last section. The distinction between the "flux tubes" involved in the triple Pomeron interactions and those involved in the vacuum production and absorption is that the former involves a potentially odd-signature (or "axial-vector") combination of gluons while the latter involves only even-signature combinations of gluons. We can briefly summarize the final flux tube interpretation of the  $QCD_{MB}$  Pomeron and the physical states coupling to the one-Pomeron exchange diagrams as follows.

Firstly the physical states (that we have found so far) are colour-zero combinations of a finite number of massive reggeized gluons (or quarks) surrounded by a superposition of large transverse "closed strings" or "flux tubes" defined strictly as gauge-invariant combinations of non-interacting zero transverse momenta gluons, which we refer to picturesquely as a thick flux tube. The thick flux-tube has three essential properties, the first two of which are properties (6.1) and (6.2) of the previous section. The third property is that the flux tube is able to interact with massive reggeons to produce an effective triple Pomeron interaction and in addition allows pairs of  $C = -1$  states to couple to the Pomeron.

This "picturesque" picture of the  $QCD_{MB}$  Pomeron is illustrated in Fig. 7.6, where we have also shown the equivalent super-critical Pomeron diagram. (We should emphasize perhaps that since we calculate only  $S$  matrix elements in our formalism we clearly have no authentic space-time picture of the states or the Pomeron.)

At this point it seems extremely likely to us that a precise comparison of the Pomeron in  $QCD_{MB}$  and the super-critical Pomeron can be made. However, to make the comparison diagram by diagram it will be necessary to go through the multi-Regge and infra-red analysis of previous sections in complete detail. As we remarked in the Introduction we also intend to publish a complete derivation of the super-critical RFT formalism direct from Reggeon unitarity which we have derived but so far left unpublished (since we believed there would be more interest in the subject if the connection with QCD was first made apparent in this paper). In the next section we shall summarize the general arguments for the connection of the critical Pomeron with  $QCD_M$ , which we also believe are very striking.

Let us accept, for the moment, that the high energy behaviour of  $QCD_{MB}$  is indeed described by the super-critical Pomeron RFT formalism that we have described in previous papers. In this case we have an exchange degenerate Pomeron, a triple (and higher) Pomeron vertex and there is vacuum production and absorption of Pomerons leading to effective singular Pomeron interactions. (The formalism is illustrated in Fig. 7.7, where we have reverted to the conventional notation of a wavy line for the Pomeron.) The odd signature component of the Pomeron couples to the even-signature component only through diagrams involving vacuum production and absorption. The critical limit in which the Pomeron intercept goes to one also involves the vanishing of vacuum production so that while the intercept of the exchange degenerate odd-signature trajectory also goes to one it completely decouples from the Pomeron and presumably also from all physical states.

Clearly if this is the behaviour of  $QCD_{MB}$  as we take the mass of the singlet  $B^8$  vector to zero it will be completely consistent that this limit should give pure  $QCD_M$ . We will then be left with the critical Pomeron as the only physical manifestation of all exchanged gluons. Our flux-tube picture of the Pomeron gives a very attractive picture of the critical limit which we briefly described in Section 2 and which is illustrated in Fig. 7.8. In the critical limit infinitely many massive (becoming massless) reggeons share the available transverse momentum and so move towards large transverse distance to be absorbed into the "thick" flux tube and define an  $SU(3)$  symmetric flux tube. Since this flux tube will



have the symmetry under rotation (in transverse space) of the familiar dual model closed string it is natural to expect it to be purely even signature, as the critical limit requires. Also as we remarked in Section 2 it is likely to give exchange degenerate trajectories before the  $SU(3)$  symmetry is restored.

The physical states of  $QCD_M$  must now be colour-zero combinations of quarks surrounded by a Pomeron flux tube carrying negative charge parity. These states will still allow the physical charge conjugation operation to be defined in terms of the quark content of the state and particle-antiparticle transformations can still be defined in terms of quark-antiquark transformations. The negative colour charge conjugation of the surrounding flux tube can clearly be simply regarded as a property of the "vacuum" - although, of course, the vacuum never appears in the  $S$  matrix and cannot be given a meaning from it. The only manifestation of the flux tube "vacuum" will indeed be in the nature of the Pomeron and also, we believe, in the Nambu-Goldstone realization of chiral symmetry.

We can briefly present our reasons for believing that the Pomeron is responsible for chiral symmetry breaking as follows. Our rough understanding of the physical states of the theory implies that they contain (in the high energy limit) an infinite number of massless, zero momentum gluons. Effectively there is an expectation value for some multigluon operators. Lorentz invariance, of course, does not allow a finite energy expectation value for a single gluon field, but many people have suggested<sup>47),48)</sup> expectation values for multiple gluon operators. Parisi<sup>49)</sup> has also argued that the origin of such expectation values is in the divergences of sums of gluon diagrams which are large in the infra-red region (the infra-red renormalons of QCD). We believe that the high energy limit forces the relevant infra-red divergences into finite-order diagrams which we have effectively regularized by the addition and subsequent removal of Higgs scalars generating the infra-red divergences we have discussed. Therefore the origin of the effective expectation values for gluon operators is really the same in our formalism as the renormalon origin suggested by Parisi. If the vacuum should also be interpreted as containing infinite numbers of zero momentum gluons then clearly we expect expectation values for quark mass operators<sup>50)</sup>, although to discuss this we again need the reggeized quark formalism. In the critical limit, moreover, all even signature combinations of gluons effectively vanish from the physical states, since their only effect is in the vacuum production and absorption of Pomerons. Therefore at the critical point the physical states (coupling to one Pomeron exchange) can be described as containing only an infinite number of zero-momentum "axial" vectors (the even signature gluons which decouple are a combination of ordinary vectors). Thus suggesting that the degeneracy of the vacuum can be entirely described by axial vector currents, as we would like.

More concretely perhaps, the removal of the odd-signature component of the Pomeron as the critical limit is reached should correspond to a reduction in the physical state spectrum. Specifying the signature of a Regge pole is essentially<sup>32),42)</sup> specifying the behaviour under a TCP transformation of the  $t$  channel states to which it couples. Since we have already specified the colour charge conjugation of the Pomeron, if we also constrain the signature properties of states we are by implication restricting the parity spectrum of particle-antiparticle states. Therefore it is plausible that the decoupling of the odd-signature component of the Pomeron in the critical limit is associated with the decoupling of potential parity doublet states from the physical state spectrum.

Actually there have been many hints in the past that the Pomeron is closely related to chiral symmetry. A particular result strongly supporting the last argument above was derived shortly after the discovery of the critical Pomeron<sup>20),21)</sup>. It was shown<sup>45)</sup> that the critical Pomeron has the following very attractive property. When allowed to interact, through the diagrams of Fig. 7.9, with a fermion reggeon which has a linear trajectory and possesses the parity doublets therefore required by McDowell symmetry, the critical Pomeron produces an output "renormalized" approximately linear trajectory with the parity doublet states hidden on unphysical sheets (in the angular momentum plane) of the multi-Pomeron/Reggeon cuts.

The conventional picture of a Nambu-Goldstone realization of chiral symmetry is, of course, that the unwanted axial states are hidden on the unphysical sheet of some "order parameter"<sup>51)</sup> and thus could in principle be recovered by analytic continuation in this parameter. The difficulty in QCD has been to locate such an order parameter, all attempts so far having failed. We would like to suggest therefore that it is in the parameters of the Pomeron that we should look for the "order parameter". The parity doublets of hadron Regge trajectories are, we believe, hidden on unphysical sheets of the multi-Pomeron/Reggeon cuts. The connection between the critical Pomeron and chiral symmetric limits gets closer as we investigate the Pomeron further.

First we note that the signature factors of reggeized quarks will also produce transverse momentum singularities as any quark mass goes to zero in analogy with the gluon singularities of previous sections. In particular, since the triple Pomeron vertex contains a quark loop it will be singular as the quark mass goes to zero. The dimensions of the conventionally defined triple Pomeron vertex  $\tau_0$  are  $(\text{mass})^{-1}$  but a consideration of diagrams such as Fig. 7.4 suggests

$$\tau_0 \sim [m_q^2]^{-1} \quad (7.3)$$

(which is in agreement with the old phenomenological result that the triple Pomeron coupling is approximately given by a pion transverse momentum loop). Equation (7.3) therefore suggests that the chiral symmetric and infinite triple Pomeron limits should coincide in  $QCD_{MB}$ . However, if the Pomeron intercept is away from the critical point the infinite coupling limit is unlikely to exist. If the Pomeron is critical, or rather the infinite coupling limit is taken along the critical surface, the result is simply to bring the critical asymptotic diffraction peak given by the Pomeron propagator down to finite energies, giving a sensible limit. Therefore we are led to the conclusion that the requirement that the chiral symmetric limit be finite may, in  $QCD_{MB}$ , be equivalent to requiring that the Pomeron be critical.

We noted in Section 2 that Banks and Rabinovici<sup>16)</sup> anticipate that the presence of massless fermions will, in general, invalidate the analytic connection between the Higgs and confinement régime and they expect a chiral phase transition. This may explain why our formalism defined from the Higgs régime with massive quarks (so that we have only gluon infra-red divergences to handle) may not give a sensible chiral limit before we take the critical limit into  $QCD_M$ . The implication would be that in  $QCD_{MB}$  we have the number of states to formally give parity doublets in the chiral symmetric limit but there will be a phase transition preventing us taking this limit. At the critical point the Regge trajectories on which the extra-states lie, move on to unphysical sheets of Pomeron cuts, thus allowing the chiral limit to be taken. This would then imply that when the Pomeron is sub-critical, which as we shall discuss, will include confining QCD with a small number of flavours, the symmetric limit can be taken but the symmetry will be realized in the Nambu-Goldstone form.

If the Pomeron is responsible for the Nambu-Goldstone realization of chiral symmetry in QCD as we are suggesting then we have a very attractive picture of confinement as follows. For most of the discussion in this paper the "short distance states" which are surrounded by a large, thick flux tube, may be either local combinations of colour zero quarks, or quarks with short "open strings" of flux between them. However, the open string is presumably what produces the conventional confinement with hadrons lying on approximately linear trajectories. It is attractive to suppose that the linear trajectories form parity doublets with chiral symmetry unbroken. Surrounding such states with a negative colour charge parity, even signature, flux tube forming the Pomeron removes the parity doublets, as described for fermions and the critical Pomeron in Ref. 45). If the Pomeron is sub-critical we would also expect the removal of the parity doublets but in this case we would expect considerable deformation of the linear trajectory by the Pomeron.

Finally we come to the requirement that we must saturate QCD with quarks to strictly obtain the critical Pomeron. We would first like to discuss why this is reasonable on general grounds. First we note that if the parameters of a theory containing a single Pomeron Regge pole are varied so that the intercept approaches the critical point, the effect on the diffraction peak at finite energy will be to spread the peak in momentum transfer, signalling the increasing importance of multi-Pomeron cuts. Therefore as the critical point is approached we expect the theory to fall off more and more slowly at large transverse momentum. If the large transverse momentum region is described by asymptotically free QCD, then the fall-off will indeed be slowest when the theory is saturated with quarks. A complementary argument based on low transverse momentum is that increasing the number of flavours clearly increases the number of hadronic states and so raises the appropriate<sup>52)</sup> multiperipherally defined "bare Pomeron intercept". At the same time the triple Pomeron vertex will be dominated by the low mass hadrons, as discussed above, and so will change little. Therefore it again follows that adding quarks to the theory necessarily moves the QCD Pomeron closer to the critical point.

We can reproduce the same result from the following (potentially) more formal argument. If we complete the infra-red analysis of the QCD<sub>MB</sub> with a transverse momentum cut-off and a small number of quarks as we have outlined in this and the previous section and match it with super-critical RFT, we should be able to find a cut-off dependent definition of the singlet ( $B^8$ ) mass such that taking the zero mass limit will give us simultaneously the critical Pomeron and pure QCD with a transverse momentum cut-off. This implies that the cut-off is necessarily a "relevant parameter" in defining the critical limit. (It is only when we have sixteen flavours that we can take the cut-off away before taking the critical limit and hence define the critical limit in terms of the physical S matrix mass of  $B^8$ ). Equivalently this implies that for any number of quarks in QCD we can find a transverse momentum cut-off which gives the critical Pomeron. Raising the cut-off will then move the theory off the critical surface. For small triple Pomeron coupling  $r_0$ , the bare critical intercept is given by<sup>53)</sup>

$$\Delta_{0c} \sim \frac{r_0^2}{\alpha'_0} \ln \left[ \frac{r_0^2 \Lambda_0}{\alpha'_0} \right] \quad (7.4)$$

where  $\alpha'_0$  is the slope (defined at low transverse momentum) and  $\Lambda_0$  is the transverse momentum cut-off. This implies that if the theory is on the critical surface and we increase  $\Lambda_0$  only, then we go sub-critical, so that, as above, we conclude that continuum QCD with less than sixteen flavours contains an even signature Pomeron with intercept less than one.

From the above discussion it is clear that sub-asymptotic QCD with a small number of flavours may well simulate the critical Pomeron since it is only at very large transverse momentum (where not all events are measured anyway) that the theory differs significantly. However, if cross-sections continue to rise at higher and higher energies (at cosmic ray energies, for example) and as increasingly large transverse momentum analyses are made then there must exist additional flavours of quarks (or conceivably non-colour triplet quarks, as discussed in Section 2).

8. - HIGHER GROUPS, WILSON LOOPS AND THE AGK CUTTING RULES

If SU(3) gauge theory is as intimately connected with the RFT critical Pomeron as we have implied in previous sections then we are immediately led to ask, what is so special about SU(3) ? We hope that this section will give the reader an adequate answer to this question in particular.

Consider repeating the foregoing analysis for SU(4) or more generally SU(N). The results<sup>18)</sup> of Cheng, Eichten and Li state that by adding N-2 fundamental representations of Higgs scalars, we can use the Higgs mechanism to break the gauge symmetry down to SU(2) and retain asymptotic freedom for the complete theory. Again, however, the theory must contain close to the maximum number of fermions allowed by asymptotic freedom, even if the symmetry breaking is less than the maximum allowed. Consider, for example, an SU(4) theory with the gauge symmetry broken down to SU(3) only. In this case only one quartet of scalars is added and (2.8) holds for the corresponding coupling constant, except that

$$A = \frac{1}{\pi^2}, \quad B' = -\frac{3.15}{8.4\pi^2} = -\frac{45}{32\pi^2}, \quad C = \frac{3.3.22}{32.4.4\pi^2} = \frac{99}{256\pi^2} \quad (8.1)$$

and now (for quartet quarks)

$$b_0 = \frac{1}{8\pi^2} \left[ \frac{44}{3} - \frac{2}{3} N_f - \frac{1}{6} \right] \quad (8.2)$$

The stability condition  $B^2 > 4AC$  where  $B = B' + b_0$  now gives

$$\left( 45 - 32\pi^2 b_0 \right)^2 > 16.99 \quad (8.3)$$

$$\sim 45 - 32\pi^2 b_0 > 40 \quad (8.4)$$

$$\Rightarrow \frac{5}{4} > 8\pi^2 b_0 = \left[ \frac{44}{3} - \frac{2N_f}{3} - \frac{1}{6} \right] \quad (8.5)$$

The different values of  $N_F$  give

$$\frac{5}{4} > [N_f = 21] = \frac{1}{2}, \quad \frac{5}{4} > [N_f = 20] = \frac{7}{6}, \quad \frac{5}{4} \not> [N_f = 19] = \frac{11}{6} \quad (8.6)$$

so the first critical point for  $SU(4)$  is reached at  $N_f = 20$ , one less flavour than the maximum allowed for asymptotic freedom of the pure gauge theory. To consider adding more representations of scalars it is necessary to discuss a more complicated set of stability equations which have been studied, on a computer only, by Cheng, Eichten and Li<sup>18)</sup>. As we stated above, they conclude that two representations of scalars, but no more can be added, allowing the gauge symmetry to be broken to  $SU(2)$ . Presumably because it was too complicated, they did not determine whether both representations can be added at  $N_f = 20$  or only at  $N_f = 21$ . It will be attractive, but not essential, in the following to assume that the gauge symmetry can be broken to  $SU(3)$  at  $N_f = 20$  and to  $SU(2)$  at  $N_f = 21$ , so that there are in effect two critical points. Similarly in  $SU(5)$  the symmetry can be broken to  $SU(4)$  at four flavours less than the maximum, and altogether the symmetry can again be broken only to  $SU(2)$ . It is attractive to assume there are three critical points distinguished by the number of flavours, and so on.

Consider first  $SU(4)$  broken to  $SU(2)$  so that we can build up the high energy behaviour of the theory as we did for  $QCD_{MB}$ . The regular  $SU(4)$  representation for the gluons generators has the form

$$\left( \begin{array}{c} \leftarrow 4 \rightarrow \\ SU(4) \end{array} \right) \equiv \left( \begin{array}{c} \leftarrow 2 \rightarrow \\ SU(2) \\ \hline \end{array} \right) \equiv \left( \begin{array}{c} \leftarrow 3 \rightarrow \\ SU(3) \\ \hline \end{array} \right) \quad (8.7)$$

so that instead of the one singlet vector  $B^8$  in  $QCD_{MB}$  we will have a quartet of reggeized massive vectors which are singlets under the remaining  $SU(2)$  gauge symmetry. This quartet will form exchange degenerate vacuum trajectories by combining with zero transverse momentum  $SU(2)$  gauge gluons. Suppose we first restore the  $SU(3)$  symmetry shown in (8.7). One of the quartet trajectories will be part of an  $SU(3)$  octet and will go to zero mass, giving the critical Pomeron as in  $QCD_{MB}$ . Two of the other vacuum trajectories will combine with doublet trajectories under the  $SU(2)$  symmetry to form confined  $SU(3)$  triplets.

There will remain a massive reggeized vector which is a singlet under the  $SU(3)$  gauge group. Knowing from the work of Abarbanel and Sugar<sup>54)</sup> that a vector boson trajectory can be left essentially unperturbed by the critical Pomeron we have no reason to doubt that this singlet trajectory can be taken smoothly to unit intercept. We also have no a priori reason to expect it to decouple from either the Pomeron or the physical spectrum. We conjecture therefore that the critical phenomenon as  $SU(2)$  gauge symmetry is restored to  $SU(4)$  involves an odd signature trajectory contributing to the Pomeron in addition to an even signature trajectory. This is the case for  $N_f = 21$ . For  $N_f = 20$  the symmetry can be broken only to  $SU(3)$  by adding only one quartet of Higgs scalars. Therefore only one gauge vector trajectory can be brought into the spectrum by the Higgs mechanism, implying that the even signature Pomeron is still critical but that the odd signature component now has intercept less than one.

We can generalize this structure to higher gauge groups and similarly construct the critical behaviour by breaking the gauge symmetry initially to  $SU(2)$ . We will conclude that when the asymptotic freedom constraint on the number of quarks is saturated there will be a critical phenomenon involving many Pomeron trajectories of both signatures. In fact the above analysis would suggest that there will be  $(N-2)$  such trajectories in  $SU(N)$ . As the number of quarks is reduced these will move successively away from unit intercept (at each "critical" value of the number of flavours), with the even signature critical Pomeron presumably the last to go. This picture becomes particularly attractive when we interpret it in terms of the Wilson flux loop structure of the gauge theories involved.

It is part of the popular wisdom on the emergence of a stringlike picture for hadrons in gauge theories<sup>2),55)-59)</sup> that closed strings (or tubes) of electric flux will be created by non-local operators which are functionals of the gauge fields. Good approximations as bare versions of such non-local operators are thought to be the familiar Wilson loops.

$$\phi(C) = \text{Tr} \left[ P \exp -g \int_C dx_\mu A_\mu(x) \right] \quad (8.8)$$

where, as in Section 2,  $\text{Tr}$  denotes a trace of the group matrices involved around the space time loop  $C$  (around which the string lies) and  $P$  refers to path ordering. The most ambitious hope<sup>55)</sup> (so far unrealized of course) is that the theory can be reformulated in terms of the operators  $\phi(C)$ . The dual string



model would then suggest that the Pomeron could be related in a first approximation to the  $t$  channel propagator for closed strings, which in the gauge theory language would be an object of the form.

$$\langle \phi(C_1), \phi(C_2) \rangle = \int [d\phi d\phi^*] \phi(C_1) \phi(C_2) e^{-S \mathcal{L}_G(\phi)} \quad (8.9)$$

where this is a functional integral<sup>55)</sup> over the fields  $\phi$  defined on loop space and  $\mathcal{L}_G$  is some Gaussian approximation to the gauge theory Lagrangian expressed in terms of  $\phi(C)$ . We would like therefore to be able to relate our results on the Pomeron in different theories to the structure of the  $\phi(C)$  in such theories.

We can make this connection heuristically as follows. We know from all the perturbation theory calculations of vector theories that the  $t$  channel exchange of vectors at high energy gives always a result of the form

$$A(s, t) \underset{s \rightarrow \infty}{\sim} s f(t) [\ln s]^N \quad (8.10)$$

where the factor of  $s$  results from the vector nature of the exchange. The logarithms, of course, sum to change the power while  $f(t)$  describes the propagation in the reduced two-dimensional transverse momentum space of the  $t$  channel state exchanged. Let us ignore the possible intercept shift for the moment and as a first approximation look at the  $s f(t)$  part of the amplitude. Let us assume that in such a first approximation the amplitude resulting from (8.9) has the form

$$A \langle \phi(C_1), \phi(C_2) \rangle \underset{s \rightarrow \infty}{\sim} s \langle \phi(C_{1T}), \phi(C_{2T}) \rangle \quad (8.11)$$

where the factor of  $S$  results from the exchange of a (very complicated) function of vector fields and  $C_{1T}$  and  $C_{2T}$  are projections of  $C_1$  and  $C_2$  into transverse space so that  $\langle \rangle$  is a projection of the propagator (8.9) onto the transverse space, or at least has analogous properties. Since the transverse space is Euclidean we can use some simple properties of (8.8) in Euclidean space to make some conclusions about the amplitudes that can arise from (8.11).

Suppose that we are considering a scattering amplitude of the form shown in Fig. 8.1a where we have shown only the quark content of the external states. They may be connected by open strings, surrounded by flux tubes as discussed in previous sections, etc. For the moment all that interests us is that the quarks must couple onto a  $t$ -channel closed string which then propagates as illustrated in Fig. 8.1b. According to 't Hooft<sup>14)</sup>, given a gauge group and a particular closed non-orientated curve  $C$  we should distinguish various operators defined on  $C$  by their commutation relations with analogous operators which create magnetic flux loops. The consequence is that in  $SU(2)$  we can associate only one operator with  $C$ , whereas in  $SU(3)$  we can distinguish two operators which can be associated with an orientation of  $C$ .

The orientation dependence of  $\emptyset(C)$  arising from (8.8) can be thought of as associated with the order in which group matrices are multiplied around the loop. It can be shown (for a unitary group, at least) that reversing the direction of multiplication simply complex conjugates  $\emptyset(C)$ . However, since all  $SU(2)$  matrices have a real trace it follows from the definition (8.8) that

$$\emptyset(C) = \emptyset^*(C) \quad \text{in } SU(2) \quad (8.12)$$

which is why  $\emptyset(C)$  cannot be given an orientation dependence. In  $SU(3)$  we can have a complex trace. It is most important in the following that since  $\emptyset^*(C)$  is obtained by reversing the path order in (8.8) it can also be obtained by the charge conjugation operation of Section 6. That is

$$\begin{aligned} \emptyset(C) &\longrightarrow \emptyset^*(C) \\ A_{\alpha\beta}^i &\rightarrow -A_{\beta\alpha}^i, \quad dx \rightarrow -dx \end{aligned} \quad (8.13)$$

implying that the real part of  $\emptyset$  is even under charge conjugation while the imaginary part is odd.

In  $SU(4)$  we can distinguish not only  $\emptyset$  and  $\emptyset^*$  but also a third operator associated with encircling  $C$  twice, which is real, and so on. In  $SU(N)$  the distinct operators, being associated with the elements of the centre of the group  $Z_N$ , are  $(N-1)$  in number. These results are, of course, well known but we summarize them in Fig. 8.2. We now wish to consider the implications of these results for the propagators of the form (8.11).

Consider an elastic amplitude at zero momentum transfer and consider the signatured amplitudes formed by adding or subtracting the amplitude for the process in which one pair of particles is crossed as in Fig. 8.3. Kinematically we will have  $s \rightarrow -s$  and since particles are simply changed to antiparticles all quarks will be changed to antiquarks and vice versa. Therefore we will calculate

$$A^{\pm} = s \langle \phi(c_{1T}) \mp \tilde{\phi}(c_{1T}), \phi(c_{2T}) \rangle \quad (8.14)$$

where  $\tilde{\phi}$  is simply obtained from  $\phi$  by changing quarks to antiquarks in the coupling to the external states. But this is just the charge conjugation or as discussed above the complex conjugation operation. So the even signature amplitude will be given by (an integral with respect to  $C_1$  and  $C_2$  of)

$$A^{\pm} \sim s \langle \phi(c_{1T}) - \phi^*(c_{1T}), \phi(c_{2T}) \rangle \quad (8.15)$$

which, since charge conjugation is preserved

$$= s \langle \text{Im } \phi(c_{1T}), \text{Im } \phi(c_{2T}) \rangle \quad (8.16)$$

which is the odd charge parity propagator. Similarly the odd signature amplitude is given by the even charge parity propagator

$$A^{\mp} \sim s \langle \text{Re } \phi(c_{1T}), \text{Re } \phi(c_{2T}) \rangle \quad (8.17)$$

Clearly this result matches exactly with our conclusion in previous sections that the Pomeron carries odd charge parity in QCD. In fact (8.11) should probably be viewed simply as a heuristic explanation of the detailed infra-red analysis of previous sections. Since  $\phi$  has no imaginary part in SU(2), (8.15) implies directly that SU(2) can have no even signature amplitude proportional to  $s$ , and hence no rising cross-section. In fact straightforward analogy with the dual string model would lead us to believe that the one non-orientated loop amplitude will (because of its symmetry under rotation through  $\pi$ ) be entirely even signature in SU(2) so that  $A^{\mp}$  will also be zero. In the language of the infra-red analysis of this paper we would say that the infra-red singularities

defining the external states in  $SU(2)$  do not occur in the leading power of  $S$  contributions from pure gluon diagrams. They either occur in diagrams involving reggeized quark exchange or in lower powers of  $s$  in the pure gluon diagrams. In either case there will be no amplitude increasing with energy and therefore no rising cross-section in  $SU(2)$ .

We conclude therefore that to obtain a rising cross-section (or even an approximately constant cross-section) in a confining gauge theory we must have at least  $SU(3)$  for the gauge group. If we move onto  $SU(4)$  then the double loop of Fig. 8.2, although real, has no reason to be purely even signature, [in particular it is not symmetric under rotation through  $180^\circ$ , unlike the simple  $SU(2)$  loop] and therefore will in general contribute to  $A^-$  through (8.17). As we increase the complexity of the group we increase the possible multiloop operators which can contribute to both  $A^+$  and  $A^-$ . In fact combining our understanding in Section 2 that the singlet vector  $B^8$  in  $QCD_{MB}$  gives the necessary orientation to  $SU(2)$  strings to convert them to  $SU(3)$  strings, with the analysis of the first part of this section, we are led to the following. As the size of the gauge group grows, the increasing complexity of the Pomeron spectrum that we expect from our general infra-red analysis will be in one-to-one correspondence with the increasing complexity of contributions to  $A^+$  and  $A^-$  that can be made via (8.15) and (8.17) by the multiloop operators. We therefore obtain a rather beautiful interpretation of the sequence of critical points reached as we come close to saturating the theory with quarks.

In a general gauge theory with a small number of fermions there will be separate vacuum trajectories associated with each of the distinct 't Hooft loop operators illustrated in Fig. 8.2. We anticipate that their intercepts will decrease as their complexity grows. As we increase the number of fermions, close to the maximum allowed number, we reach the first critical point where the simple orientated loop becomes critical. At this point a small variation of the parameters will break the loop down into a non-orientated loop plus a local reggeized vector. At the next critical point (reached by simply adding quarks) the double loop becomes critical also and a small parameter variation can break both critical loops down to non-orientated loops plus four local reggeized vectors. At the next critical point the three loop trajectory becomes critical, and so on, until we saturate the theory with quarks. At which point all possible loop trajectories are critical. Whether such a phenomenon is compatible with unitarity may be a deeper question. In any case we note that none of this rich structure will be seen in the  $1/N$  expansion of the theory keeping the number of quarks finite. Only the simple orientated loop trajectory will appear as the leading (non-critical) vacuum trajectory. For small groups with small numbers of fermions

there is no reason for the non-leading multiloop trajectories to be down by a power of  $s$ . This being the case it seems that if the Pomeron is to contain only a single even signature Regge pole, with intercept close to or at one, then SU(3) gauge theory is the unique choice (amongst the unitary groups at least).

Having seen that SU(3) is picked out as the unique (unitary) group with the structure to generate a simple even signature Pomeron, the remaining question is, perhaps, if QCD<sub>MB</sub> is described by super critical RFT, how does the RFT formalism know about the group structure involved in the gauge theory. The answer is at first sight surprising, since it depends on the AGK cutting rules, which would appear to have little to do with a gauge group. However, as we shall explain, this is really not the case once the gauge theory is confining and we are concerned with closed string structures which really depend only on the centre of the group, as 't Hooft has emphasized<sup>14)</sup>.

We can briefly describe the emergence of the group structure in RFT as follows (although more details will be given in our paper on super critical RFT). The AGK cutting rules are incorporated in the Pomeron RFT by introducing three ("non-relativistic") Pomeron fields -  $\bar{\psi}^+$ ,  $\bar{\psi}^-$ ,  $\bar{\psi}_c$  are creation operators and  $\psi^+$ ,  $\psi^-$ ,  $\psi_c$  are destruction operators - with the three Green's function

$$\langle \psi^+, \bar{\psi}^+ \rangle, \langle \psi^-, \bar{\psi}^- \rangle, \langle \psi_c, \bar{\psi}_c \rangle \quad (8.18)$$

describing the physical amplitude respectively, above its (invariant) energy cut, below its energy cut and with the discontinuity taken. The AGK cutting rules include the equality

$$\langle \psi^+, \bar{\psi}^+ \rangle = \langle \psi^-, \bar{\psi}^- \rangle = \langle \psi_c, \bar{\psi}_c \rangle \quad (8.19)$$

which is produced in perturbation theory by the "cut RFT" Lagrangian

$$\begin{aligned} \mathcal{L}_c = & \mathcal{L}_0 + \frac{i\tau_0}{2} (\bar{\psi}_+ \psi_+^2 + \bar{\psi}^2 \psi_+) - i \frac{\tau_0}{2} (\bar{\psi}_- \psi_-^2 + \bar{\psi}^2 \psi_-) \\ & + \frac{\tau_0}{32} (\bar{\psi}_c \psi_c^2 + \bar{\psi}_c^2 \psi_c) + \frac{\tau_0}{32} (\bar{\psi}_c \psi_+ \psi_- + \psi_c \bar{\psi}_+ \bar{\psi}_-) \\ & + i \frac{\tau_0}{2} (\bar{\psi}_c \psi_c \psi_+ + \psi_c \bar{\psi}_c \bar{\psi}_+) - i \frac{\tau_0}{2} (\bar{\psi}_c \psi_c \psi_- + \psi_c \bar{\psi}_c \bar{\psi}_-) \end{aligned} \quad (8.20)$$

This Lagrangian also produces immediately

$$\langle \psi^+, \bar{\psi}_c \rangle = \langle \psi^+, \bar{\psi}_- \rangle = \dots = 0 \quad (8.21)$$

which is important, since all such Green's functions would be unphysical.  $\mathcal{L}_C$  does, however, give some non-zero non-physical multiple Green's functions. To express the AGK cutting rules in terms of a symmetry we must therefore look for a symmetry of the physical Green's functions and not the Lagrangian  $\mathcal{L}_C$ . In fact we can perform global SU(3) transformations on the complex fields  $\bar{\psi} = (\bar{\psi}_+, \bar{\psi}_-, \bar{\psi}_c)$ ,  $\psi = (\psi_+, \psi_-, \psi_c)$  by transforming  $\bar{\psi}$  as an SU(3) triplet and  $\psi$  as a complex conjugate triplet. The Green's functions (8.19) and (8.21) therefore in principle transform as a  $3^* \otimes 3$  representation of this SU(3). Although  $\mathcal{L}_C$  is not invariant under this transformation it can be shown that the Green's functions are and so in fact form a singlet under SU(3). In fact we believe, although we have not checked it completely, that the statement of the AGK cutting rules is equivalent to the statement that physical Pomeron Green's functions are invariant under SU(3) transformations.

In the supercritical phase a linear combination of  $\bar{\psi}_+, \bar{\psi}_-, \bar{\psi}_c$  (and the same combination of  $\psi_+, \psi_-, \psi_c$ ) acquires an expectation value. Consequently the global symmetry of the Greens functions is reduced to SU(2) and the matrix of Green's function has the structure

$$\left( \begin{array}{cc|c} \times & 0 & \times \\ 0 & \times & \times \\ \hline \times & \times & \times \end{array} \right) \quad (8.22)$$

with the additional non-diagonal Green's functions transforming under a  $3^* \otimes 3$  representation of the original SU(3). Consequently the new set of Green's functions has all the right symmetry properties to be identified with those derived from SU(3) gauge theory, with the Higgs mechanism applied to break the gauge symmetry from SU(3) to SU(2). In fact it was by determining which must be the physical Greens functions in (8.22) that we first discovered that there was an odd signature reggeon coupling pairwise to the Pomeron in the supercritical phase<sup>19)</sup>. This gives us confidence that all the numbers (resulting from the symmetry breaking patterns) will match nicely when we finally compare QCD<sub>MB</sub> and supercritical RFT precisely.

Nevertheless the connection between the  $SU(3)$  global symmetry derived from the AGK cutting rules, and  $SU(3)$  gauge theory may still seem bizarre. Let us, however, look at the origin of the AGK cutting rules in the usual phenomenological language<sup>22),60)</sup> which can be adapted to a string picture of the Pomeron. We proceed as follows.

- 1) Consider events with close to the average multiplicity  $\langle n \rangle$  and describe them by a multiperipheral approximation as illustrated in Fig. 8.3.
- 2) Form the unitarity sum to define the "bare Pomeron", as in Fig. 8.4.
- 3) Consider events with close to twice the average multiplicity and similarly describe them by a double multiperipheral approximation as in Fig. 8.5.
- 4) The AGK cutting rules now tell us that these events are totally counted by the two Pomeron graph as illustrated in Fig. 8.6.
- 5) Similarly events with  $3 \langle n \rangle$  multiplicity are counted by three Pomerons, etc. and fluctuations of multiplicity on the rapidity plot are represented by Pomeron interaction graphs as illustrated in Fig. 8.7.

Repeating this description in a string theory we obtain

- 1) the average multiplicity events are represented by cutting a  $t$  channel closed string in the  $s$  channel, as illustrated in Fig. 8.8.
- 2) A closed string bare Pomeron is formed from the unitarity sum as in Fig. 8.9.
- 3) Events with twice the average multiplicity are counted by two cut closed strings, for simplicity we represent the unitarity sum by the  $t$  channel projection in Fig. 8.10.

It is clear from our previous discussion that if we consider  $SU(4)$  closed strings, then at this point there is a second possibility corresponding to forming a double loop which we can illustrate roughly as in Fig. 8.11. It is rather simple therefore to see that in this case events with twice the average multiplicity will not be counted completely by the double Pomeron graph if the bare Pomeron is defined from the average multiplicity events. Instead such events will generate a new (from our previous discussion) odd signature trajectory representing the double loop.

This effect immediately breaks the AGK cutting rules and so we see that these rules uniquely represent the situation when a simple  $SU(3)$  closed string structure becomes critical. Actually it is clear that in the string context the cutting rules really describe the way strings can be cut and sewn together

by unitarity so that they essentially carry the same information on the topological structure of the gauge group as is carried by the centre of the gauge group. Therefore it may well be that it is only the centre of the  $SU(3)$  group defined above from the AGK rules that we should think of as identified with the centre of the gauge group. The centre tells us the topological structure of the strings involved, and therefore how unitarity is satisfied at high energy by such strings. Finally we note that the arguments above generalize to an  $SU(N)$  group to tell us that new trajectories will be generated by events with up to  $(N-2)$  times the average multiplicity. Presumably there exists a multi-Pomeron theory with cutting rules to describe the situation when all such trajectories become simultaneously critical. However, one may seriously doubt whether this is consistent with unitarity.



REFERENCES

- 1) I have no published references for this, it is a personal experience.
- 2) See, for example, Polyakov's emphasis of the importance of closed strings :  
A.M. Polyakov - Nuclear Phys. B164 (1979) 171, or Mandelstam's review :  
S. Mandelstam - Proceedings of the Lepton-Photon Conference (Fermilab, 1979),  
or Migdal's recent paper :  
A.A. Migdal - Landau Institute Preprint (1980).
- 2) A.R. White - Lectures at the Les Houches Institute (1975).
- 4) V.S. Fadin, E.A. Kuraev and L.N. Lipatov - Phys.Letters 60B (1975) 50 ;  
Soviet Phys. JETP 44 (1976) 443, 45 (1977) 199.
- 5) H. Cheng and C. Lo - Phys.Rev. D13 (1976) 1131, D15 (1977) 2959.
- 6) J. Bartels - DESY Preprint 79/68 ; Summer School Lectures at Cracow, Jaca  
and Kaiserslautern, DESY Preprints 80/09, 80/54 (1980).
- 7) J. Bronzan and R.L. Sugar - Phys.Rev. D17 (1978) 585.
- 8) G. Parisi - Phys.Letters 76B (1978) 65.
- 9) H. Cheng, J. Dickinson, K. Olaussen and P.S. Yeung - Stony Brook Preprint  
(1979).
- 10) P.S. Yeung - MIT Preprint (1979).
- 11) Ya.Ya. Balitsky, L.N. Lipatov and V.S. Fadin - in "Materials of the 14th  
Winter School of Leningrad Institute of Nuclear Research" (1979).
- 12) P. Carruthers, P. Fishbane and F. Zachariasen - Phys.Rev. D15 (1977) 3675.
- 13) J.M. Cornwall and G. Tiktopoulos - "New Pathways in High Energy Physics,  
Plenum, New York (1976).
- 14) G. 't Hooft - Nuclear Phys. B138 (1978) 1.
- 15) E. Fradkin and S.H. Shenker - Phys.Rev. D19 (1979) 3682.
- 16) T. Banks and E. Rabinovici - Nuclear Phys. B160 (1979) 349.
- 17) D.J. Gross and F. Wilczek - Phys.Rev. D8 (1973) 3633.
- 18) T.P. Cheng, E. Eichten and L.F. Li - Phys.Rev. D9 (1974) 2259.
- 19) A.R. White - Proceedings of the Marseilles Conference on High Energy Physics  
(1978), Proceedings of the 2nd International Symposium on Hadron Structure,  
Kazimierz, Poland (1979).
- 20) A.A. Migdal, A.M. Polyakov and K.A. Ter Martirosyan - Zh.Eksp.Teor.Fiz.  
67 (1974) 84.
- 21) H.D.I. Abarbanel and J.B. Bronzan - Phys.Rev. D9 (1974) 2397.
- 22) V.A. Abramovskii, V.N. Gribov and O.V. Kancheli - Soviet J.Nucl.Phys. 18  
(1974) 308.

- 23) H.P. Stapp - Lectures at the Les Houches Institute (1975).
- 24) J. Bros, H. Epstein and V. Glaser - Lectures at the Les Houches Institute (1975).
- 25) T. Jaroszewicz - Cracow Preprints (1980).
- 26) J.M. Cornwall and G. Tiktopoulos - D13 (1976) 3370.
- 27) A.R. White - Nuclear Phys. B159 (1979) 77.
- 28) B.W. Lee and J. Zinn-Justin - Phys.Rev. 5 (1972) 3137.
- 29) I am very grateful to M. Peskin for clarifying discussions of this issue.
- 30) An introductory review of reggeon field theory (RFT) and its motivation can be found in :  
H.D.I. Abarbanel, J.B. Bronzan, R.L. Sugar and A.R. White - Physics Reports 21C (1975) 119.
- 31) M. Toller - Nuovo Cimento 62A (1969) 341.
- 32) P. Goddard and A.R. White - Nuclear Phys. B17 (1970) 45.
- 33) V.N. Gribov, I.Ya. Pomeranchuk and K.A. Ter Martirosyan - Phys.Rev. B139 (1965) 184.
- 34) A.R. White - Nuclear Phys. B50 (1972) 130.
- 35) J.L. Cardy, R.L. Sugar and A.R. White - Phys.Letters 55B (1975) 384.
- 36) H.D.I. Abarbanel, J. Bartels, J.B. Bronzan and D. Sidhu - Phys. Rev. D12 (1975) 2459.
- 37) See, for example, the dimensional regularization of G.M. Cicuta - Phys. Rev. Letters 43 (1979) 826.
- 38) M.T. Grisaru and H.J. Schnitzer - Phys.Rev. D20 (1979) 784 ;  
see also L. Lukaszuk and L. Szymanowski - Warsaw Preprint (1979).
- 39) J. Kwiecinski and M. Praszalowicz - Cracow Preprints (1979, 1980).
- 40) V.A. Novikov, L.B. Okun, M.A. Shifman, A.I. Vainshtein, M.B. Voloshin and V.I. Zakharov - Physics Reports 41C (1978) 3.
- 41) L.N. Lipatov - Soviet J.Nucl.Phys. 23 (1976) 642.
- 42) M. Toller - Nuovo Cimento 54A (1968) 295.
- 43) J.B. Bronzan and R.L. Sugar - Phys.Rev. D17 (1978) 2813.
- 44) V.N. Gribov, E.M. Levin and A.A. Migdal - Soviet J.Nucl.Phys. 11 (1970) 378.
- 45) J. Bartels and R. Savit - Phys.Rev. D11 (1975) 2300.
- 46) G.M. Cicuta, G. Marchesini and E. Montaldi - Milan Preprint IFUM 240 FT (1980).
- 47) M.A. Shifman, A.I. Vainshtein and V.I. Zakharov - Nuclear Phys. B147 (1979) 385.

- 48) R. Fukuda and Y. Kazama - Fermilab Preprint 80/55-TH4 (1980).
- 49) G. Parisi - Nuclear Phys. B150 (1979) 163.
- 50) For a review of the expected characteristics of a Nambu-Goldstone realization of chiral symmetry in QCD, see :  
R.J. Crewther - Proceedings of the Kaiserslautern Summer Institute (1979).
- 51) For example : S. Coleman and E. Witten - Phys.Rev.Letters 45 (1980) 100.
- 52) J.W. Dash, E. Manesis and S.T. Jones - Phys.Rev. D18 (1978) 303.
- 53) R.L. Sugar and A.R. White - Phys.Rev. D10 (1974) 4074.
- 54) H.D.I. Abarbanel and R.L. Sugar - Phys.Rev. D10 (1974) 721.
- 55) F. Gliozzi and M.A. Virasoro - Nuclear Phys. B164 (1980) 141.
- 56) C. Thorn - Phys. Rev. D19 (1979) 639.
- 57) Y.M. Makeenko and A.A. Migdal - Phys.Letters B, 88B (1979) 135.
- 58) J.L. Gervais and A. Neveu - Nuclear Phys. B153 (1979) 445.
- 59) T. Eguchi - Chicago Preprint, EFI 22 (1979).
- 60) A.H. Mueller - Proceedings Aix-en-Provence Conference (1973).

FIGURE CAPTIONS

- Fig. 2.1 : A possible coupling constant trajectory.
- Fig. 2.2 : Possible open strings.
- Fig. 2.3 : Phase diagram for a non-Abelian lattice gauge theory with fundamental representation scalars.
- Fig. 2.4 : Representation of a lattice line integral.
- Fig. 2.5 : Addition of operators.
- Fig. 2.6 : A sequence of trajectories defining the limit  $L$ .
- Fig. 3.1 : A Toller diagram.
- Fig. 3.2 : A planar Toller diagram from Fig. 3.1.
- Fig. 3.3 : Vertices generating hexagraphs.
- Fig. 3.4 : Some hexagraphs associated with the planar Toller diagram of Fig. 3.2.
- Fig. 3.5 : Insertion of "polygraphs" in hexagraphs.
- Fig. 3.6 : Transformation of a hexagraph to a flow-graph.
- Fig. 3.7 : Cuts of some simple flow-graphs.
- Fig. 3.8 : T, D and V lines.
- Fig. 3.9 : A hexagraph containing a T line and its flow-graph.
- Fig. 3.10 : The six combinations of five cuts through the flow-graph of Fig. 3.9.
- Fig. 3.11 : Notation for signature factors.
- Fig. 3.12 : Hexagraph analysis of a  $t$  channel intermediate state.

- Fig. 3.13 : The simplest hexagraph.
- Fig. 3.14 : Flow-graphs involved in the unitarity integral for the hexagraph of Fig. 3.13.
- Fig. 3.15 : The flow-graph for a fixed pole residue.
- Fig. 3.16 : A cross product of hexagraphs.
- Fig. 3.17 : The correspondence between Pomeron graphs and hexagraph loops.
- Fig. 3.18 : Two-particle / multi-Pomeron couplings.
- Fig. 3.19 : Flow-graphs involved in multi (external) particle unitarity integrals.
- Fig. 3.20 : The two Regge-pole cut in the eight particle amplitude.
- Fig. 3.21 : The fixed pole residue hexagraph involved in Fig. 3.20.
- Fig. 3.22 : A four Pomeron graph in the eight particle amplitude.
- Fig. 3.23 : An illustration of the AGK cutting rules.
- Fig. 4.1 : The leading log reggeon diagrams.
- Fig. 4.2 : The vertices appearing in Fig. 4.1.
- Fig. 4.3 : The unitarity bootstrap.
- Fig. 4.4 : The intermediate state sum giving the four reggeon vertex.
- Fig. 4.5 : Infra-red finite, off mass-shell gluon diagrams.
- Fig. 4.6 : Diagrams summed by the integral equation with an  $N$  gluon irreducible kernel.
- Fig. 5.1 : The simplest hexagraph loop together with its multiperipheral cut.

- Fig. 5.2 : The discontinuity of the six point function giving the triple reggeon vertex.
- Fig. 5.3 : AGK cuts of Fig. 5.1.
- Fig. 5.4 : Notation for the three reggeon vertex.
- Fig. 5.5 : Reggeon diagrams summed to renormalize the propagator.
- Fig. 5.6 : A hexagraph loop diagram for the three reggeon vertex.
- Fig. 5.7 : Notation for the diagram of Fig. 5.6 including the reggeon intermediate states.
- Fig. 5.8 : A hexagraph loop diagram for the elastic amplitude.
- Fig. 5.9 : A sum of hexagraph loop diagrams.
- Fig. 5.10 : The sum of Fig. 5.9 expressed in terms of renormalized quantities.
- Fig. 5.11 : A loop diagram containing a three reggeon cut.
- Fig. 5.12 : A simple diagram violating signature rules.
- Fig. 5.13 : Signature conservation satisfied in elastic amplitudes by the summation of diagrams.
- Fig. 5.14 : A further breakdown of signature conservation.
- Fig. 5.15 : A similar failure of signature rules to that of Fig. 5.14.
- Fig. 5.16 : Hexagraph loops coupling through a four reggeon vertex.
- Fig. 5.17 : A multiparticle hexagraph loop involving the four reggeon vertex and the associated hexagraph tree diagram.
- Fig. 5.18 : An elastic loop diagram containing Fig. 5.17.
- Fig. 5.19 : The simplification of hexagraph diagrams.

- Fig. 5.20 : The mapping of a hexagraph loop diagram onto a tree diagram by the evolution of intermediate states.
- Fig. 5.21 : The construction of a general hexagraph loop diagram.
- Fig. 5.22 : A subset of the hexagraph loop diagrams giving the reggeon diagrams of Fig. 4.1.
- Fig. 5.23 : A T line with no zero.
- Fig. 5.24 : Possible signature violation in an elastic amplitude.
- Fig. 5.25 : Summation of diagrams to restore signature conservation.
- Fig. 6.1 : Notation for reggeons.
- Fig. 6.2 : Triple reggeon vertices.
- Fig. 6.3 : The one loop trajectory functions.
- Fig. 6.4 : Infra-red cancellations.
- Fig. 6.5 : Separation of the trajectory function for a doublet reggeon.
- Fig. 6.6 : Infra-red finite one loop trajectory functions.
- Fig. 6.7 : Infra-red finite gluon and reggeon interactions.
- Fig. 6.8 : Allowed couplings to external particles.
- Fig. 6.9 : General amplitude involving mass-shell gluon singularities.
- Fig. 6.10 : Summation of gluon self-interactions when  $K$  is singular.
- Fig. 6.11 : Summation of diagrams with a reggeon-gluon interaction.
- Fig. 6.12 : A combination of gluons and singlet reggeon whose charge parity and signature forbids a local interaction.
- Fig. 6.13 : The simplest hexagraph loop diagram containing the combination of Fig. 6.12.

- Fig. 6.14 : The hexagraph tree diagram for Fig. 6.13 and the essential structure of the central loop.
- Fig. 6.15 : Gluon self-interactions in diagrams with the same structure as Fig. 6.13.
- Fig. 6.16 : The "external state" arising from Fig. 6.13 in transverse co-ordinate space.
- Fig. 6.17 : Interaction of the singlet reggeon with an even signature combination of gluons.
- Fig. 6.18 : A signature non-conserving, non-local vertex.
- Fig. 6.19 : A signature non-conserving local vertex.
- Fig. 6.20 : The non-local signature non-conserving vertex in conjunction with an energy non-conserving vertex.
- Fig. 6.21 : Notation for the diagram of Fig. 6.20.
- Fig. 6.22 : A rapidity ordering giving a simple production vertex.
- Fig. 6.23 : Rapidity ordering giving a singular vertex.
- Fig. 6.24 : A general diagram with infra-red singularities giving vacuum production and absorption.
- Fig. 6.25 : Vacuum production of Pomerons.
- Fig. 7.1 : General structure for a triple Pomeron vertex.
- Fig. 7.2 :  $d$  tensor triple reggeon vertices.
- Fig. 7.3 : Possible tensors for the triple Pomeron vertex.
- Fig. 7.4 : A possible triple Pomeron vertex.



- Fig. 7.5 : The zero momentum triplet structure of Pomeron interaction diagrams.
- Fig. 7.6 : Illustration of the "flux tube" Pomeron interactions.
- Fig. 7.7 : Diagrammatic representation of the supercritical RFT formalism.
- Fig. 7.8 : The flux tube picture of the critical limit.
- Fig. 7.9 : Pomeron interactions with a reggeized fermion.
- Fig. 8.1 : Colour zero external quark amplitude.
- Fig. 8.2 : The structure of electric flux closed strings in the unitary groups.
- Fig. 8.3 : A multiperipheral representation of average multiplicity events.
- Fig. 8.4 : The unitarity sum defining the "bare Pomeron".
- fig. 8.5 : Multiperipheral representation of double multiplicity events.
- Fig. 8.6 : The AGK counting of double multiplicity events.
- Fig. 8.7 : Multiplicity fluctuations represented by Pomeron interactions.
- Fig. 8.8 : String representation of average multiplicity events.
- Fig. 8.9 : The bare Pomeron in the string picture.
- Fig. 8.10 : The two Pomeron graph from double multiplicity events.
- Fig. 8.11 : The  $SU(4)$  two loop trajectory from double multiplicity events.

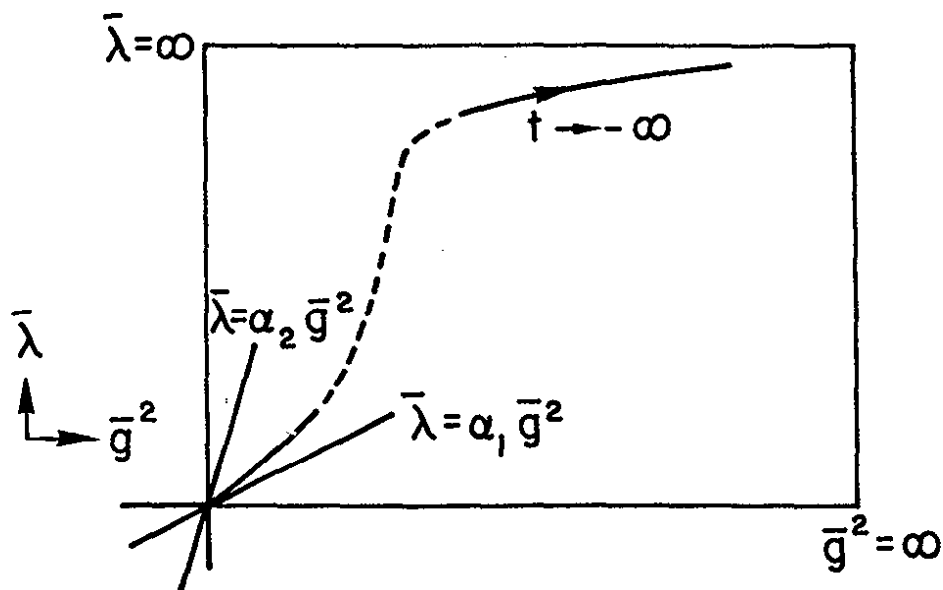


Fig. 2.1

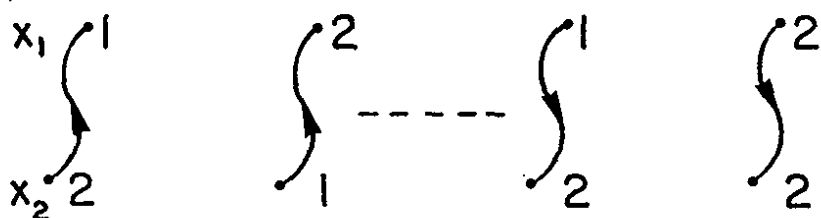


Fig. 2.2

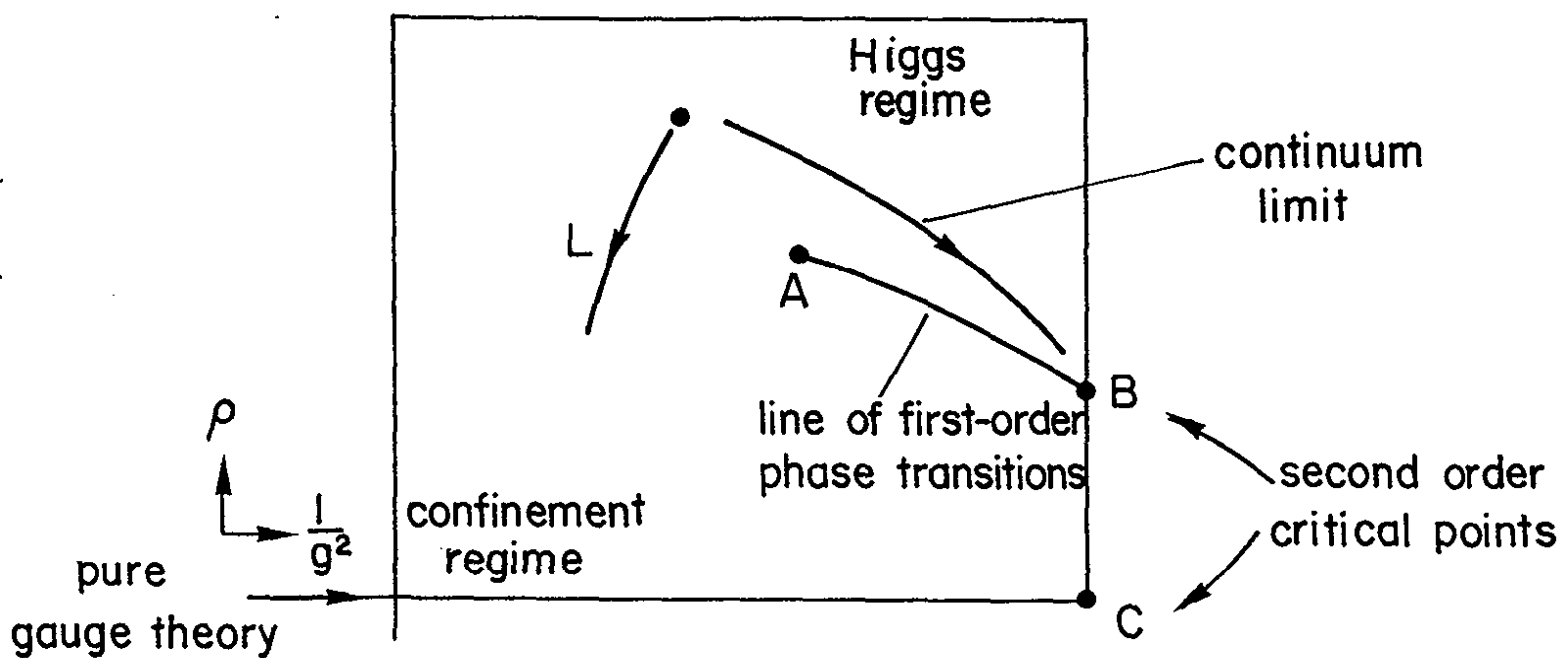
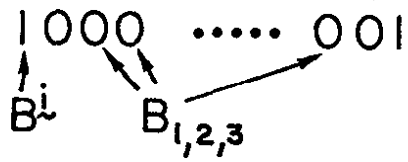


Fig. 2.3



line-integral

\*

$B_8$

local operator

Fig. 2.4

$$\begin{aligned}
 &100 \dots 00000 \dots 01 \\
 + &100 \dots 01100 \dots 01 \\
 + &100 \dots 00110 \dots 01 \\
 + &100 \dots 01*10 \dots 01 \\
 \equiv &100 \dots 00 \blacksquare 00 \dots 01
 \end{aligned}$$

$\blacksquare \equiv A_\mu$

Fig. 2.5

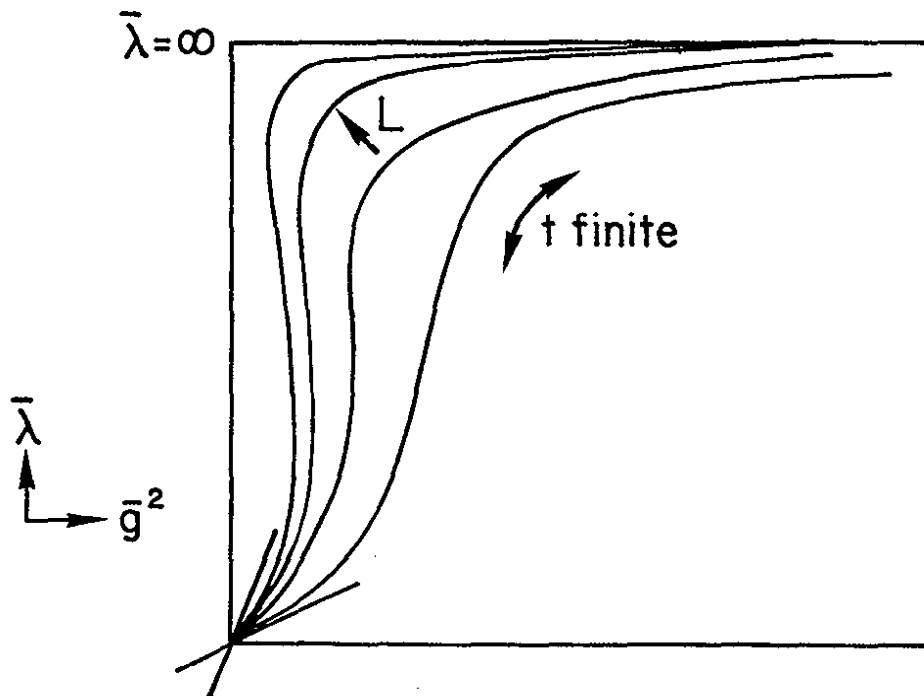


Fig. 2.6

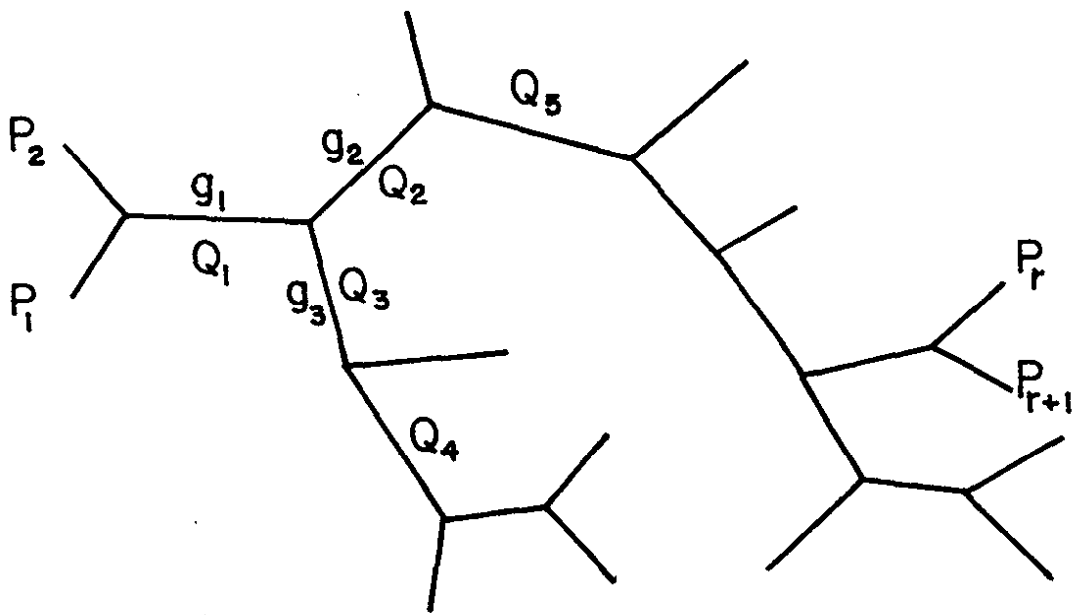


Fig. 3.1

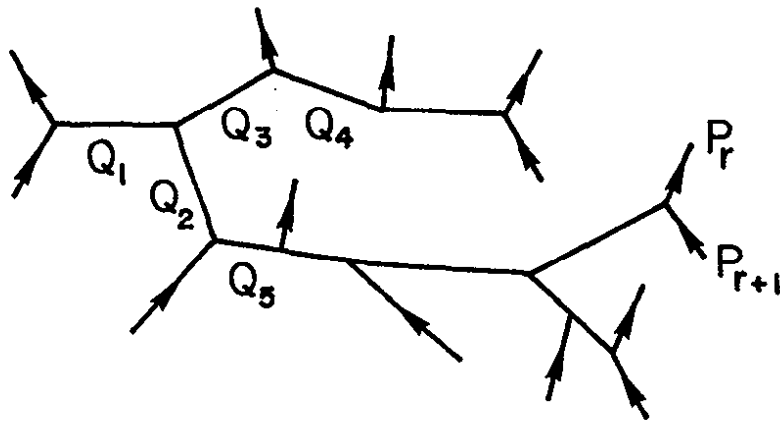


Fig. 3.2

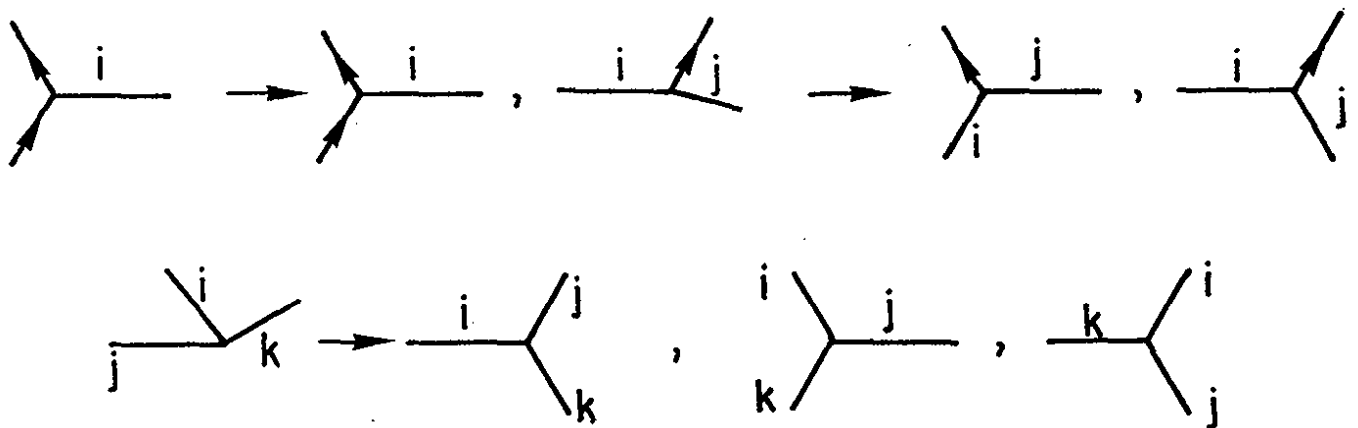


Fig. 3.3

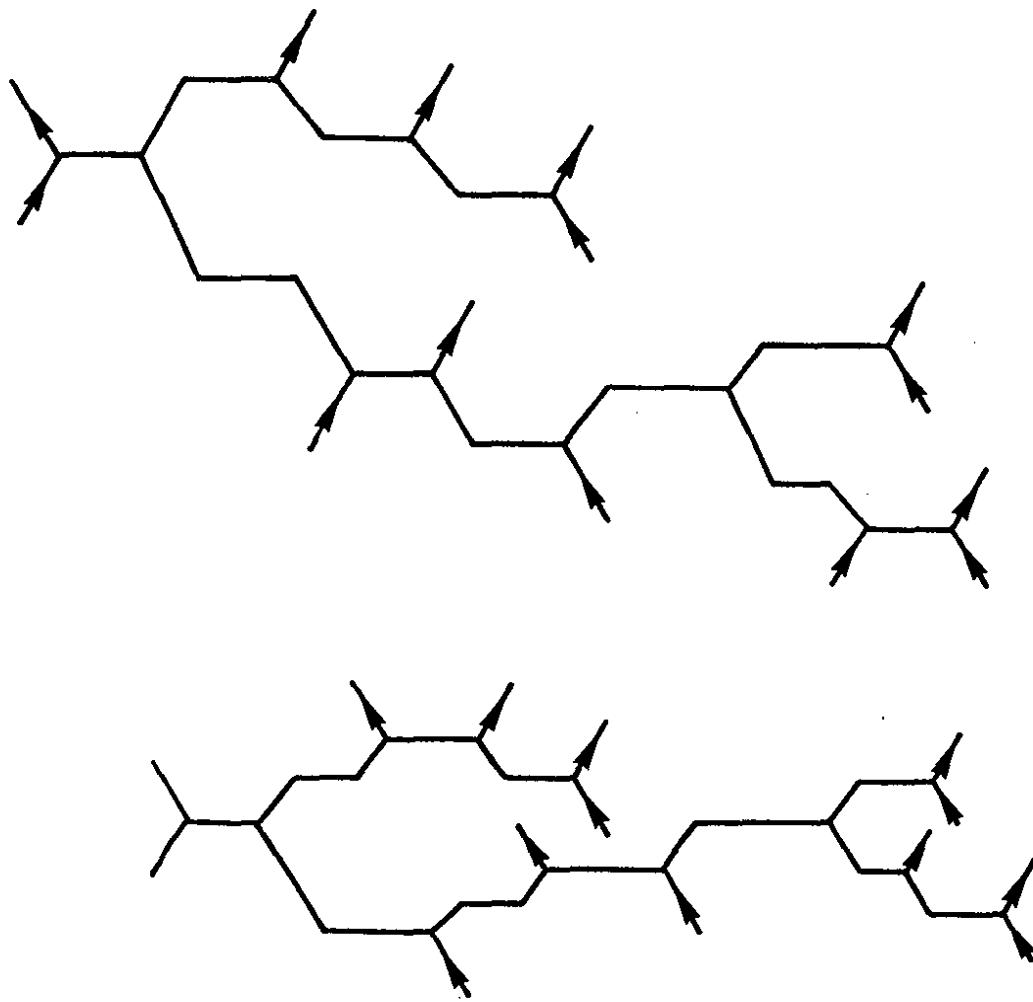


Fig.3.4

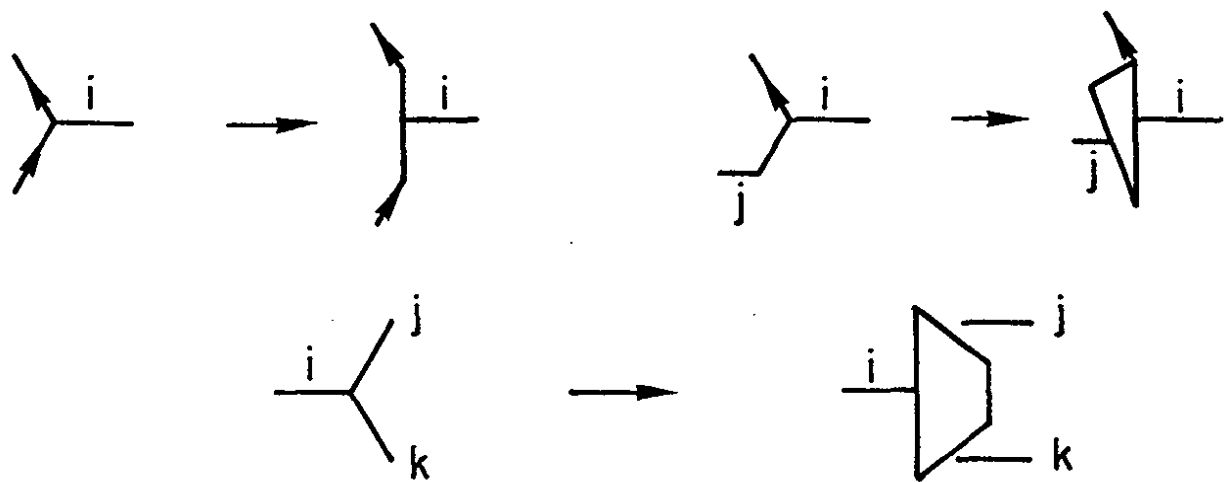


Fig. 3.5

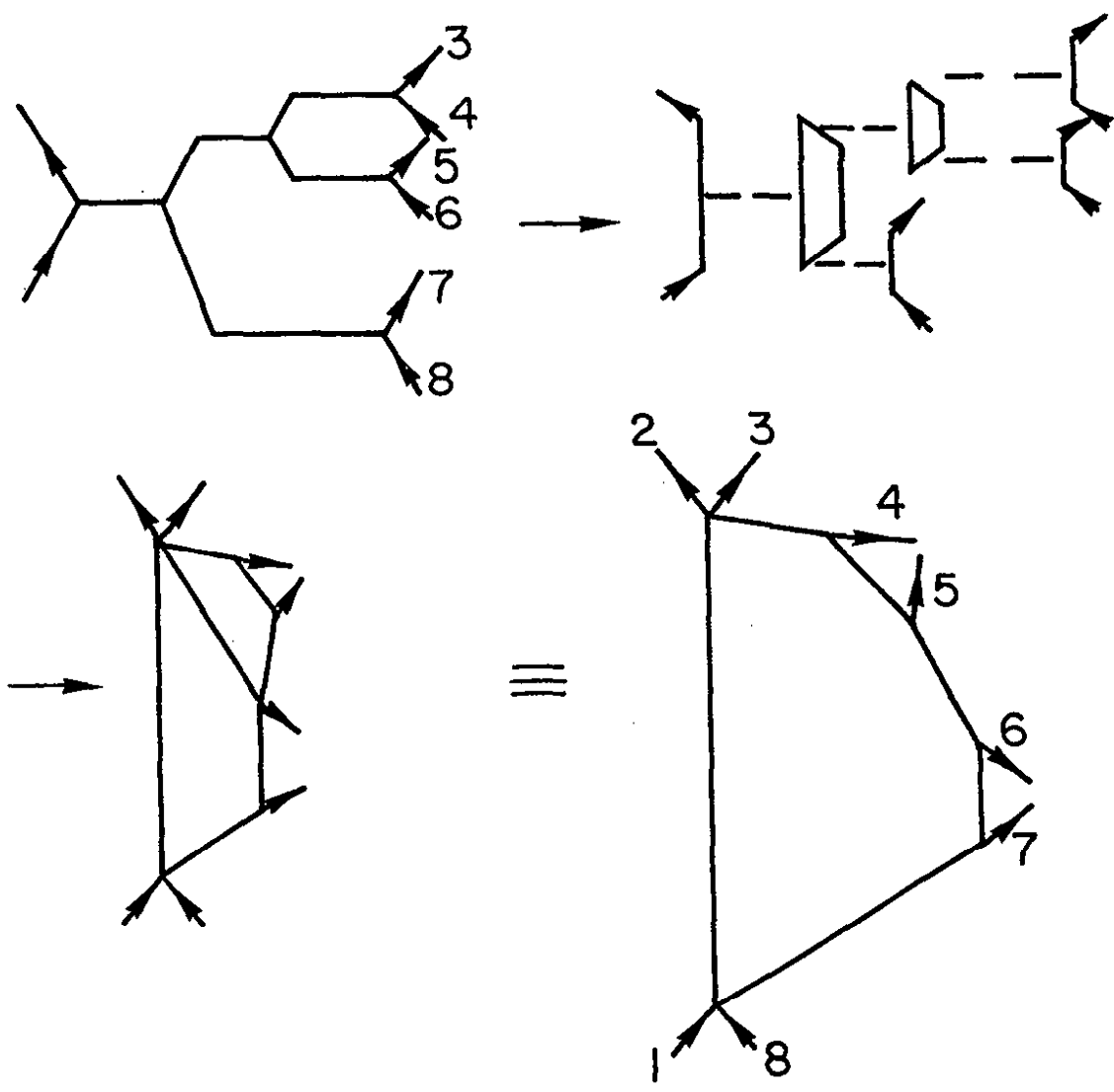


Fig. 3.6

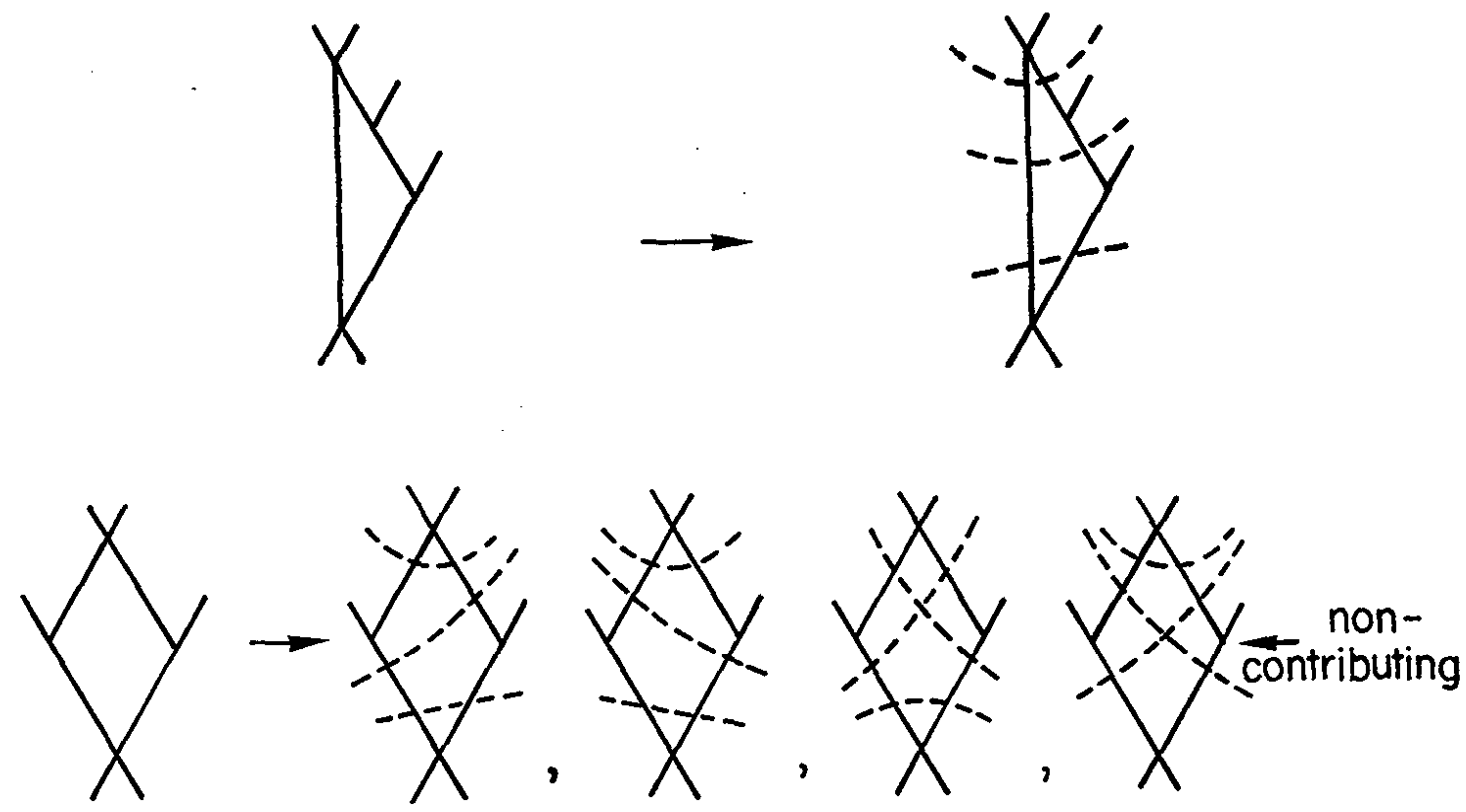


Fig. 3.7

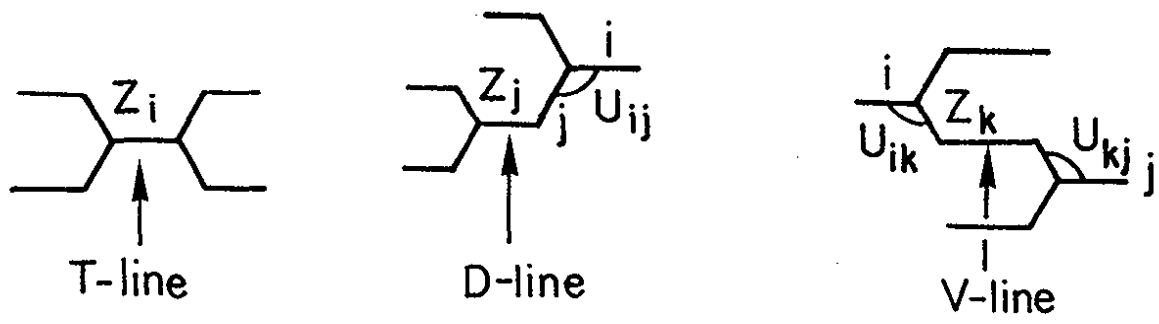


Fig. 3.8

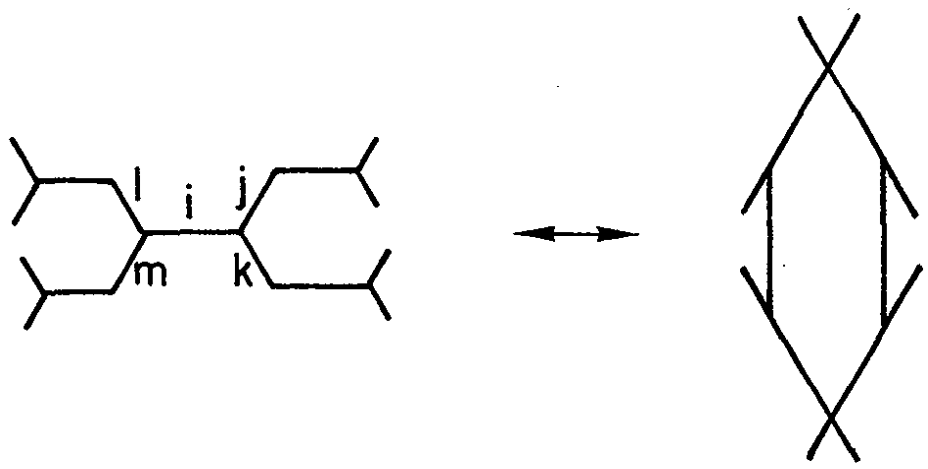


Fig. 3.9

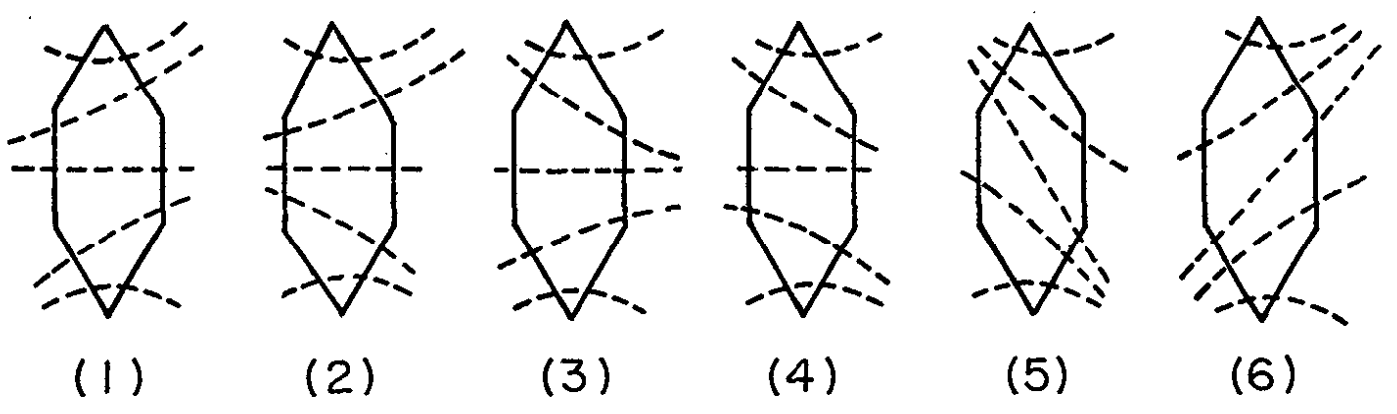


Fig. 3.10

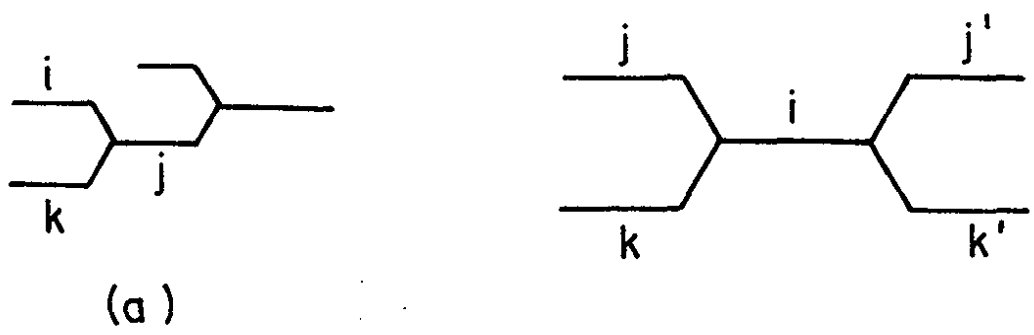


Fig. 3.11

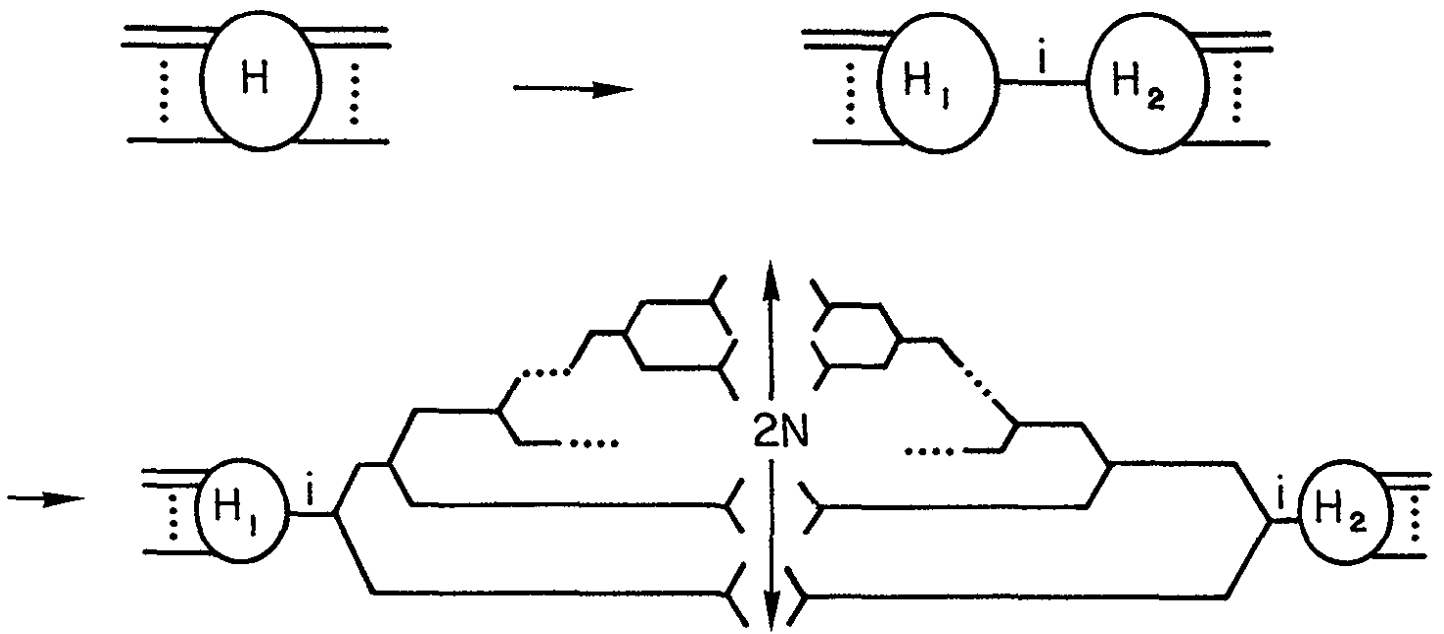


Fig. 3.12



Fig. 3.13

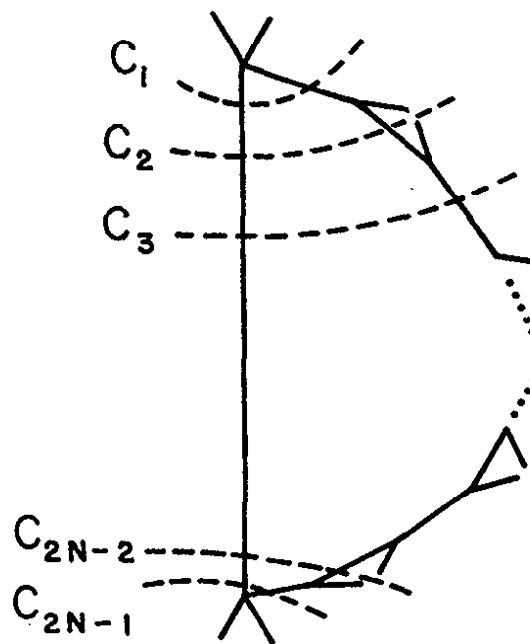


Fig. 3.14



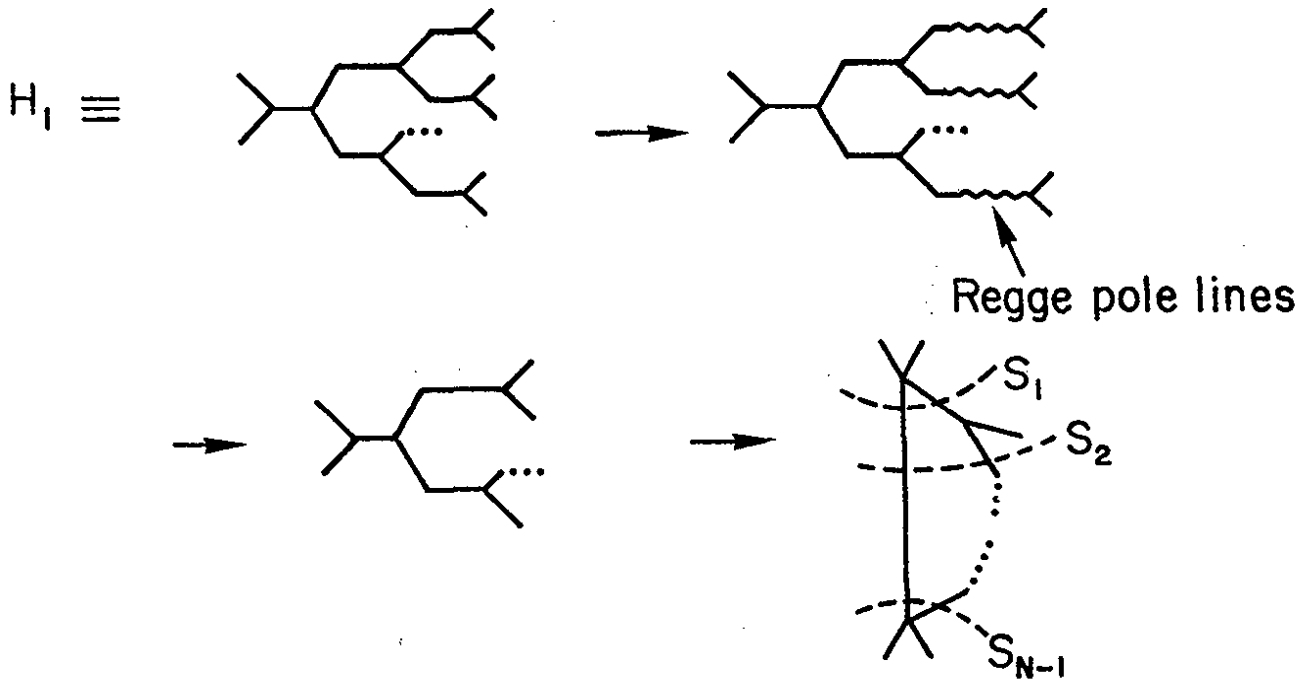


Fig. 3.15

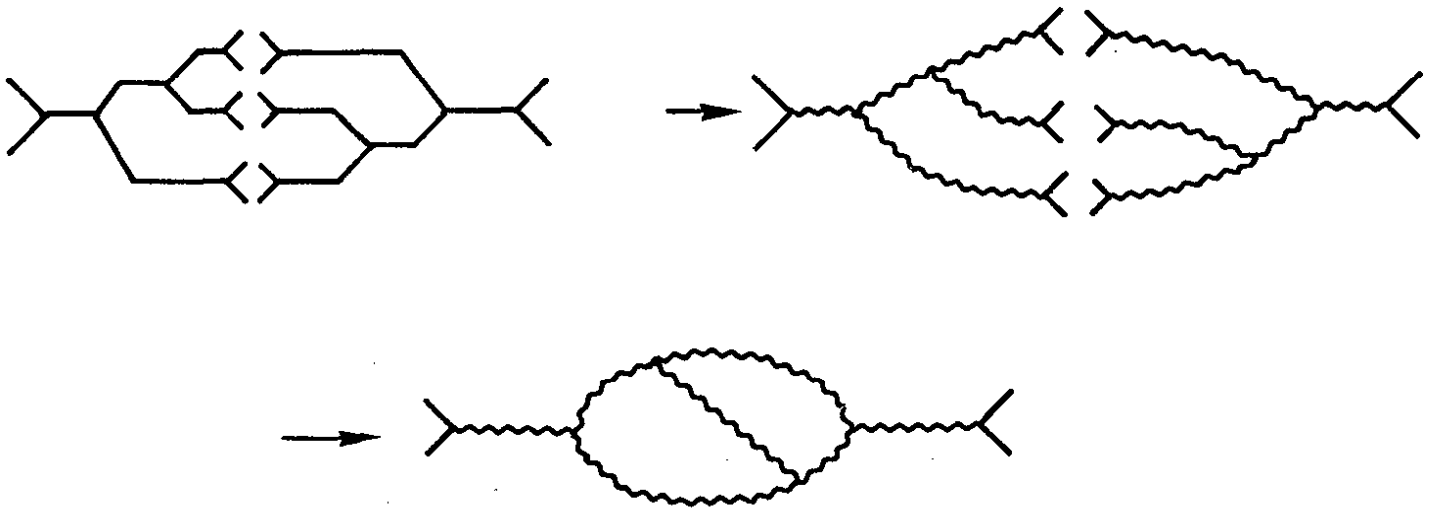


Fig.3.16

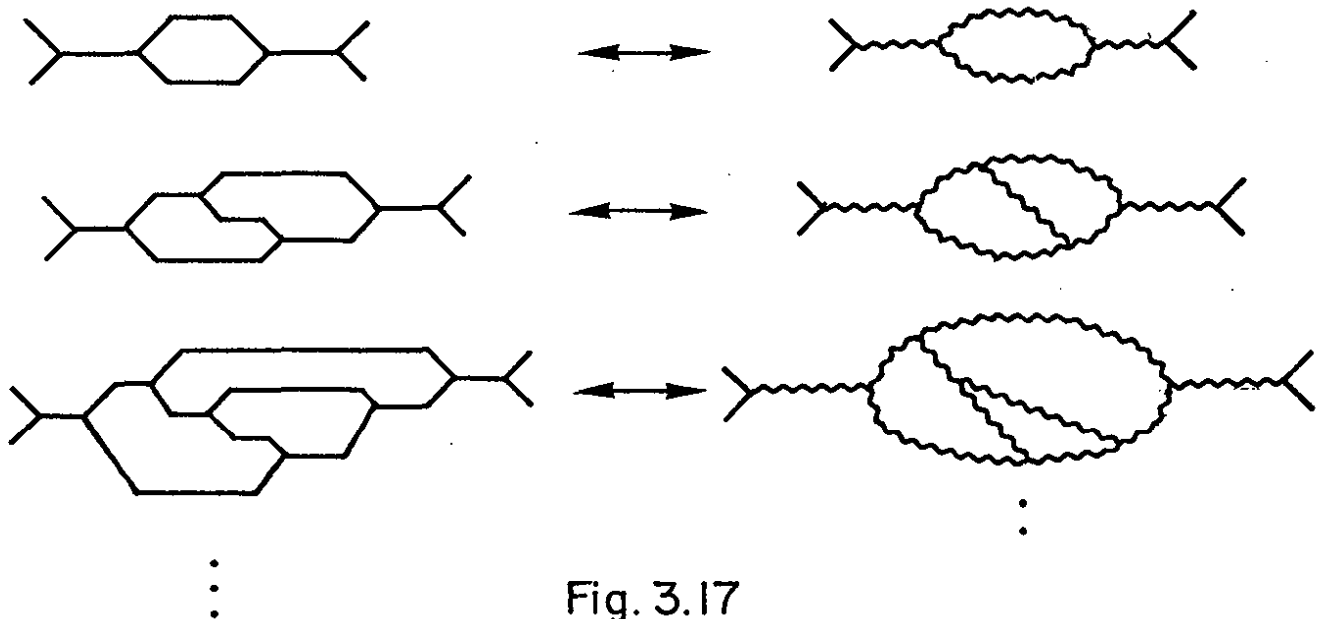


Fig. 3.17

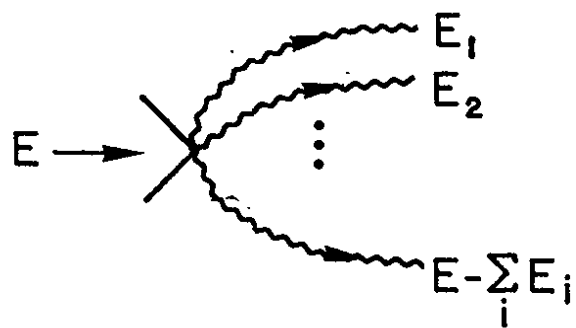


Fig. 3.18

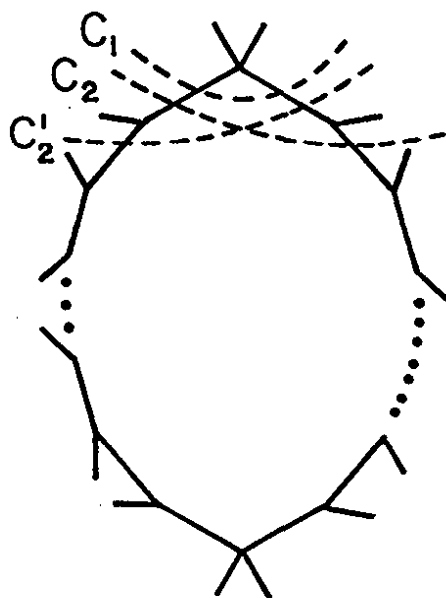


Fig. 3.19

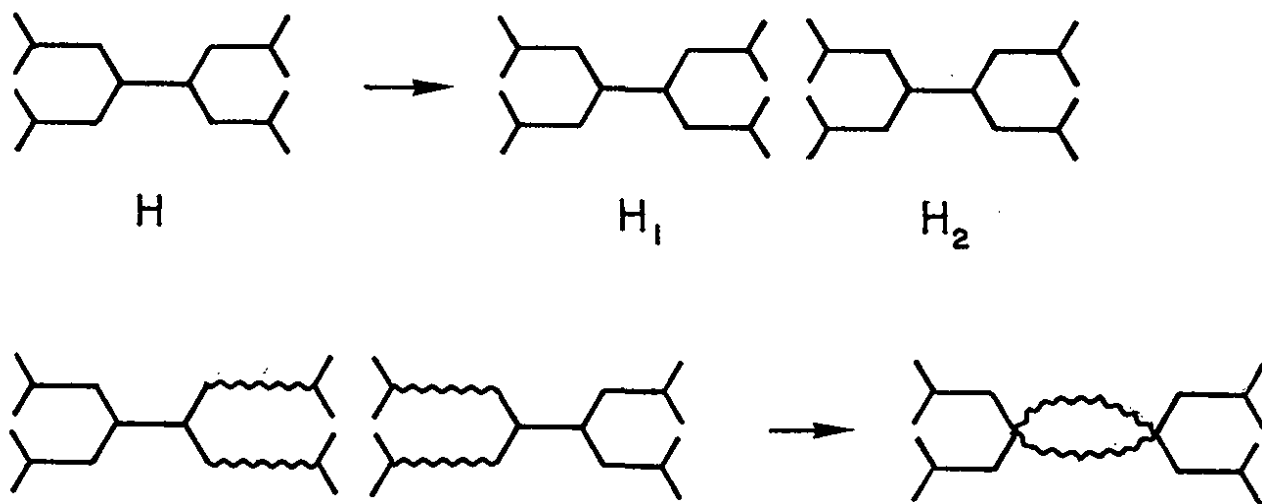


Fig. 3.20

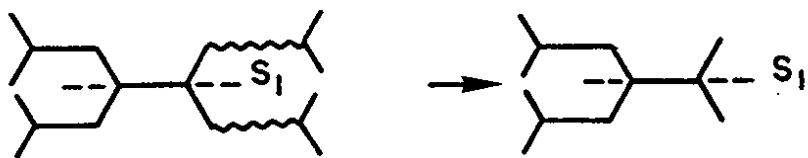


Fig. 3.21

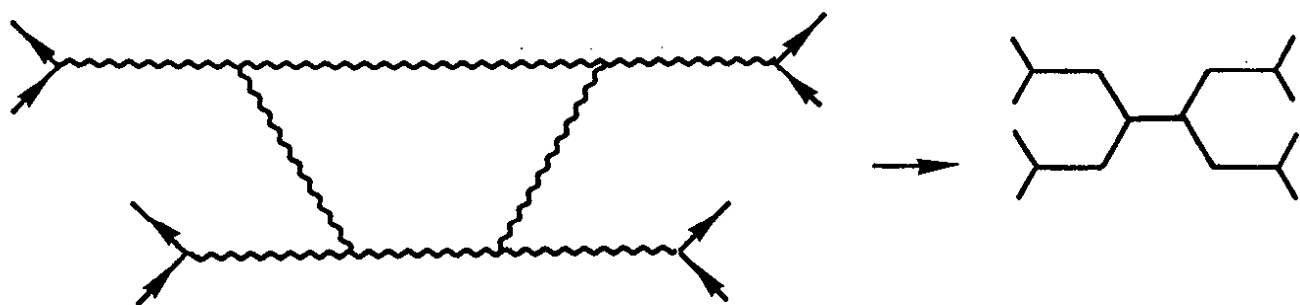


Fig. 3.22

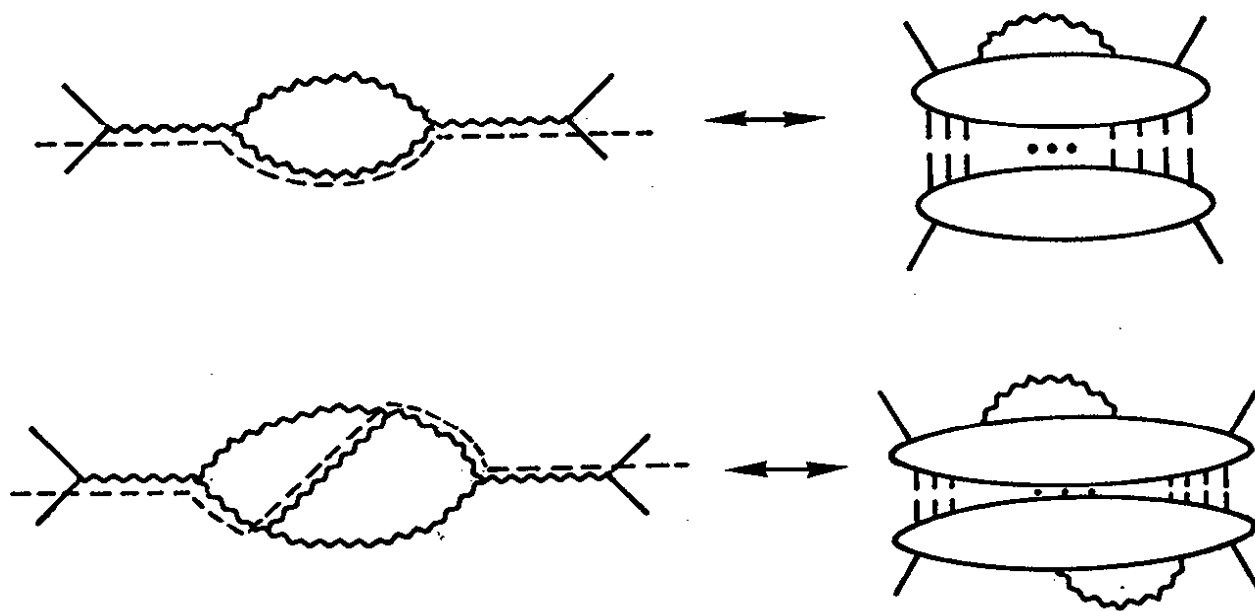


Fig. 3.23

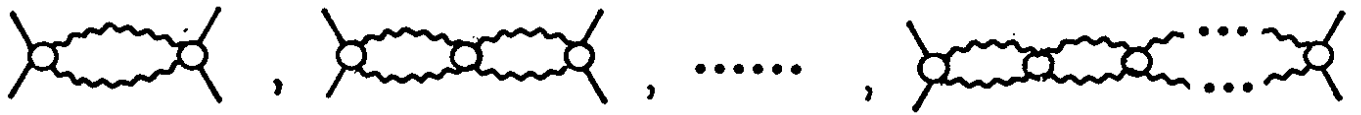


Fig. 4.1



Fig. 4.2

$$\Sigma \int d\Omega \left[ \text{diagram with } S_{ij} \text{ bracket} \right] = \text{disc}_{S_{ij}} \left[ \text{diagram with } S_{ij} \text{ bracket} \right]$$

Fig. 4.3

$$\begin{matrix} \underline{q-k} & & \underline{q-k'} \\ & \diagdown & / \\ & \text{O} & \\ & / & \diagdown \\ \underline{k} & & \underline{k'} \end{matrix} = \Sigma \begin{matrix} & & \text{O} \\ & & | \\ & & \text{O} \\ & & | \\ & & \text{O} \end{matrix}$$

Fig. 4.4

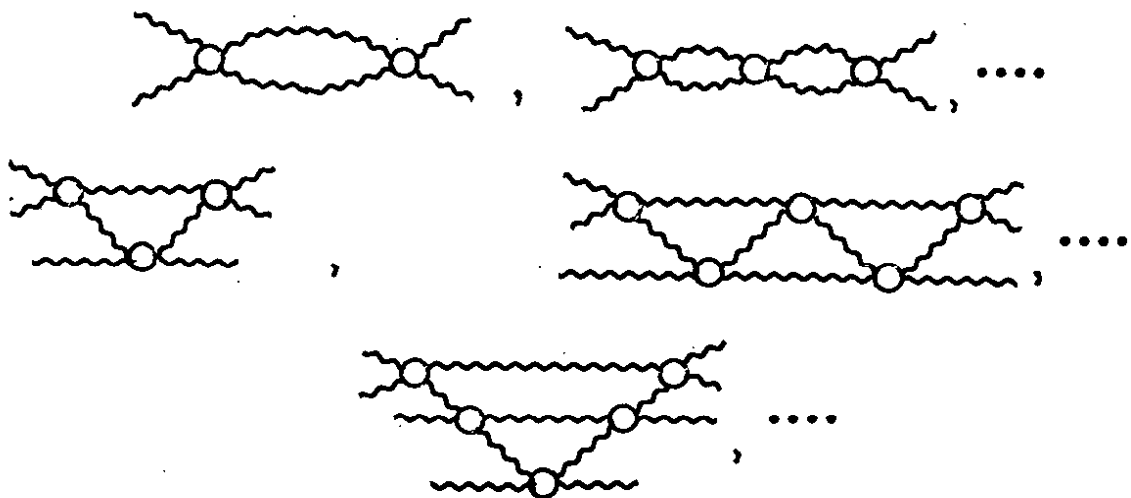


Fig. 4.5

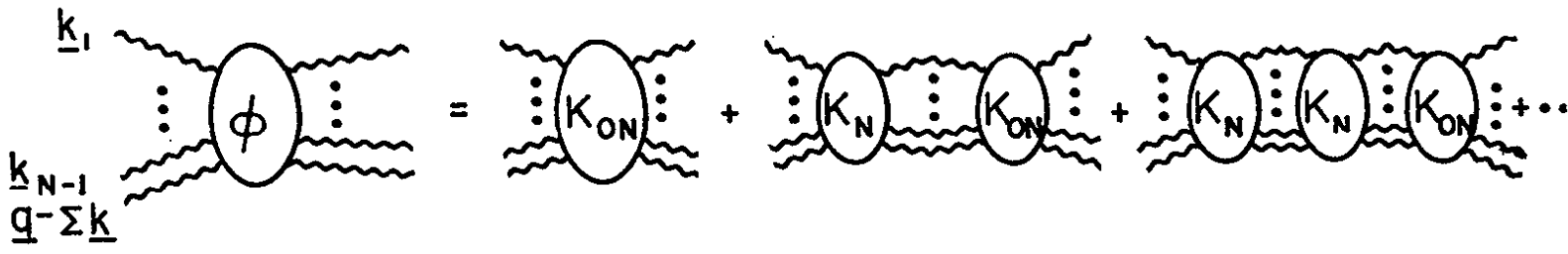


Fig. 4.6

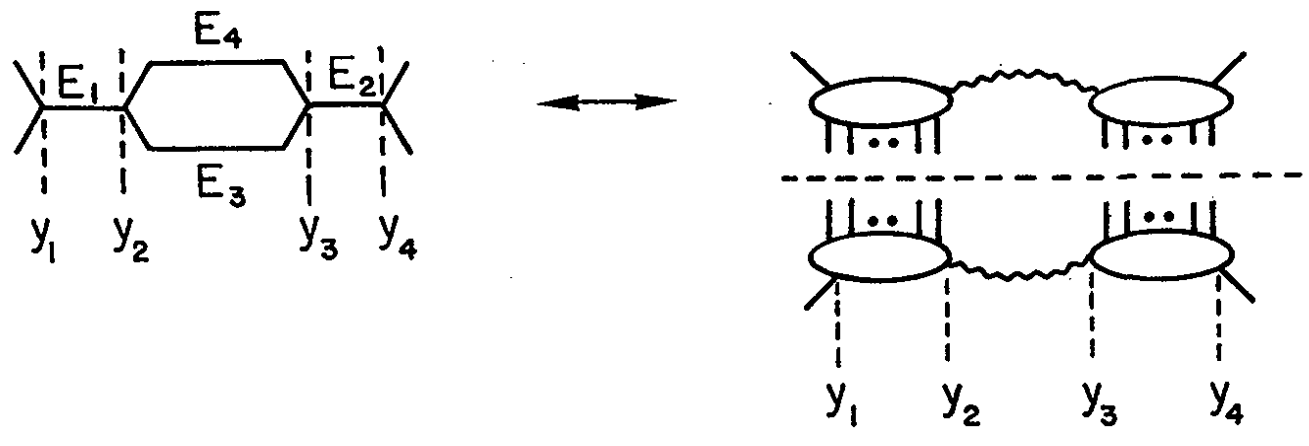


Fig. 5.1

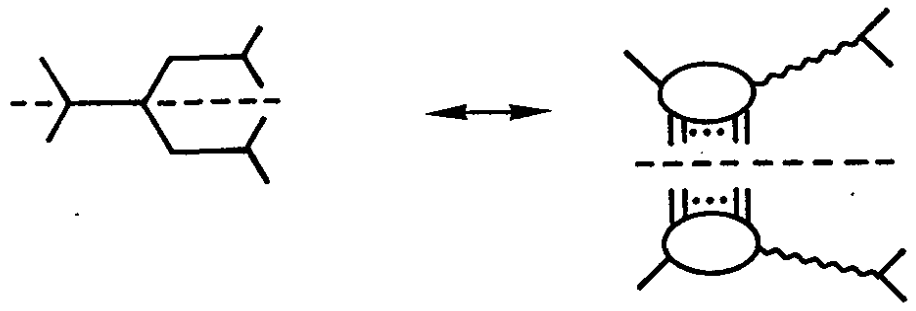


Fig. 5.2

Diagram illustrating a vertex with momentum  $E$  and outgoing momenta  $k_1, k_2$ . The vertex is represented by a horizontal line with two diagonal lines branching out to the right, labeled  $k_1$  and  $k_2$ .

$$\sim \tau_0 \left[ E - \alpha' (k_1^2 - M^2) - \alpha' (k_2^2 - M^2) \right]$$

Fig. 5.3

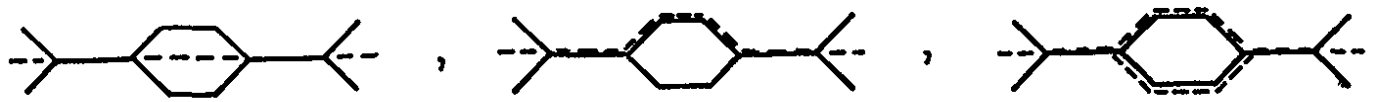


Fig. 5.4

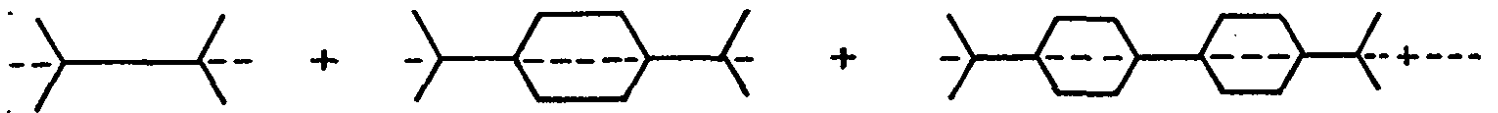


Fig. 5.5

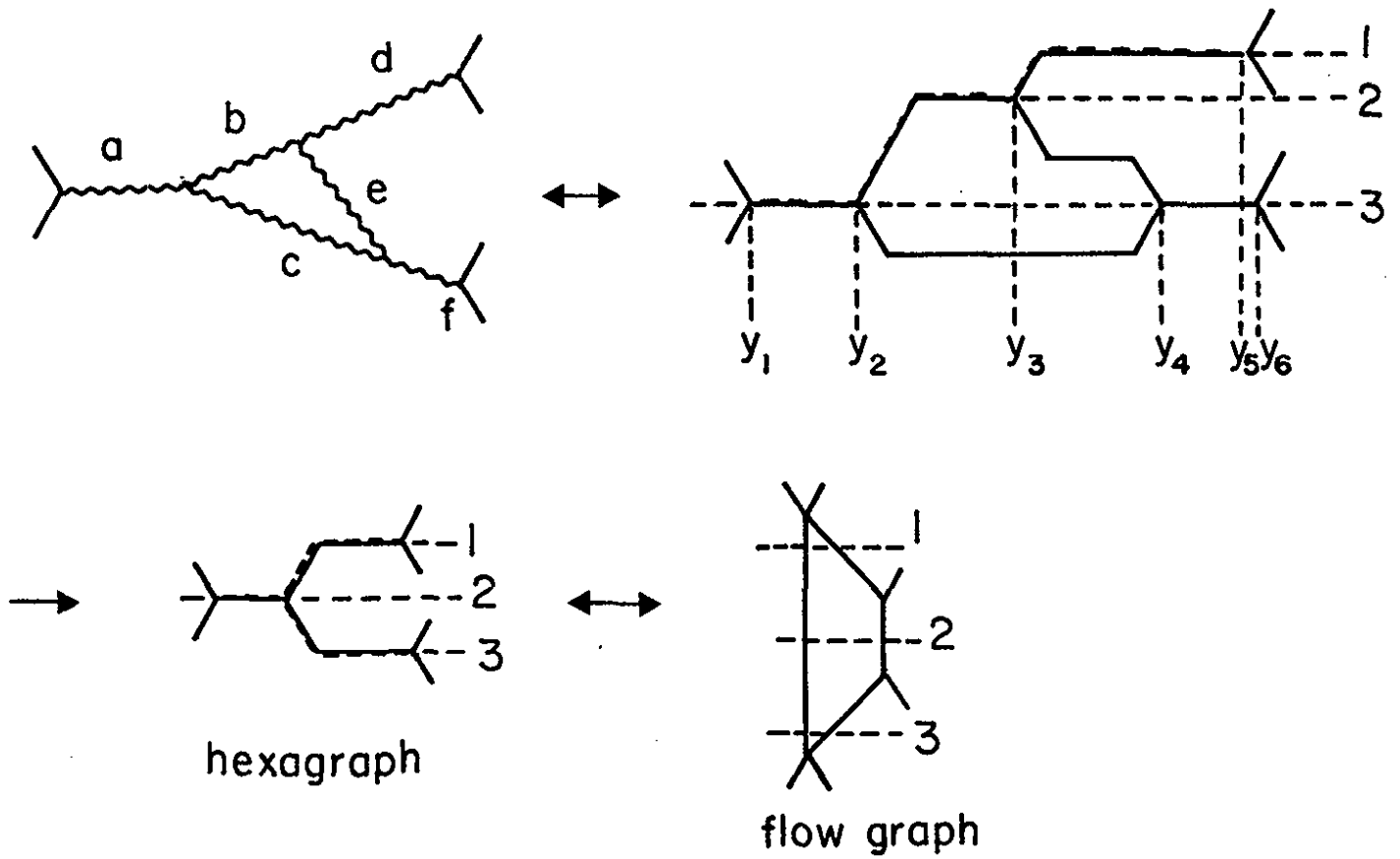


Fig. 5.6

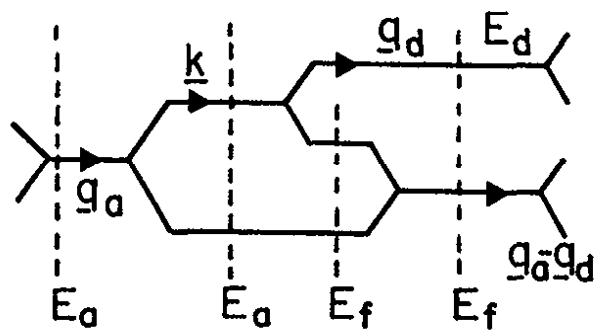


Fig. 5.7

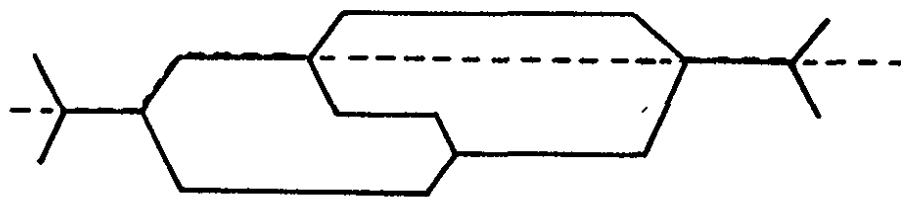


Fig. 5.8

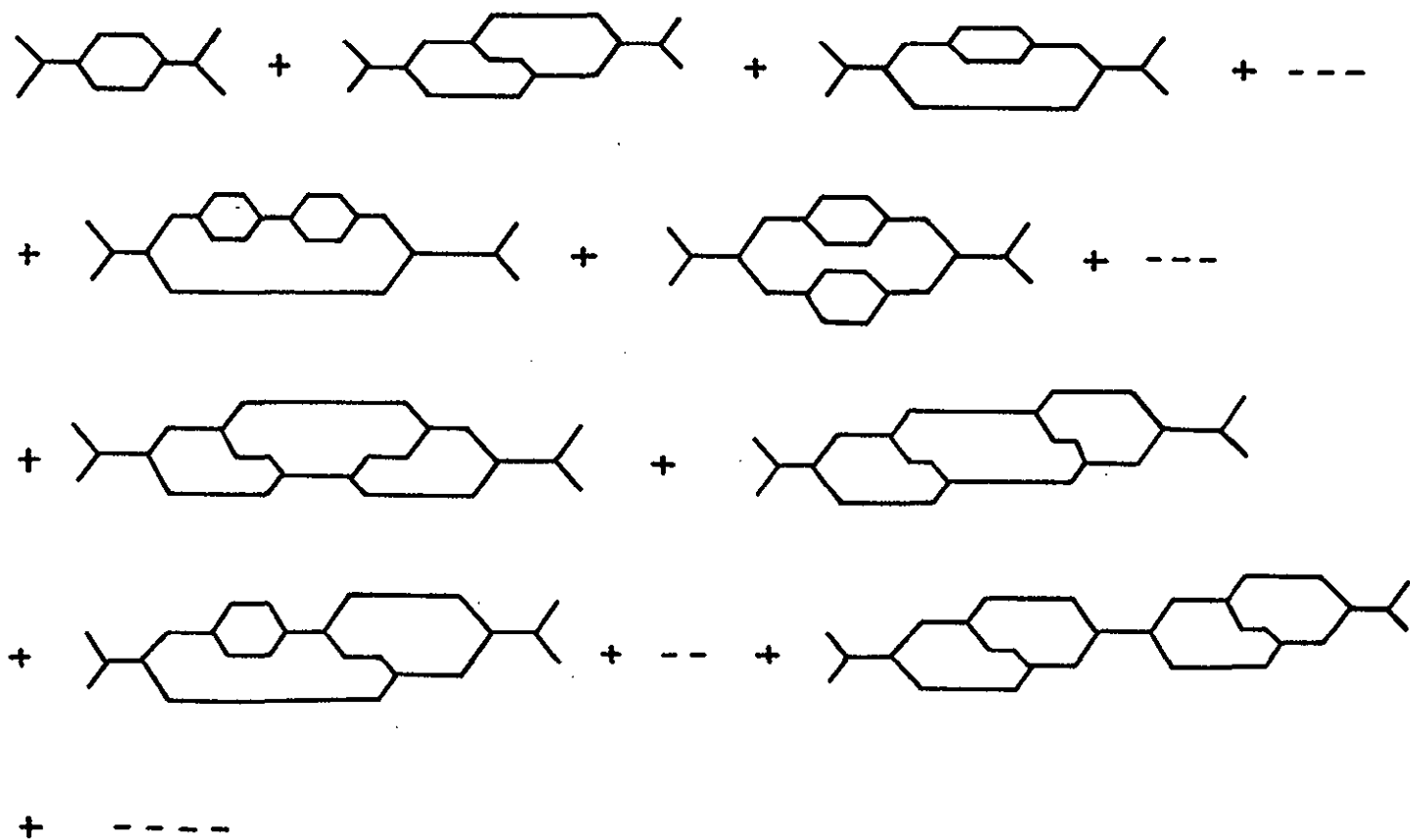
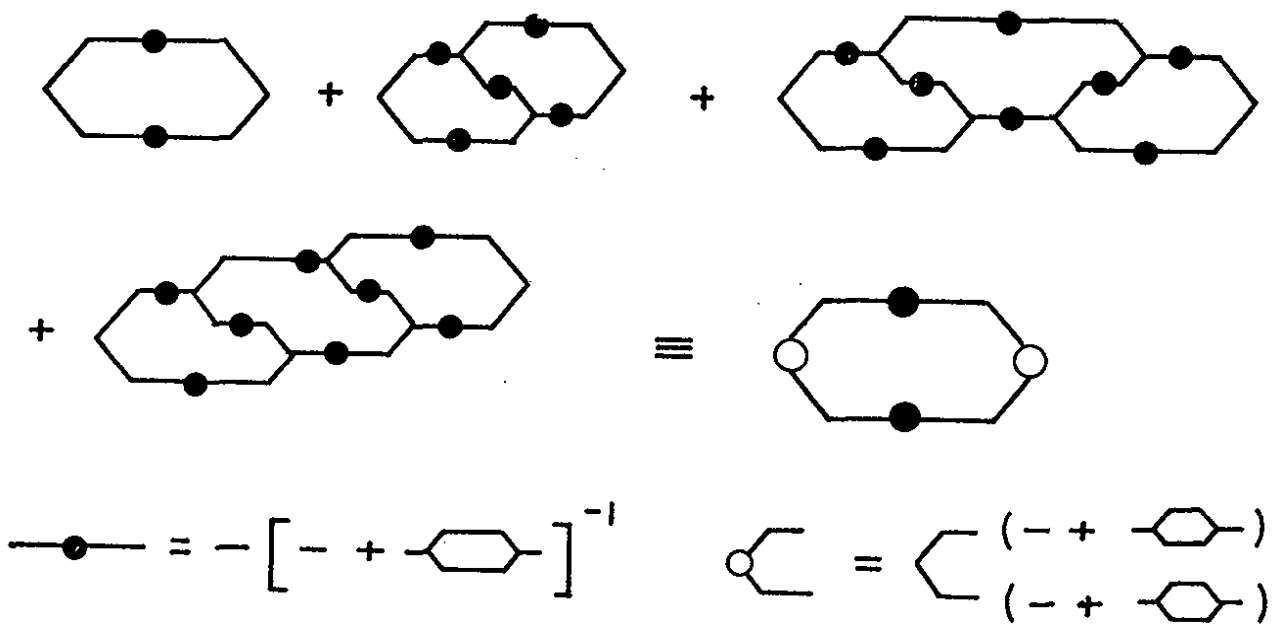
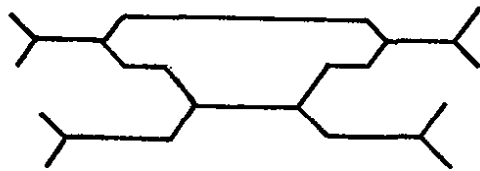
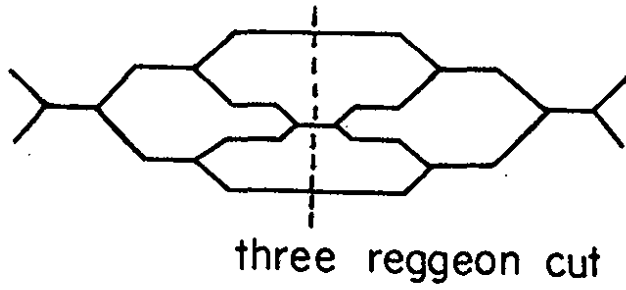
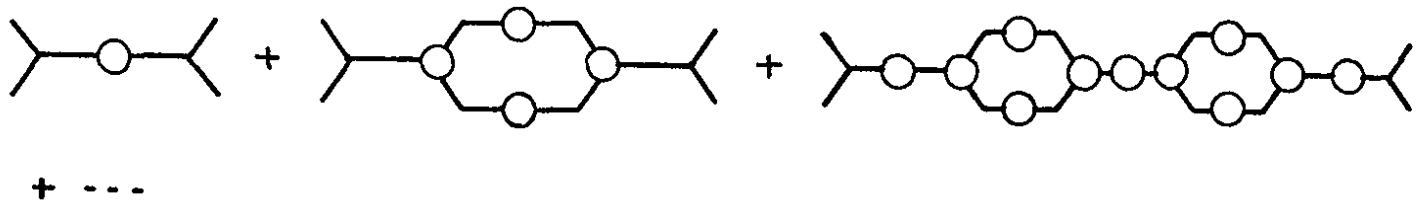


Fig. 5.9





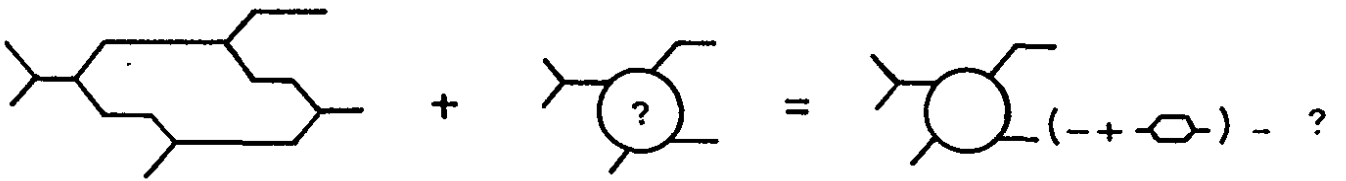


Fig. 5.14

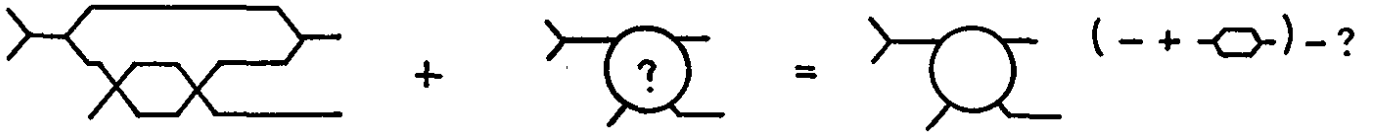


Fig. 5.15

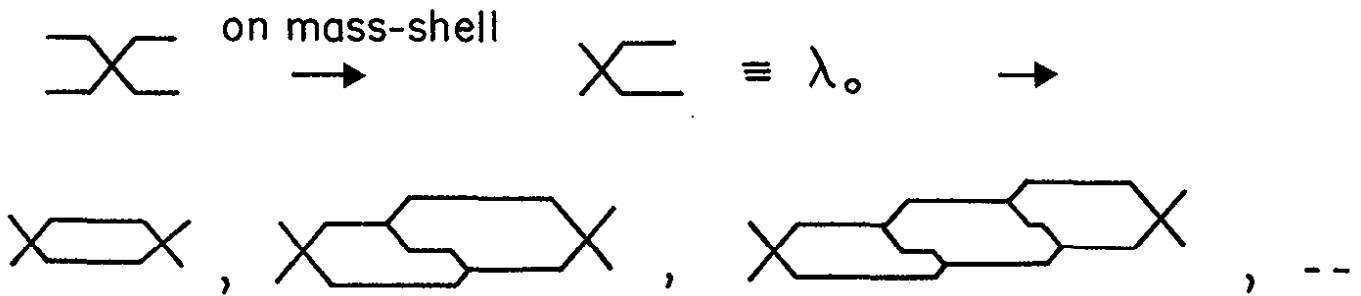


Fig. 5.16



Fig. 5.17

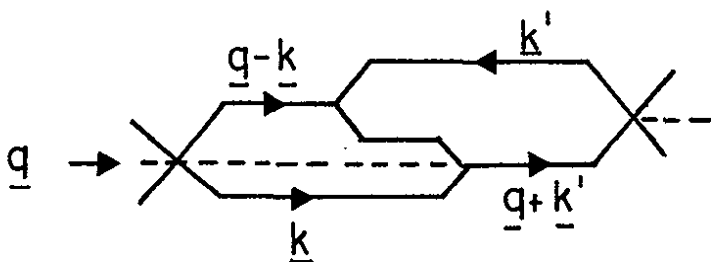


Fig. 5.18

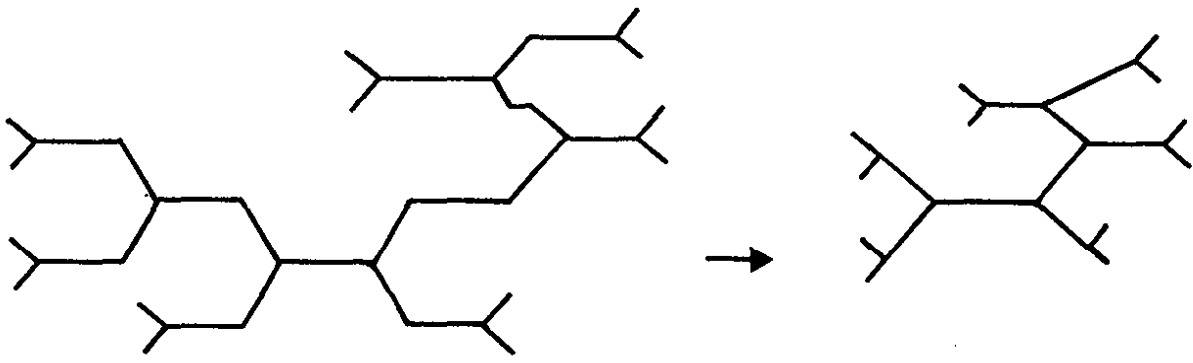


Fig. 5.19

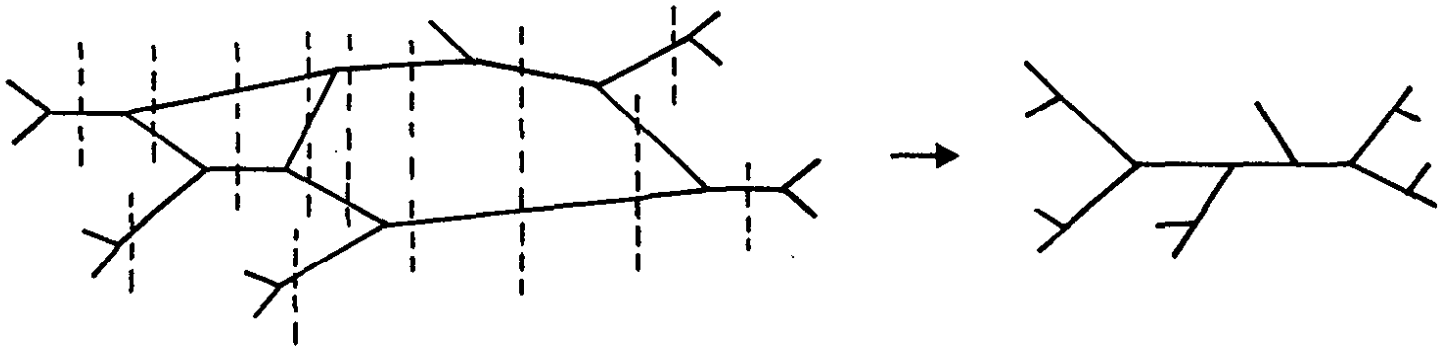
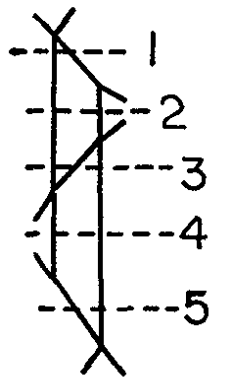
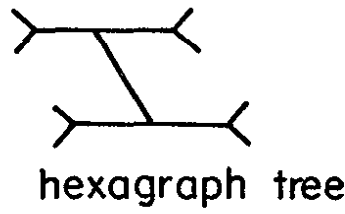
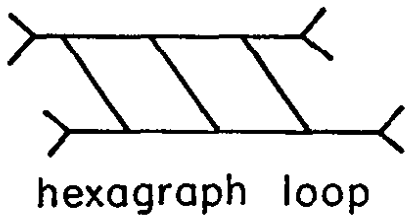


Fig. 5.20



flow-graph

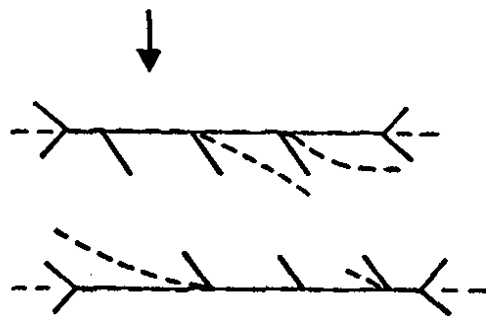
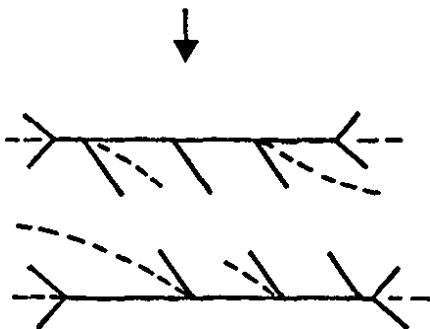
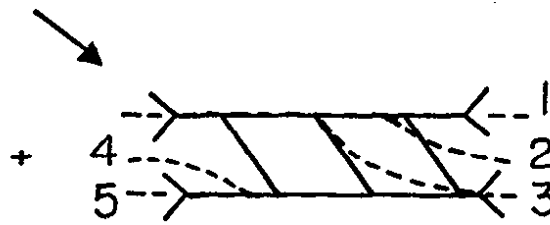
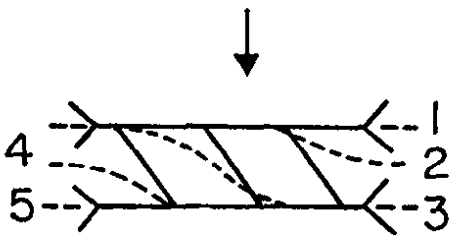


Fig. 5.21

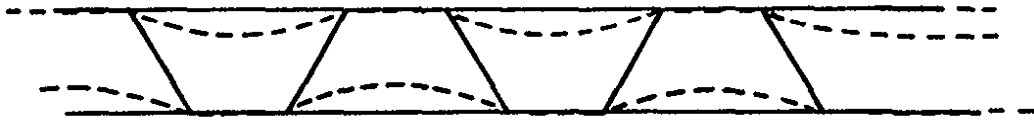
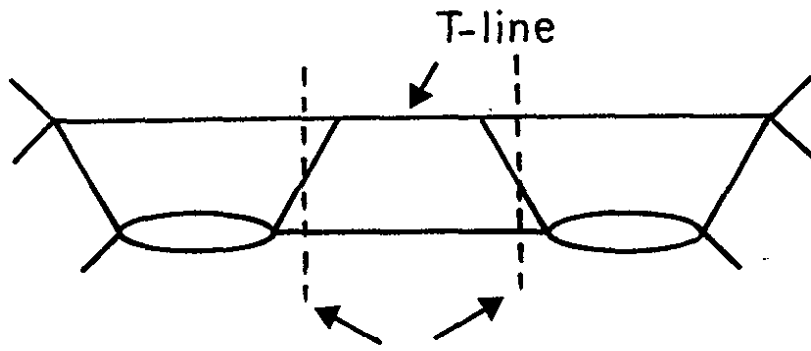
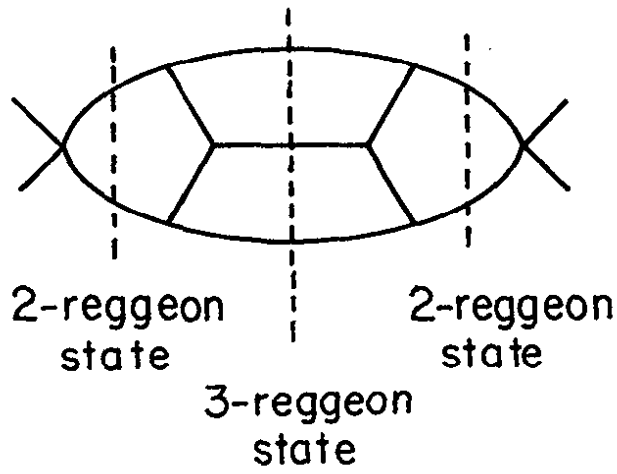


Fig. 5.22



3-reggeon states

Fig. 5.23



2-reggeon state

2-reggeon state

3-reggeon state

Fig. 5.24

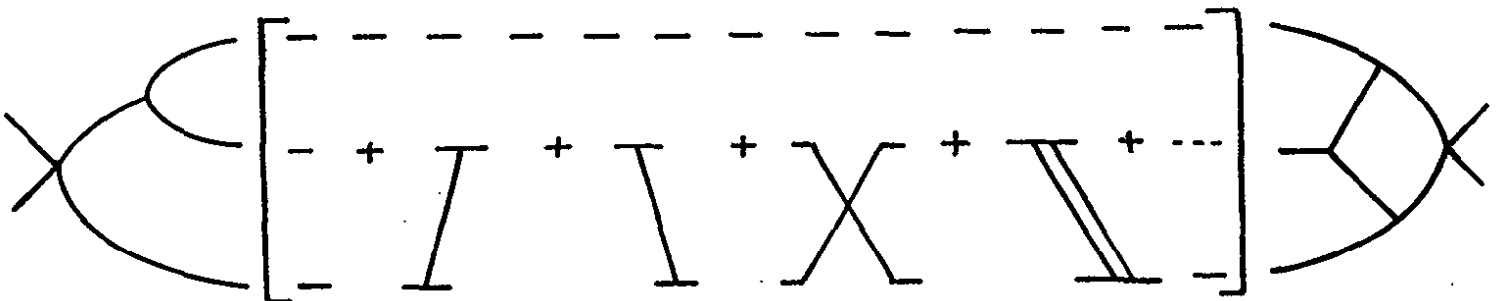


Fig. 5.25

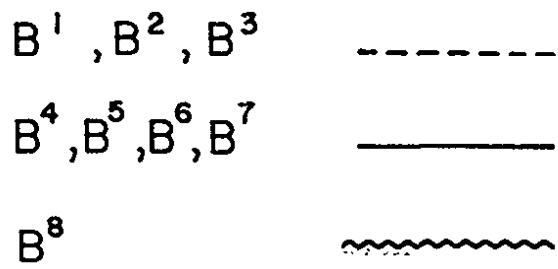


Fig. 6.1

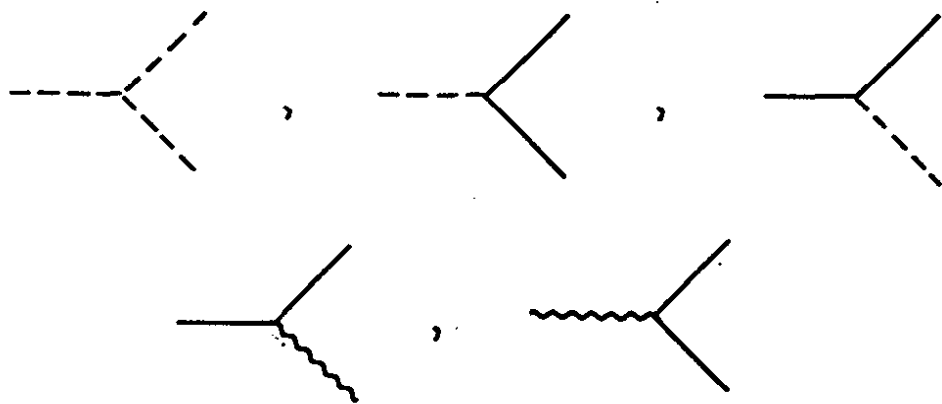


Fig. 6.2

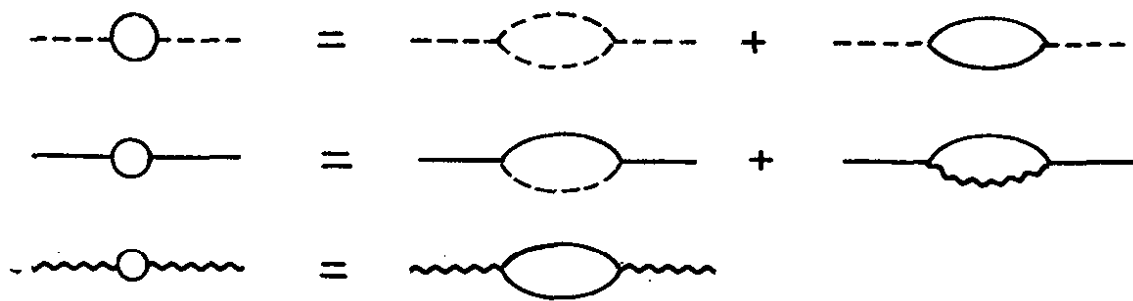


Fig. 6.3

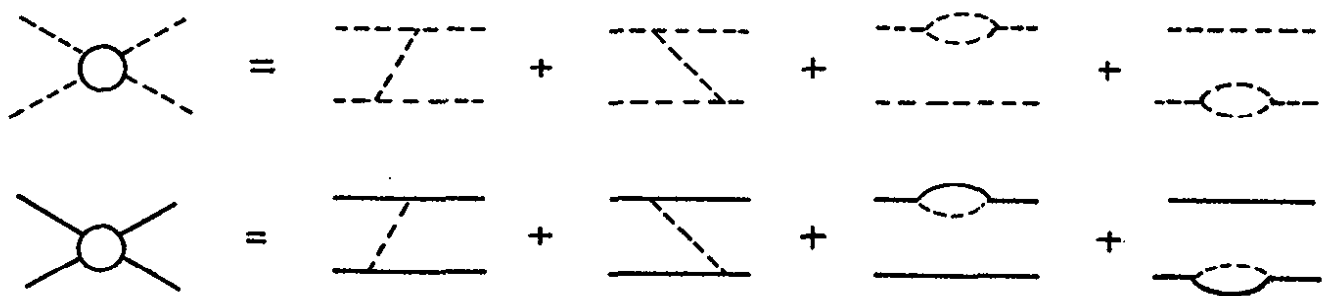


Fig. 6.4

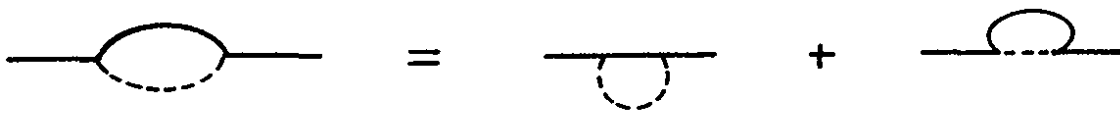


Fig. 6.5

$$\Delta_0(\underline{k}^2) = \text{---} \circ \text{---} = \text{---} \text{---} \text{---}$$

$$\Delta(\underline{k}^2) = \text{---} \circ \text{---} = \text{---} \text{---} \text{---} + \text{---} \text{---} \text{---}$$

$$\Delta_8(\underline{k}^2) = \text{---} \text{---} \text{---}$$

Fig. 6.6

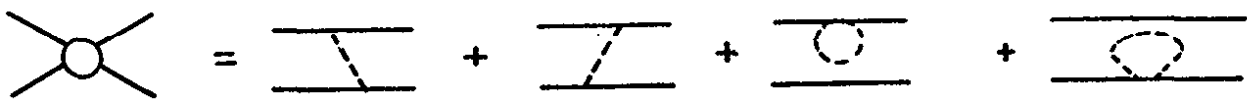
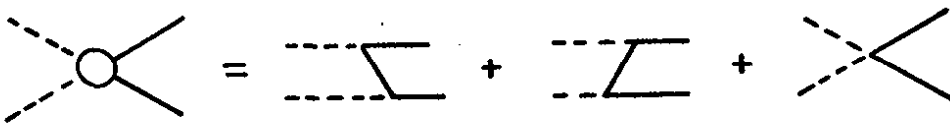
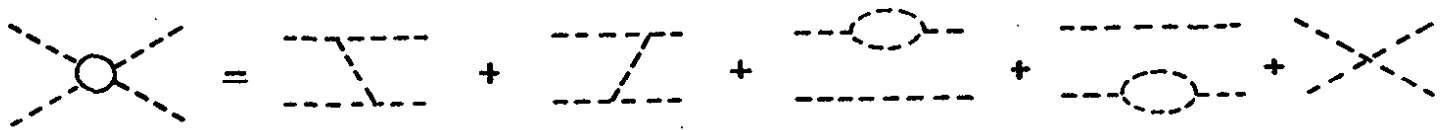


Fig. 6.7

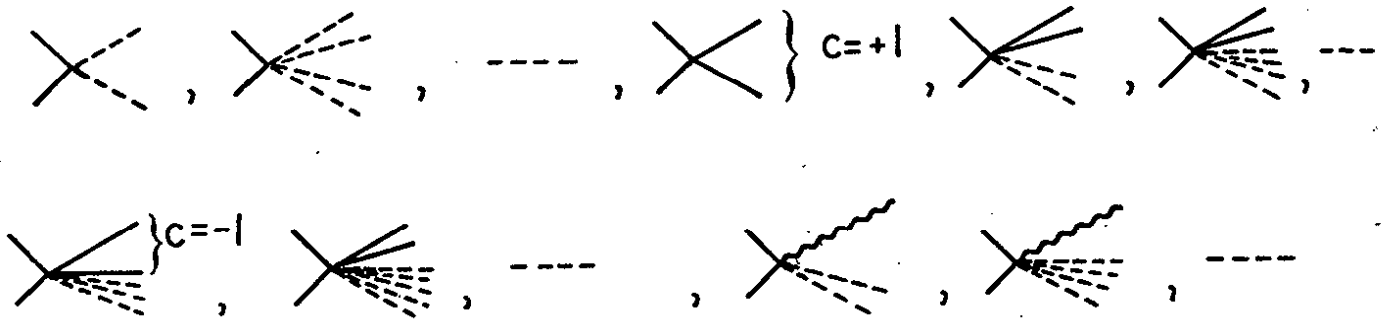


Fig. 6.8

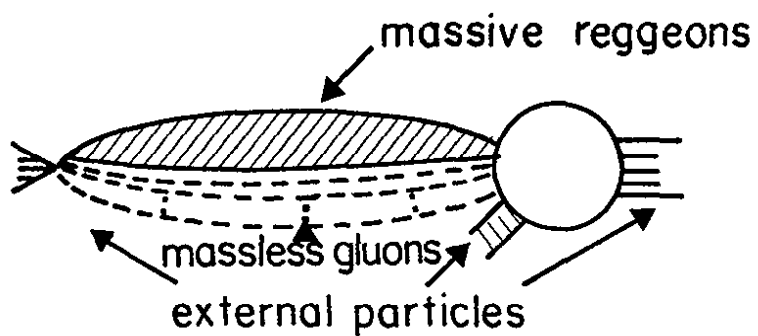


Fig.6.9

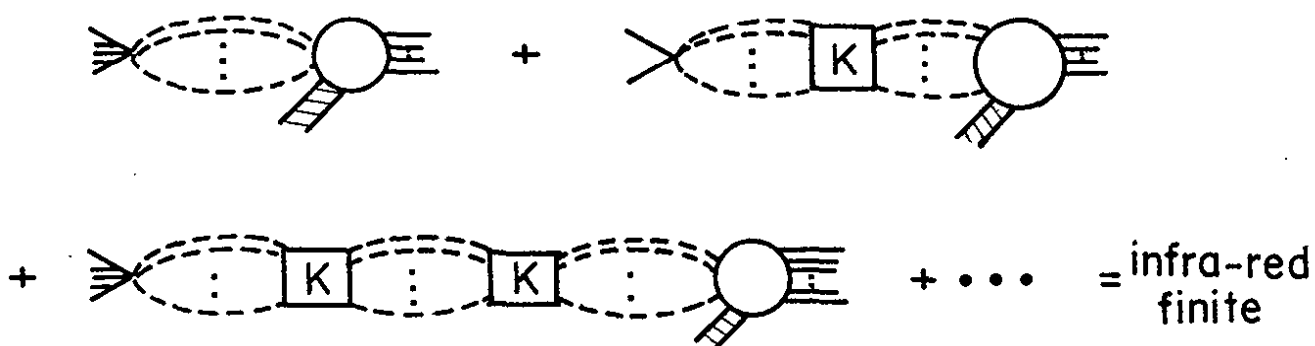


Fig.6.10

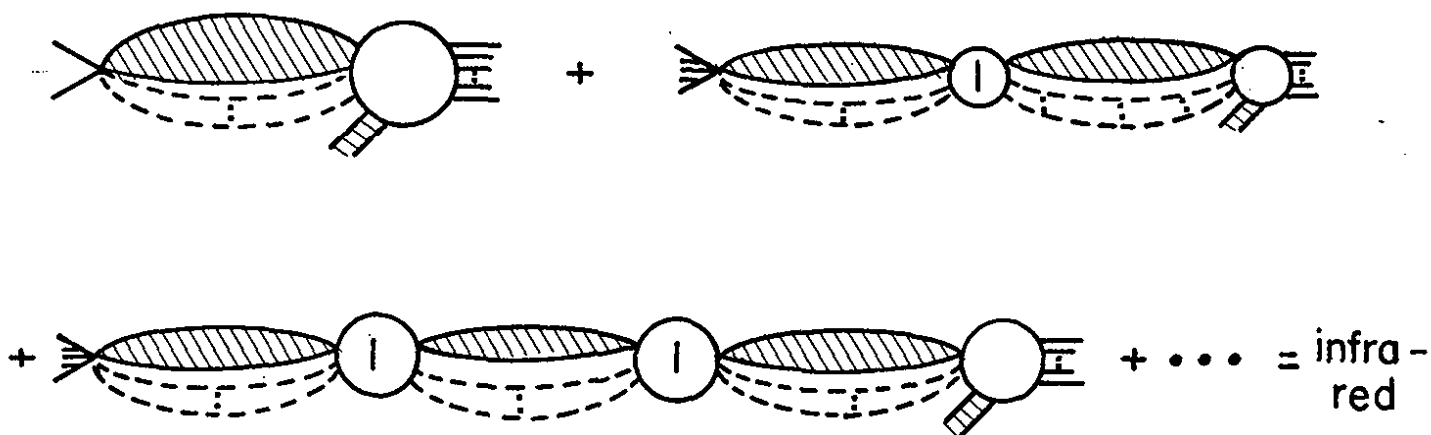


Fig.6.11

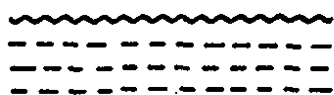


Fig.6.12

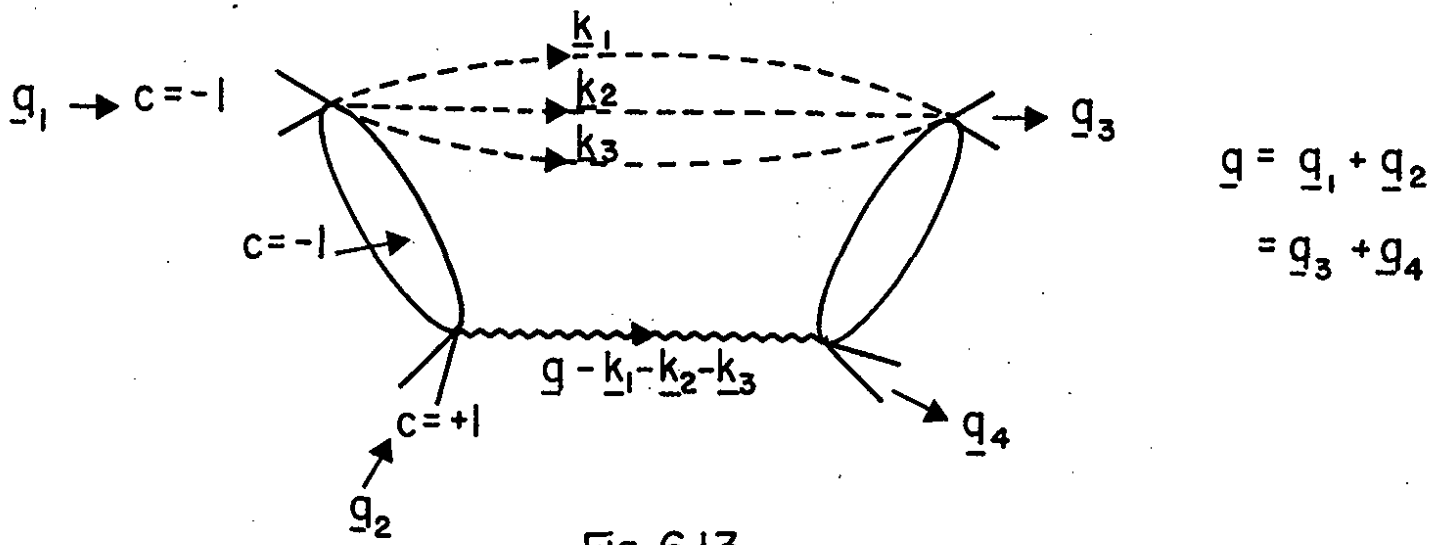


Fig. 6.13

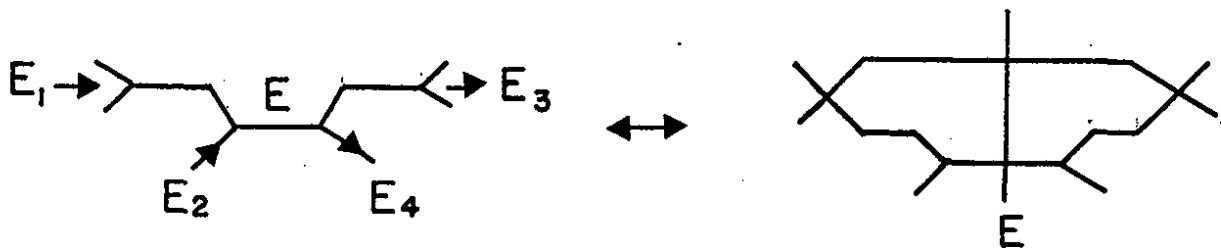


Fig. 6.14

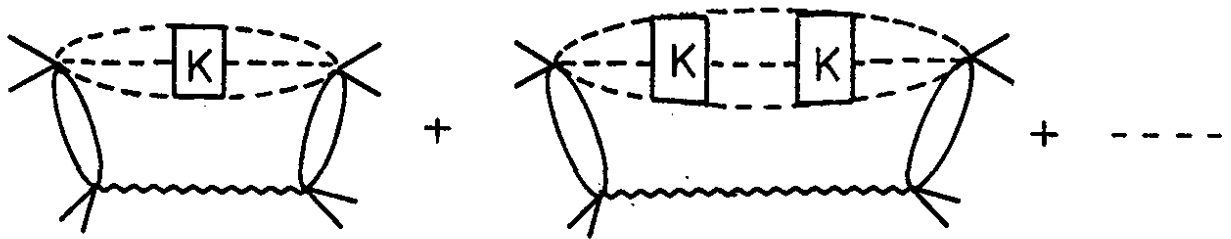


Fig. 6.15

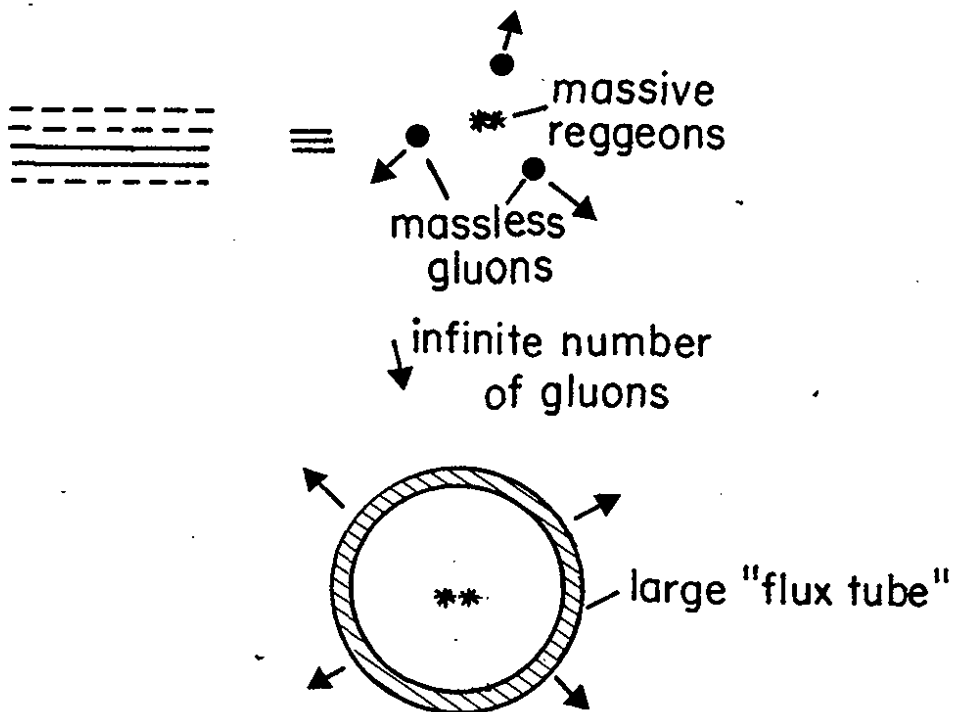


Fig. 6.16

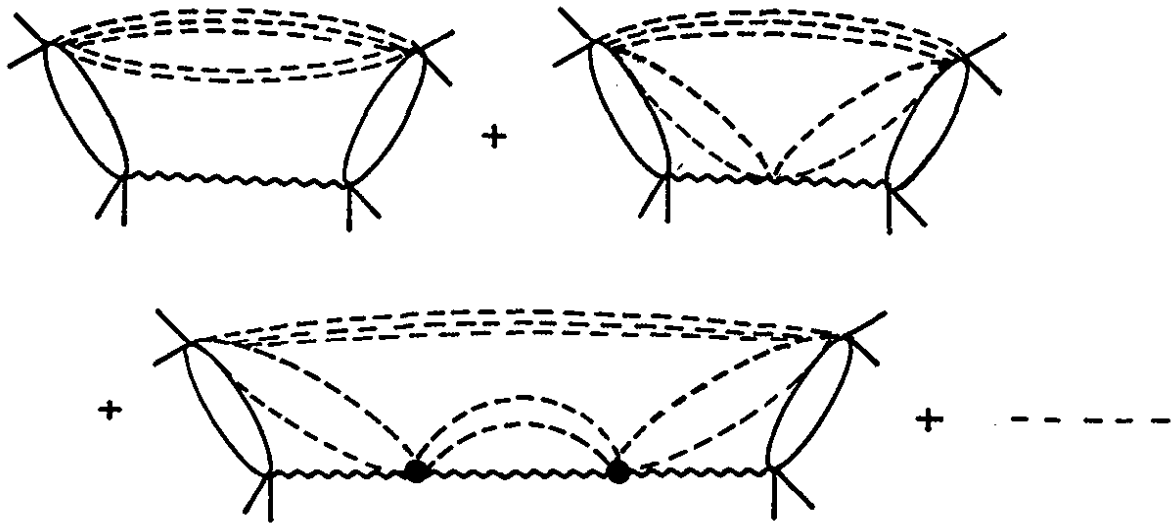


Fig.6.17

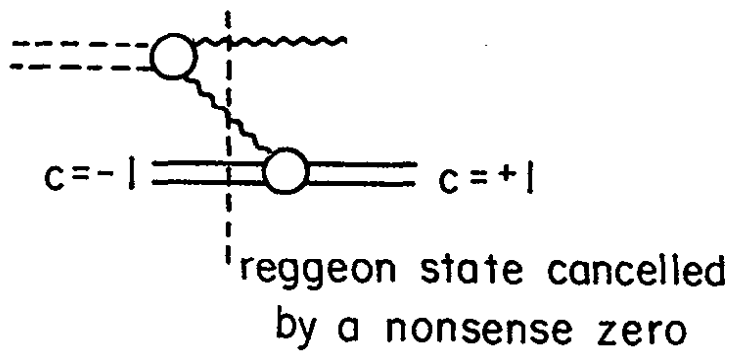


Fig. 6.18



Fig.6.19

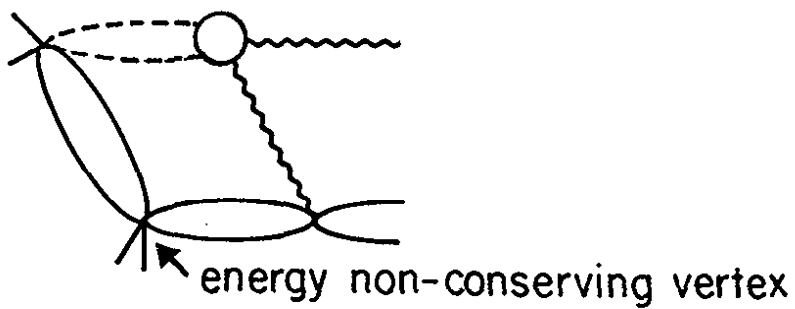


Fig. 6.20



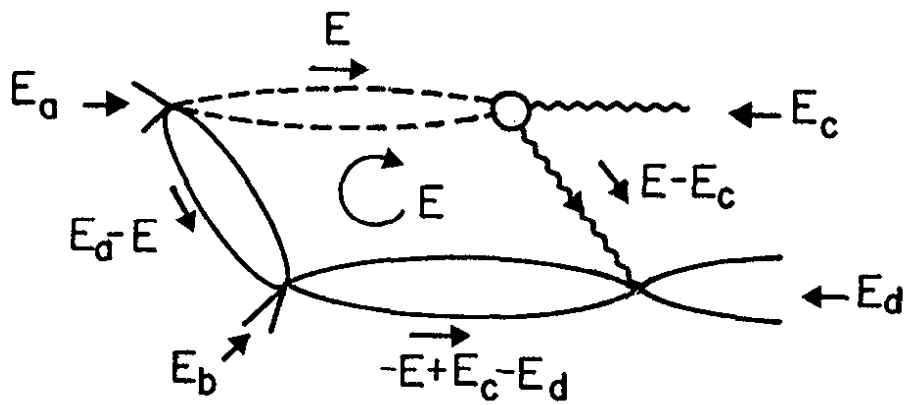


Fig. 6.21

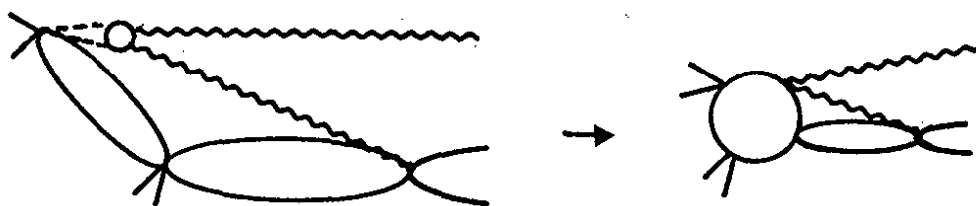


Fig. 6.22

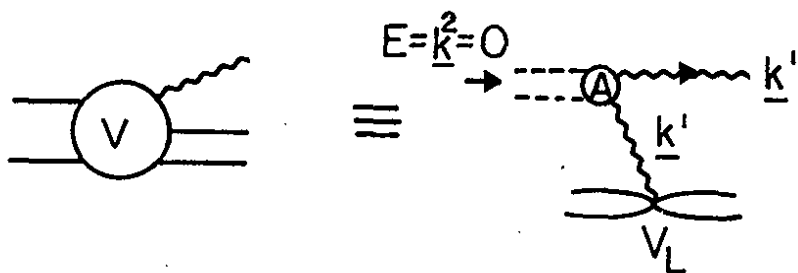
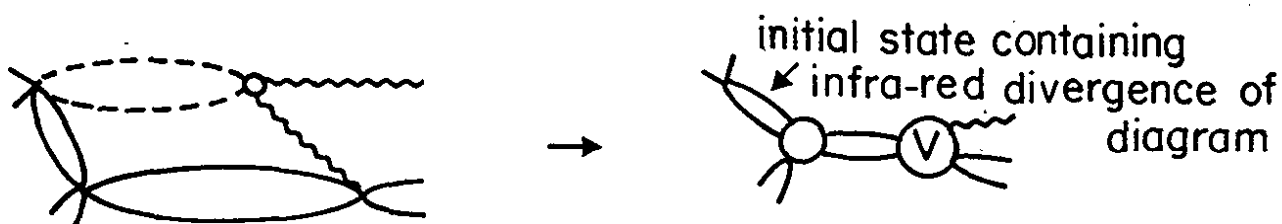


Fig. 6.23

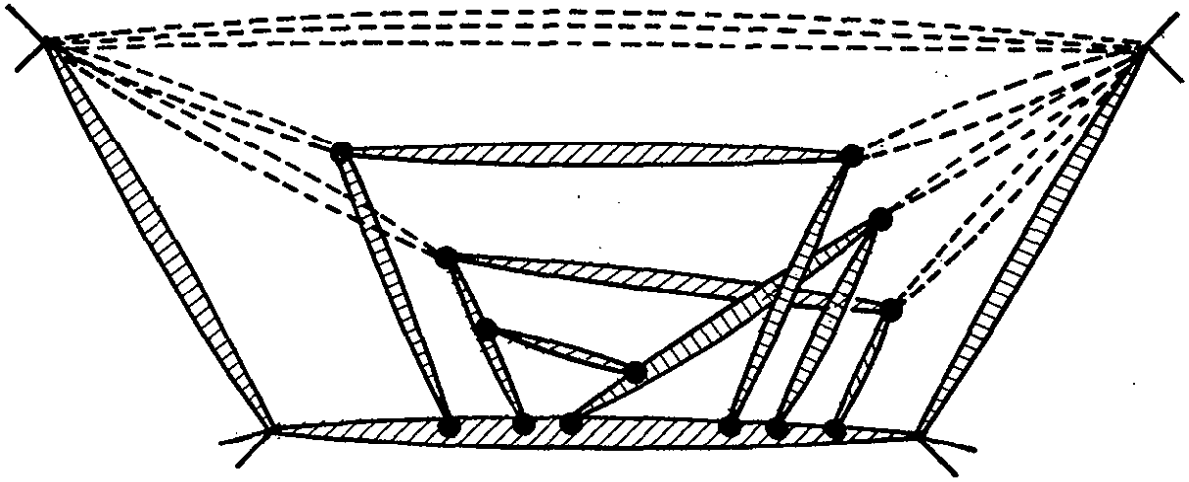


Fig. 6.24

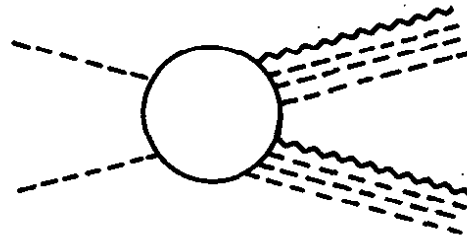


Fig. 6.25

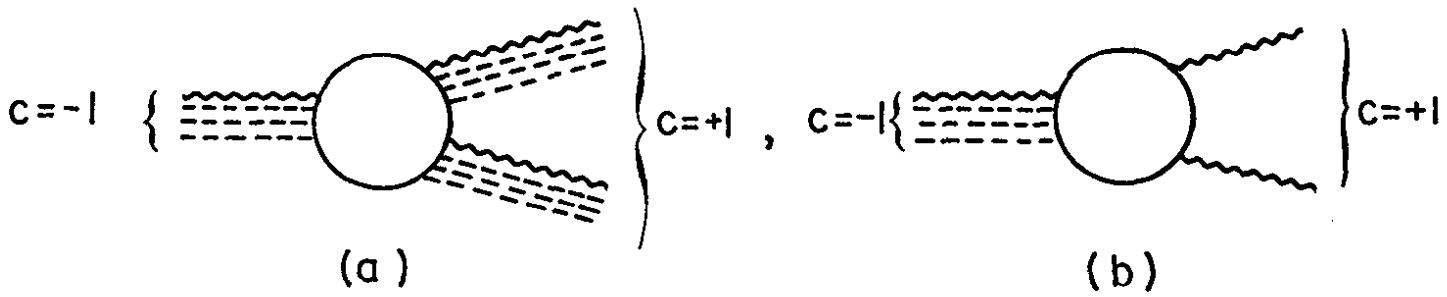


Fig. 7.1



Fig. 7.2

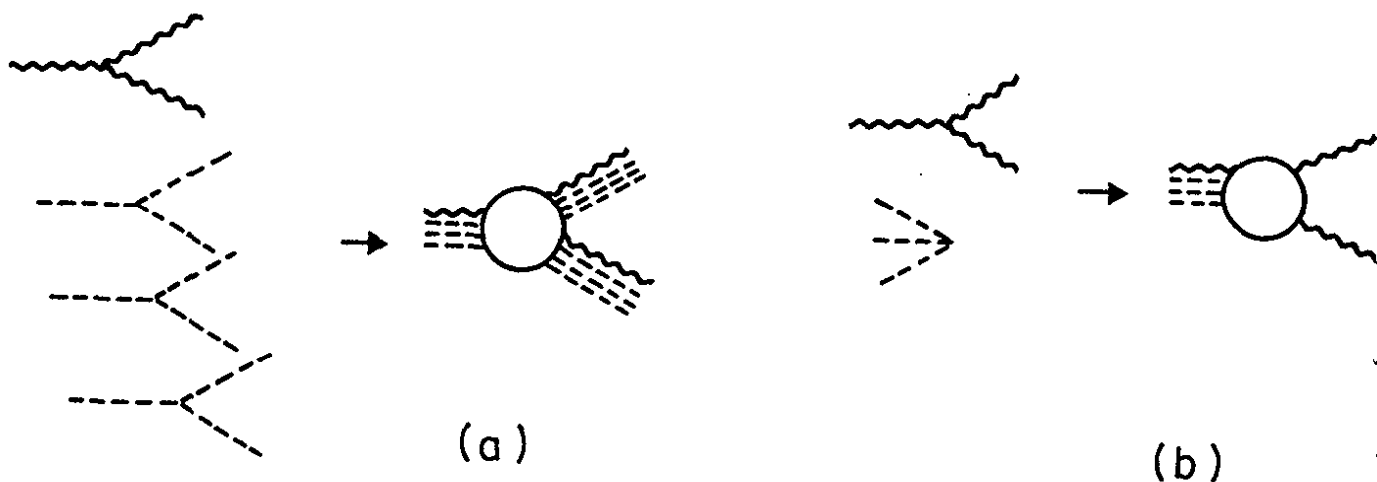


Fig. 7.3

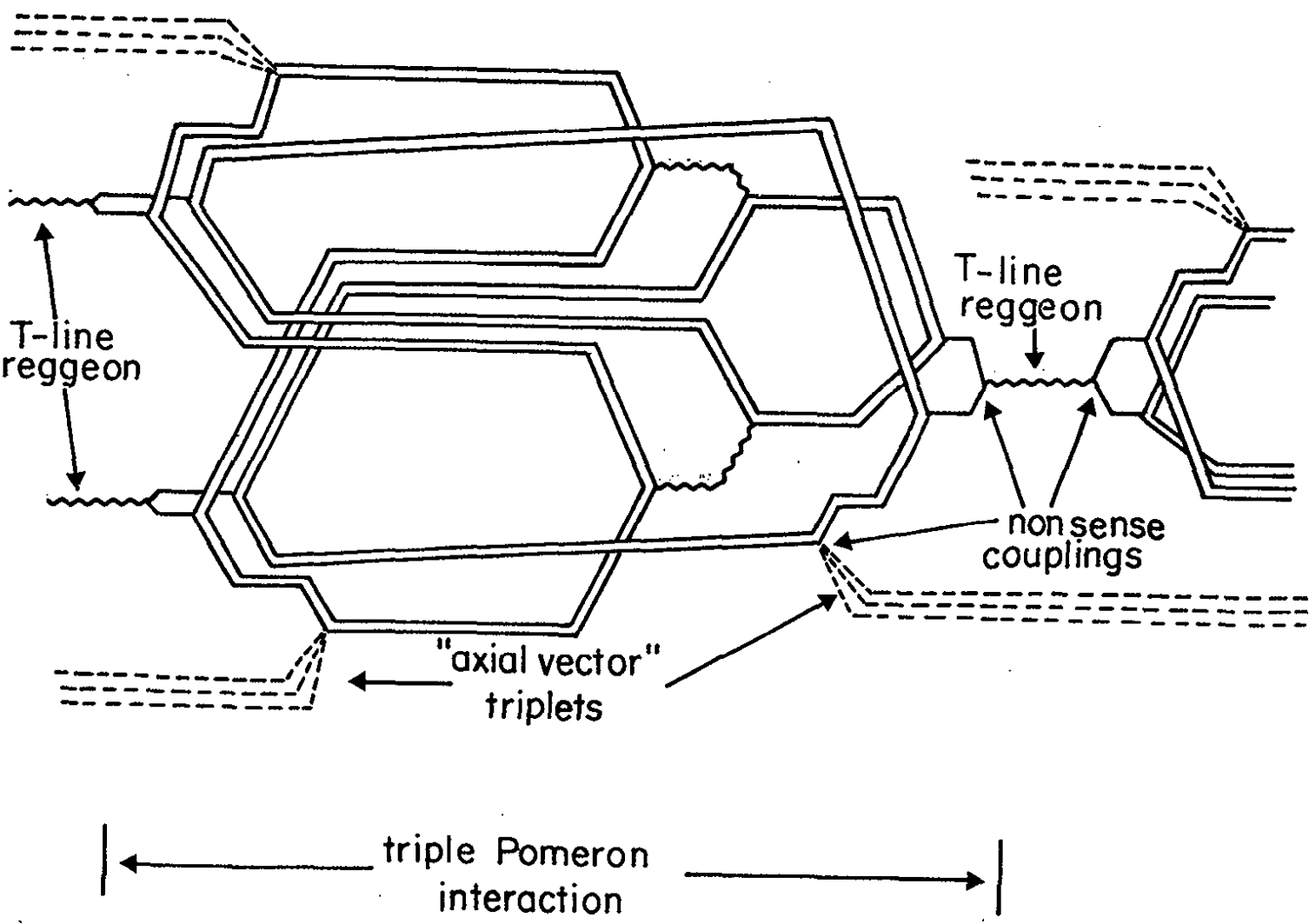


Fig. 7.4

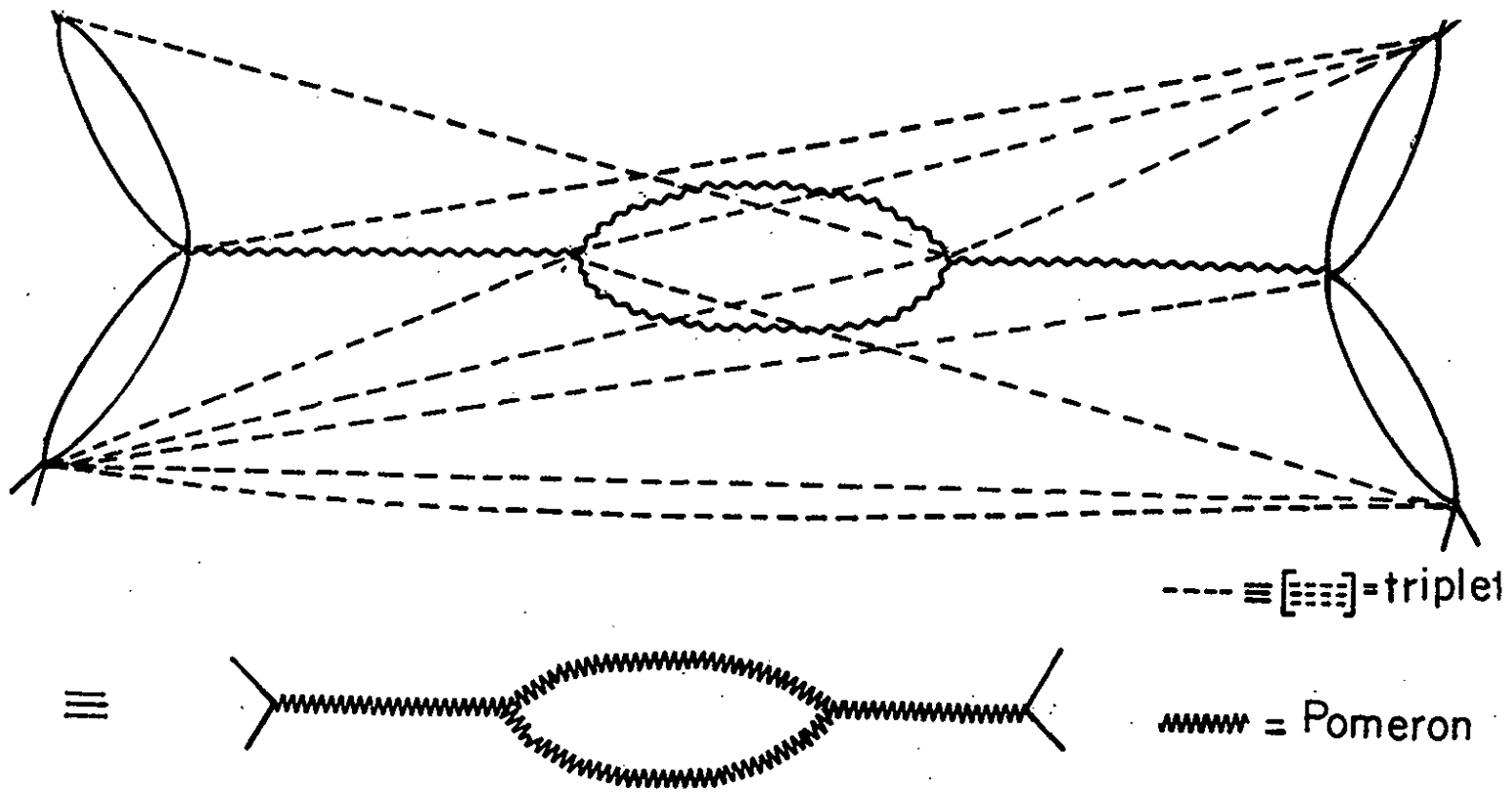


Fig. 7.5

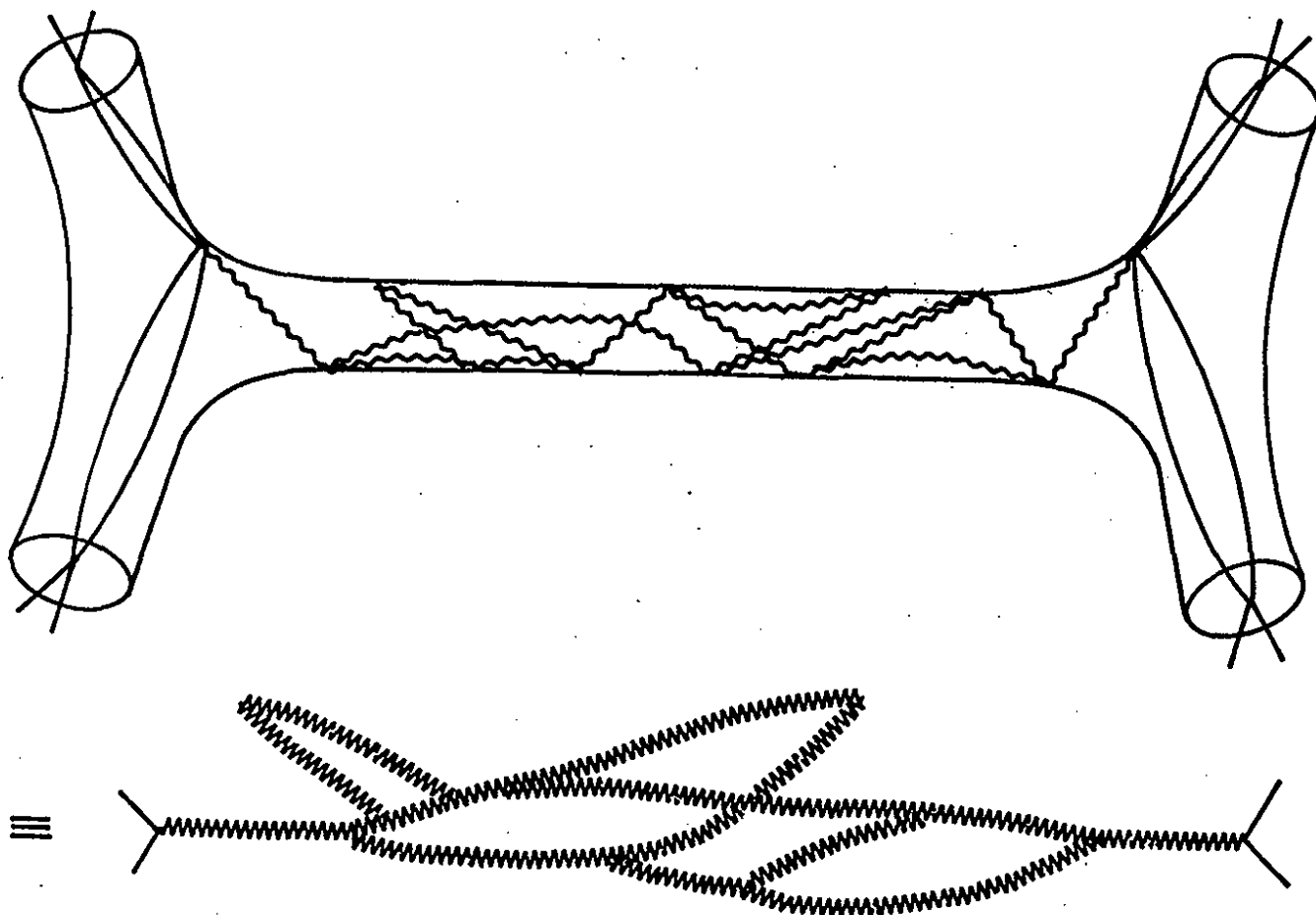

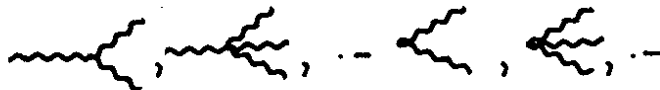


Fig. 7.6

Pomeron  $\equiv$  , interactions : 

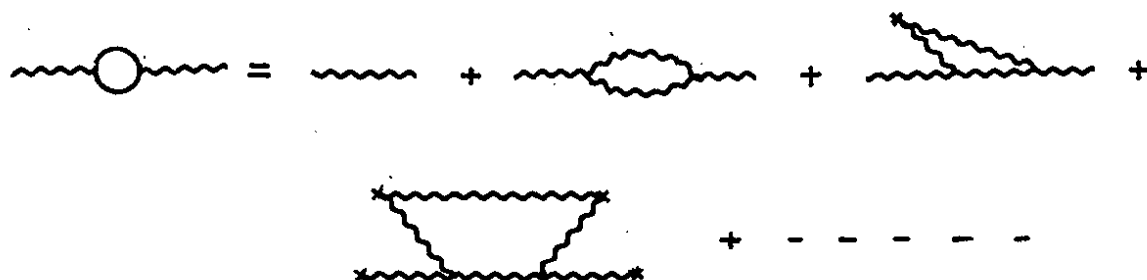
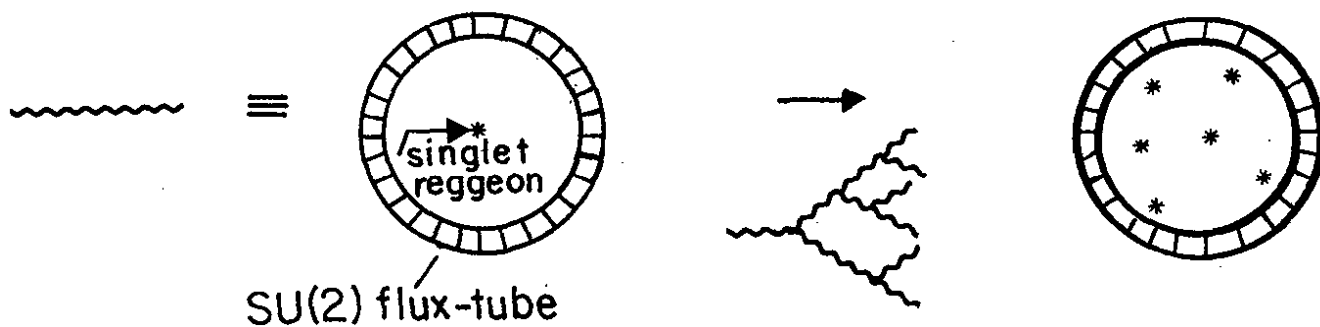


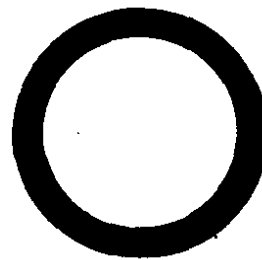
Fig. 7.7



critical limit  $\rightarrow$

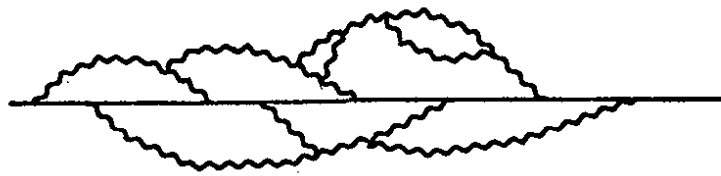


$\equiv$



SU(3) symmetric, even-signature flux-tube  $\equiv$  Pomeron

Fig. 7.8



— ≡ reggeised fermion  
 ~~~~~ ≡ Pomeron

Fig. 7.9

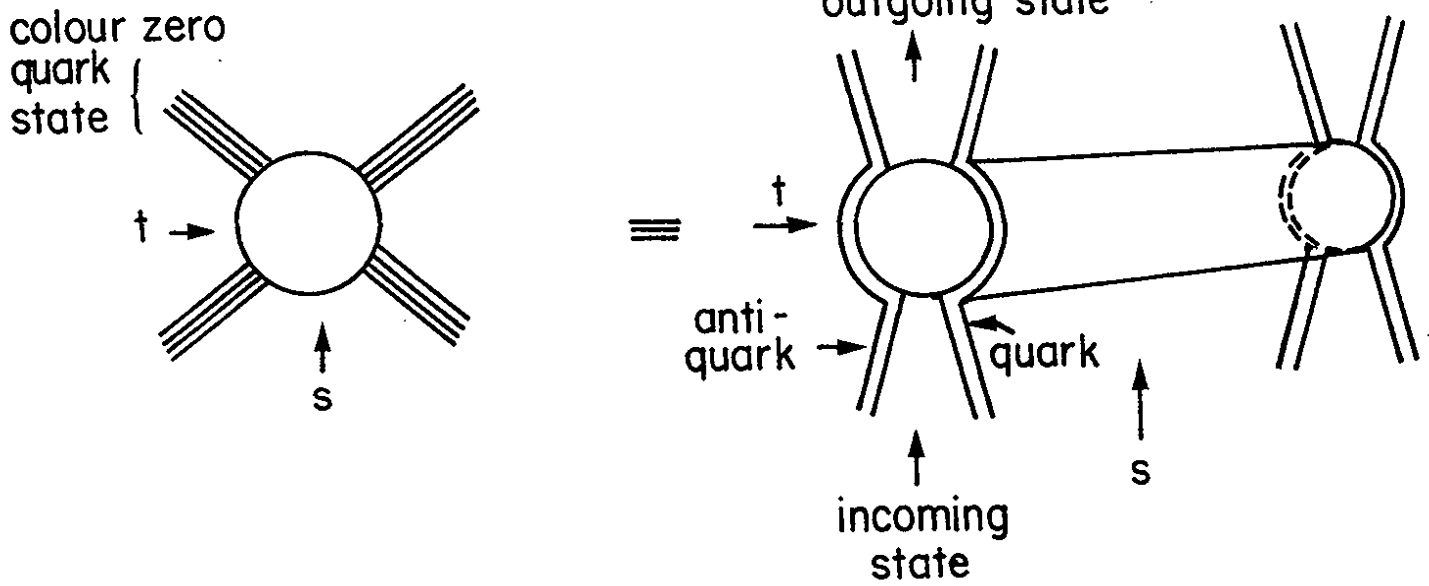


Fig. 8.1

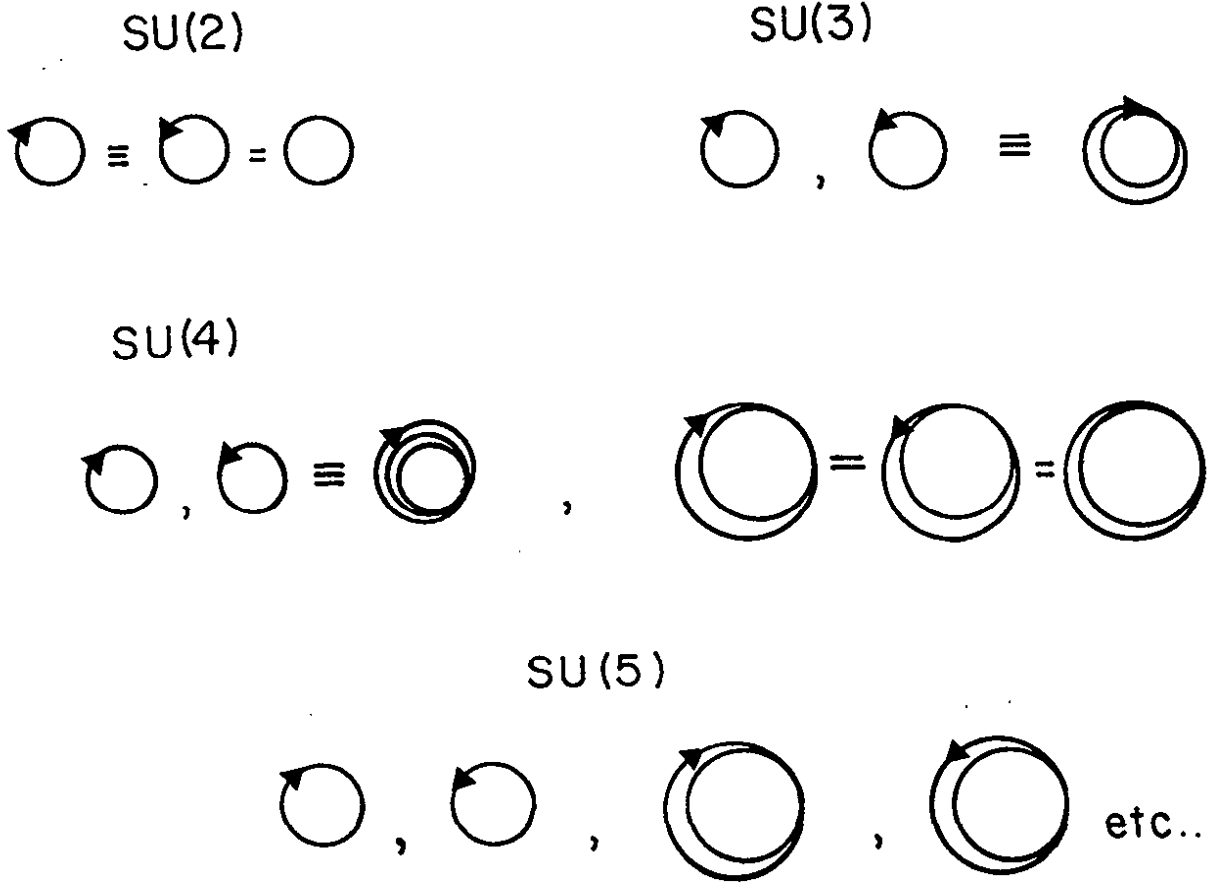


Fig 8.2

$$\langle n \rangle \sim \text{||||}\dots\text{||||}$$

Fig. 8.3

$$\text{>}< \text{wavy} = \sum \int d\Omega \left| \text{||||}\dots\text{||||} \right|^2$$

Fig. 8.4

$$2 \langle n \rangle \sim \text{>}< \text{trapezoidal}$$

Fig. 8.5

$$\text{>}< \text{blob} \supset \sum \int d\Omega \left| \text{>}< \text{trapezoidal} \right|^2$$

Fig. 8.6

$$\left| \langle n \rangle \right| \left| \langle 2n \rangle \right| \left| \langle n \rangle \right| \xrightarrow{\text{rapidity}} \text{>}< \text{blob}$$

Fig. 8.7

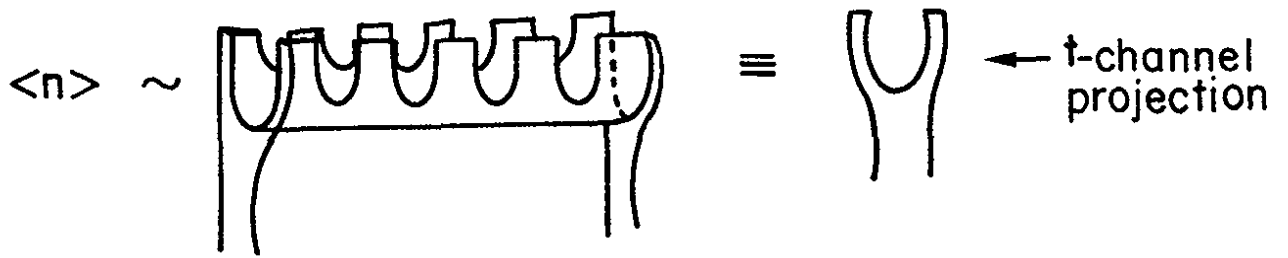


Fig. 8.8

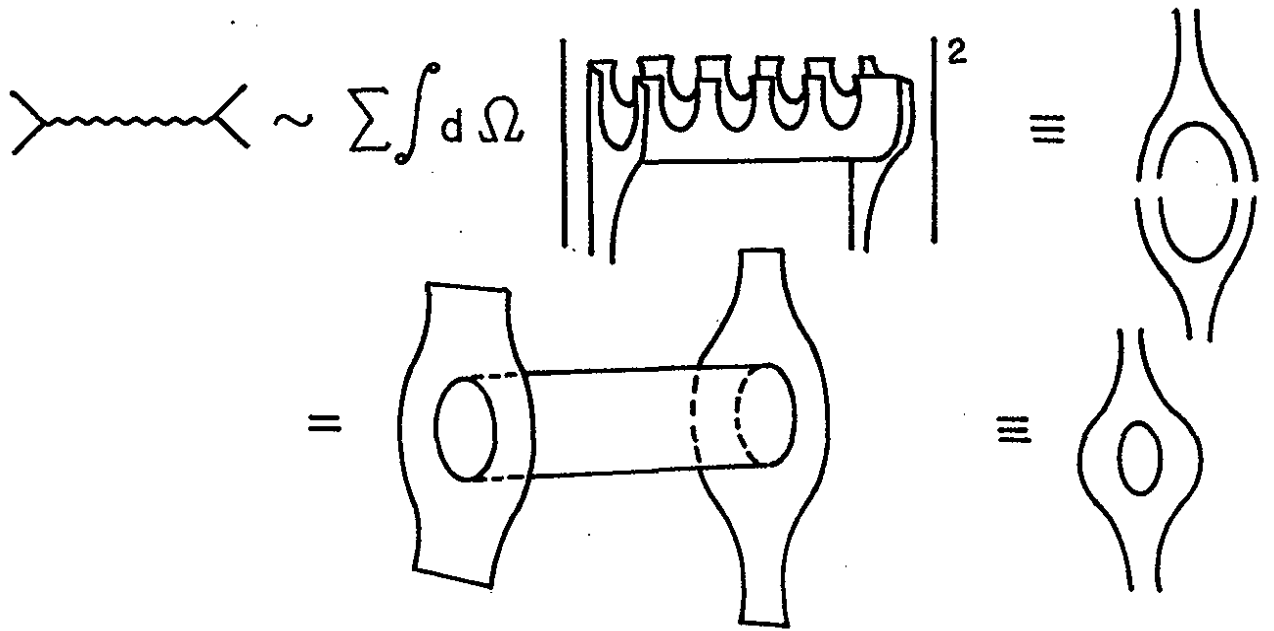


Fig. 8.9

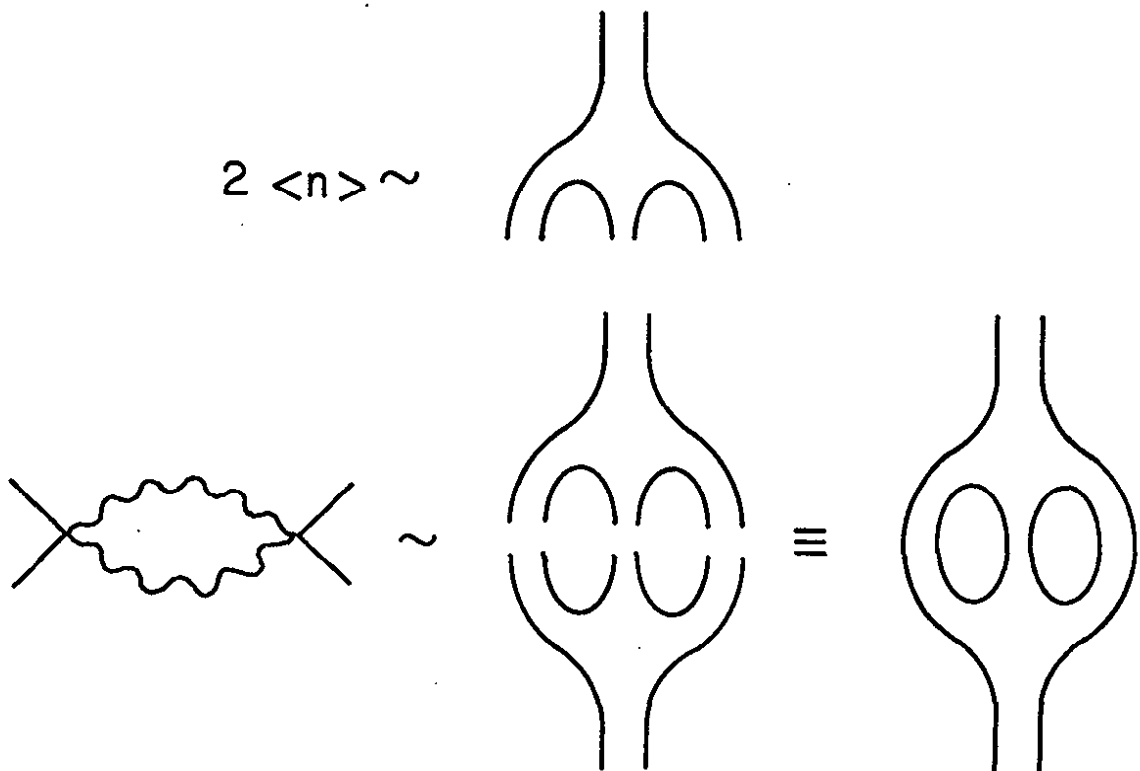


Fig. 8.10



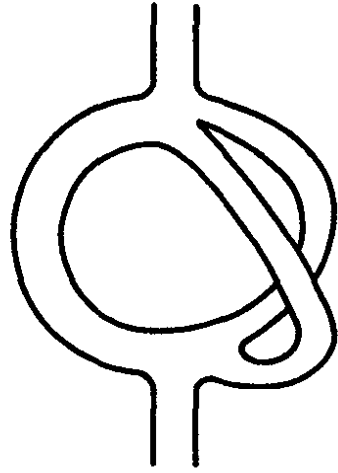


Fig. 8.11